CHAPTER SIX: FLUID INCLUSION STUDIES IN HOSTS OTHER THAN QUARTZ-Cu,Fe SULPHIDE VEINS

QUARTZ PHENOCRYSTS

Samples with quartz phenocrysts were taken from the Biotite Granodiorite, from an Intrusive Breccia, from a Feldspar-Quartz Porphyry dyke cutting the Biotite Granodiorite and from the Biuro Granodiorite. All phenocrysts contain fluid inclusions of types I, II and III and the suite of solid inclusions described in Chapter 3. Type II inclusions are more abundant than type III, and type I inclusions are variable in abundance, usually less common still. Primary type II inclusions are found adhering to solid inclusions of glass and Cu,Fe sulphide (fig. 4-5, 6-1). Definite primary type III inclusions are rare, and are again associated with solid inclusions (fig. 4-5). Many phenocrysts exhibit one prominent growth zone (commonly near the rim) marked by plentiful glass and primary type II inclusions. A few type III inclusions may also be associated with these zones.

It seems from the fluid inclusion assemblages that three fluids - silicate liquid, salt-rich liquid and vapour - coexisted in the Biotite Granodiorite magma at the level of the ore-zone. In the other intrusions, only vapour and silicate liquid are proven to have coexisted, although salt-rich liquid is present as inclusions of indeterminate habit. Fluid and solid inclusions are much less abundant in quartz phenocrysts from the Biuro Granodiorite than from phenocrysts in the Biotite Granodiorite and its associated intrusive phases. The presence in the phenocrysts of solid inclusions of Cu,Fe sulphide, (?) anhydrite and hematite, all characteristic hydrothermal solid inclusions at Panguna, suggests that some of the quartz in the phenocrysts may have been deposited from the

Fig. 6-1 Photomicrographs of inclusions.

A. A silicate solid inclusion, originally probably glass, from a quartz phenocryst in 103001. The dark objects are gas-rich inclusions.

B. The same inclusion after heating to 950°C. The rim has melted, and the gas-rich inclusions have coalesced and become rounded.

C. Another silicate solid inclusion from the same phenocryst in 103001, after heating to 950°C.

D. Type II and III inclusions in quartz from an amphibole-bearing vein, 103049. g = gas, h = halite.

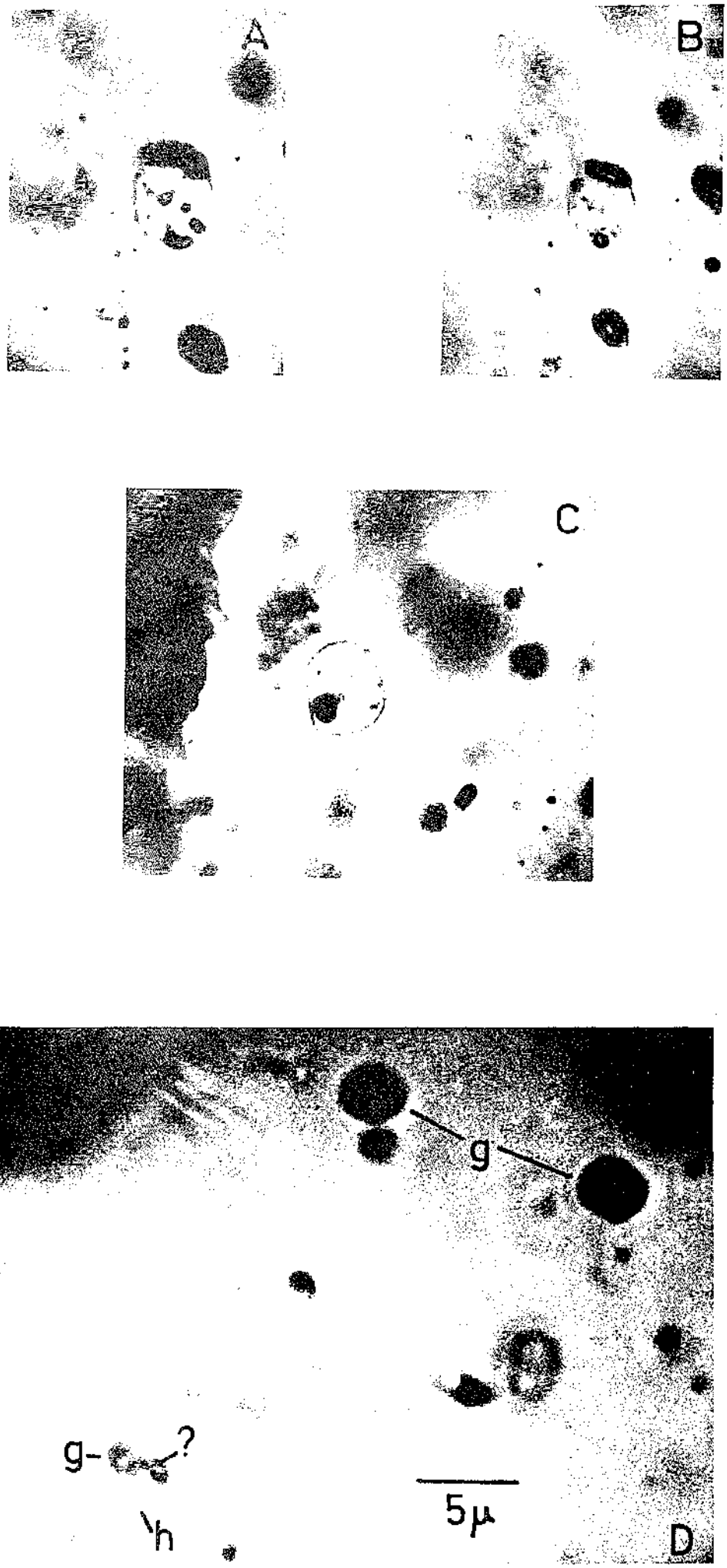
A
B
C
g
g-
?
h
5μ
D

salt-rich liquid. In the same way, the glass inclusions suggest the deposition of igneous quartz. This indicates the presence of several fluids at equilibrium, all saturated with respect to silica.

The prominent growth-zones marked by glass and type II inclusions may represent a sudden change in physical conditions - perhaps a pressure release - causing the evolution of vapour.

Temperatures were measured for type III inclusions from 103001, 103011 and 103015 (Biotite Granodiorite), 103006 (Intrusive Breccia) and 103021 (Quartz-Feldspar Porphyry). In each case the phenocrysts were taken from near quartz veins, so that salt-rich liquid from the veins could have been preserved as secondary inclusions in the phenocrysts. The T_SNaCl values in vein and phenocryst are essentially indistinguishable in 103006 and 103011, but one of the inclusions in the phenocryst in 103001 is apparently primary. For 103001, 103015 and 103021 the T_SNaCl values are distinct in vein and phenocryst; in 103001 the distinction is reinforced by the presence of a primary inclusion in the phenocryst and a difference in T_h values (cf. figs. 5-6 and 6-2).

The T_SNaCl range of salt-rich liquids from the phenocrysts is broad, 400 - 560°C to include most T_SNaCl data (fig. 6-2). Paired (T_SNaCl, T_SKCl) readings were obtained for seven inclusions, three of them in 103006. These are plotted with (T_SKCl, T_SNaCl) data from quartz-Cu,Fe sulphide veins in fig. 5-10 and all data conform to the same trend. Likewise, $T_S$salt A data from the phenocrysts conform to the patterns established for the veins (fig. 5-13). Two cases where $T_S$salt A exceeded 580°C were noted.

T_h readings also covered a broad range. They were generally less than T_SNaCl in 103006, 103011 and 103021. In 103001 and 103015 all T_h values were beyond the range of the Chaixmeca apparatus (>580°C). However, four type III inclusions in a phenocryst from 103001 were

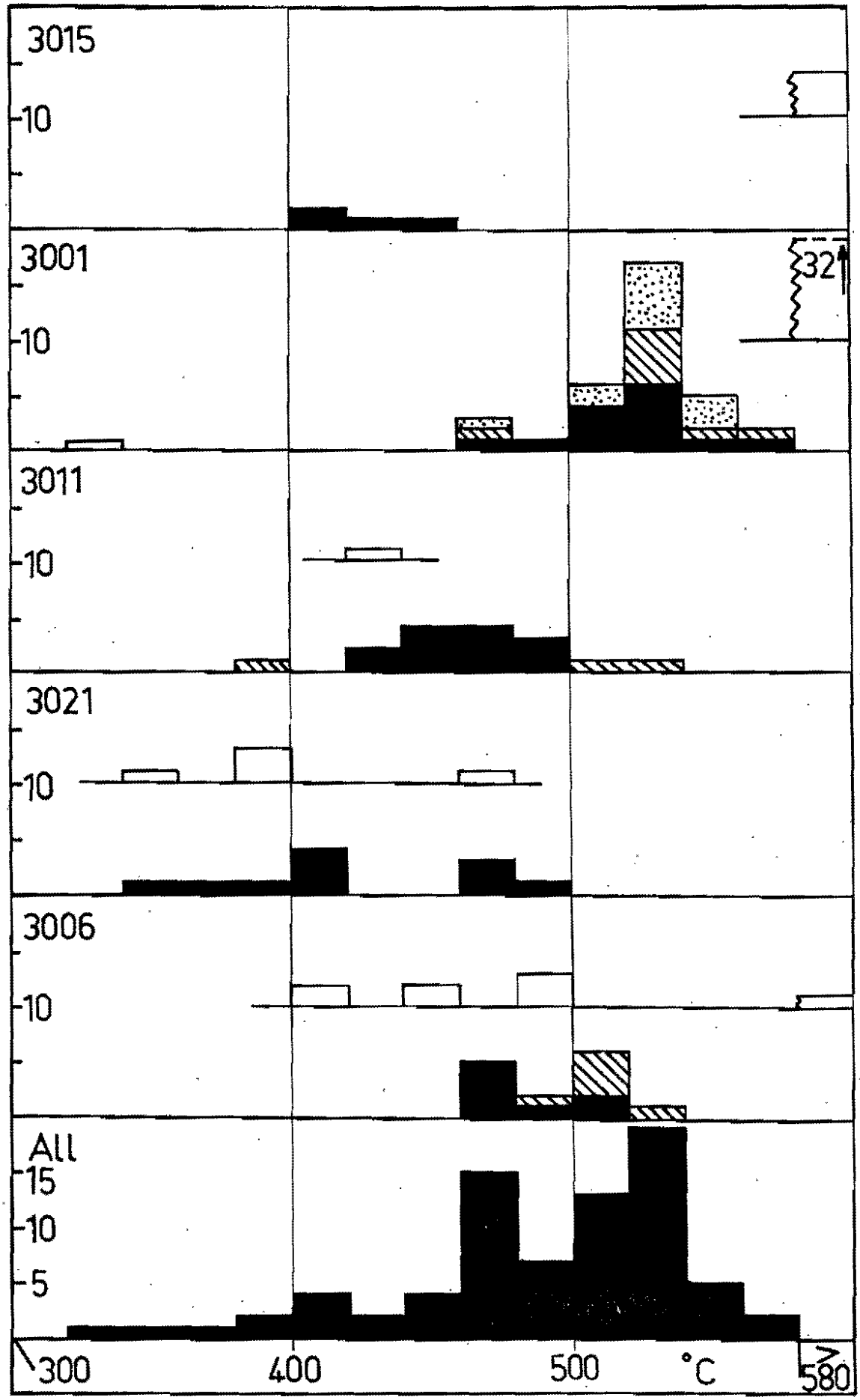

Fig. 6-2 Data from type III inclusions in quartz phenocrysts. Specimen numbers, shown at top left of each part, are prefixed by 10 in the University of Tasmania catalogue. T_h data are shown as white columns, T_sNaCl as black or patterned columns. The patterns distinguish data from different phenocrysts.

Table 6-1

ANALYSES OF A SOLID INCLUSION IN A QUARTZ PHENOCRYST FROM 103001

	Core (poorly polished)		Half way to rim	
Na_2O	2.32	0.41	11.34	1.93
Al_2O_3	19.03	2.02	20.05	2.07
SiO_2	66.68	6.01	67.58	5.93
K_2O	10.85	1.25	0.47	0.05
CaO	1.12	0.11	0.56	0.05
Total (pre-normalisation	91.30	9.80	98.10	10.03
	Half way to rim		Rim	
Na_2O	7.14	1.23	11.23	1.91
Al_2O_3	19.39	2.04	20.41	2.11
SiO_2	67.02	5.97	66.81	5.87
K_2O	5.89	0.67	0.43	0.05
CaO	0.56	0.05	1.11	0.10
Totals	101.10	9.96	100.60	10.05

Left hand columns: weight percentages.

Right hand columns: molecular proportions (per 16 oxygens).

examined on the heating stage of the C.S.I.R.O. Minerals Research Laboratories by Dr. P.J. Eadington, who obtained T_h readings of 944, 945, 1023 and 1023°C. At such temperatures, the solid inclusions thought to be devitrified glass were observed to melt around the edges, and bubbles in or on the surface of one of them disappeared. Other bubbles on the surface became rounded. The inclusion in fig. 6-1 was heated briefly to 950°C, so must have begun to melt at a lower temperature. The surface bubbles are thought to have been magmatic vapour attached to the impurity on the surface of the growing quartz phenocryst. Near the bubbles, therefore, the included silicate material would be melting in the presence of water and quartz.

The phase diagram of muscovite granite - H_2O (Wyllie, 1977, fig. 6) is appropriate for the compositions of the Panguna intrusive rocks. At 800 - 1000 bars, the likely pressure of crystallisation of the plutons (the lithostatic pressure corresponding to a hydrostatic pressure of 300 bars), quartz crystallises at temperatures below 800°C. Thus the type III fluid inclusions are indicating unreasonably high temperatures. It is not known whether quartz can contain fluid tightly at these high temperatures. As for the silicate solid inclusions, they too may be indicating unreasonable temperatures in that very little melting has taken place by 950°C. They may not, in fact, represent the melt composition at all. One of them, exposed on the surface of the polished section, was analysed in detail on the electron microprobe and found to contain sodic alkali feldspar with a potassic core (Table 6-1). There was no excess silica (this may have diffused into the host) and no concentration of Ca, Fe or Mg at the polished section. Diffusion appears to have separated Na from K within the inclusion.

The measurements do not help greatly in establishing the temperature of formation of the quartz phenocryst. The only indisputable observation

is that type III inclusions in this phenocryst as a group have much higher minimum T_h values than the groups of type III inclusions examined in vein quartz.

In the light of the discussion in Chapter 5, it seems unlikely that fluid inclusions with $T_h < T_s$NaCl could have been trapped under magmatic conditions. Thus only the salt-rich liquids in 103001 and 103015 remain as candidates for salt-rich liquid in equilibrium with magma.

The similar chemical variation patterns of the salt-rich liquids from the quartz phenocrysts and the quartz-Cu,Fe sulphide veins, and the occurrence of primary inclusions as described above, strongly suggest that some, at least, of the liquids share a common origin, namely within the magmas of the intrusive suite at Panguna. In addition, the occurrence in phenocrysts of Cu,Fe sulphides both as solid inclusions and as trapped or daughter-mineral phases in type III inclusions indicates the association of magmatic salt-rich liquid and copper.

AMPHIBOLE-MAGNETITE-QUARTZ VEINS

A single specimen, 103049, was studied for fluid inclusions. The amphibole contains abundant type II inclusions and rare reddish solid inclusions (hematite ?). The quartz also contains these, and less abundant type I and type III inclusions. No definite primary or secondary inclusions were identified. The data are presented in fig. 6-3.

Type I inclusions homogenised at 330 ± 10°C. The salinity was 0 - 3% eq. NaCl, corresponding to a T_f range of 0 to -1.8°C. For a formation pressure of 300 bars the pressure correction is 15 - 20°C (Potter, 1978) so that the trapping temperature of these fluids was 348 ± 13°C.

Type III inclusions have nucleated only one daughter mineral, which appears to be halite. The salt-rich liquid may have been boiling, because one gas-rich inclusion of composition intermediate between types II and III was observed. The data from type III inclusions are heterogeneous, and of little help in specifying the properties of a single fluid. The T_sNaCl range is 320 - 440°C, and this gives maximum formation temperature estimates for the inclusions since $T_h < T_s$NaCl in all but one inclusion, i.e. the liquids were probably supersaturated. This behaviour differs from that of type III inclusions in quartz-Cu,Fe sulphide veins in which T_h is generally greater than T_sNaCl in inclusions with T_sNaCl < 400°C. This vein may have formed from a boiling salt-rich liquid. Alternatively, the deposition of the vein minerals may have been a high temperature pneumatolytic event, (accounting for the abundance of type II inclusions in the amphibole) the salt-rich liquid in the quartz having been incorporated during later copper mineralisation. The salt-rich liquid does not, however, resemble salt-rich liquids from quartz-Cu,Fe sulphide veins, either in the daughter salts observed, or in homogenisation order. Ford & Green (1977) suggested a temperature of 600 - 650°C, based on the $\delta^{18}O$ of the quartz, for another of these veins.

QUARTZ-PYRITE VEINS

All quartz-pyrite veins contain type I inclusions, and some contain types II and III. In specimens 103015 and 103028 it was possible to distinguish two generations of quartz filling the one fracture. The younger generation in each case was associated with pyrite and contained only type I inclusions, and the older contained fluid and solid inclusions typical of quartz-Cu,Fe sulphide veins. Other quartz-pyrite veins were distinguished from quartz-Cu,Fe sulphide veins by the presence

Fig. 6-3 Fluid inclusion data from type I and III inclusions in quartz from in the amphibole-bearing vein 103049.

Fig. 6-4 The distribution of QP association fluids (see text for explanation). Geological contacts and the outer 0.3% Cu contour are as in fig. 2-3.

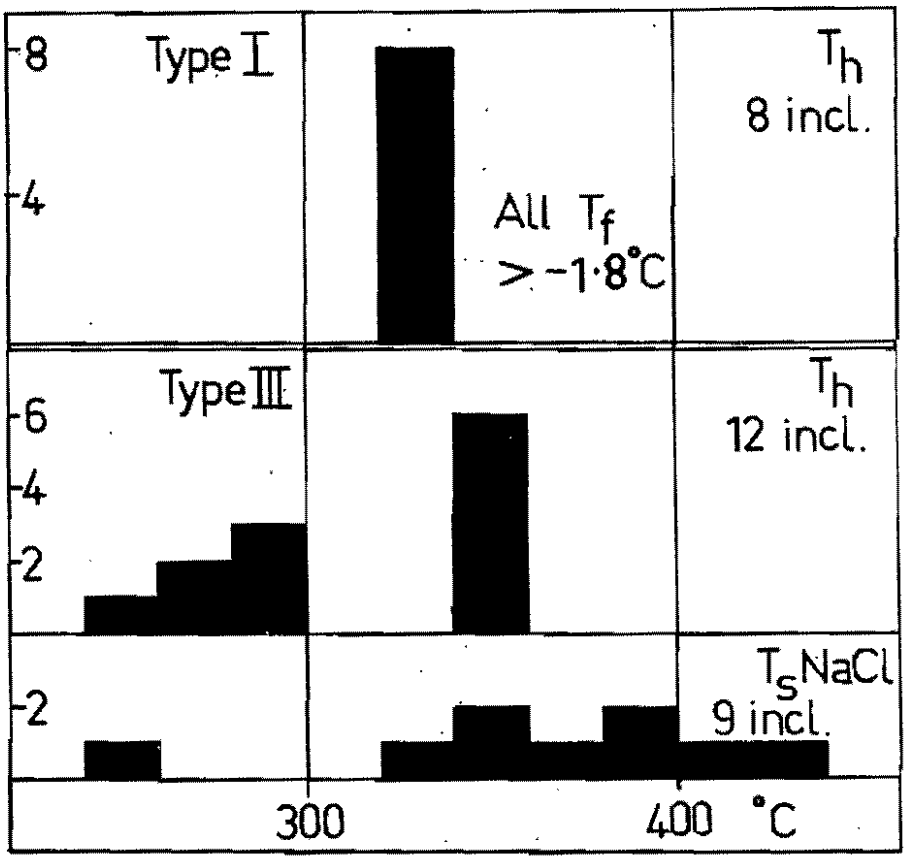
8
Type I
T_h
8 incl.
4
All T_f
> -1·8°C
6
Type III
T_h
12 incl.
4
2
T_sNaCl
2
9 incl.
300
400 °C

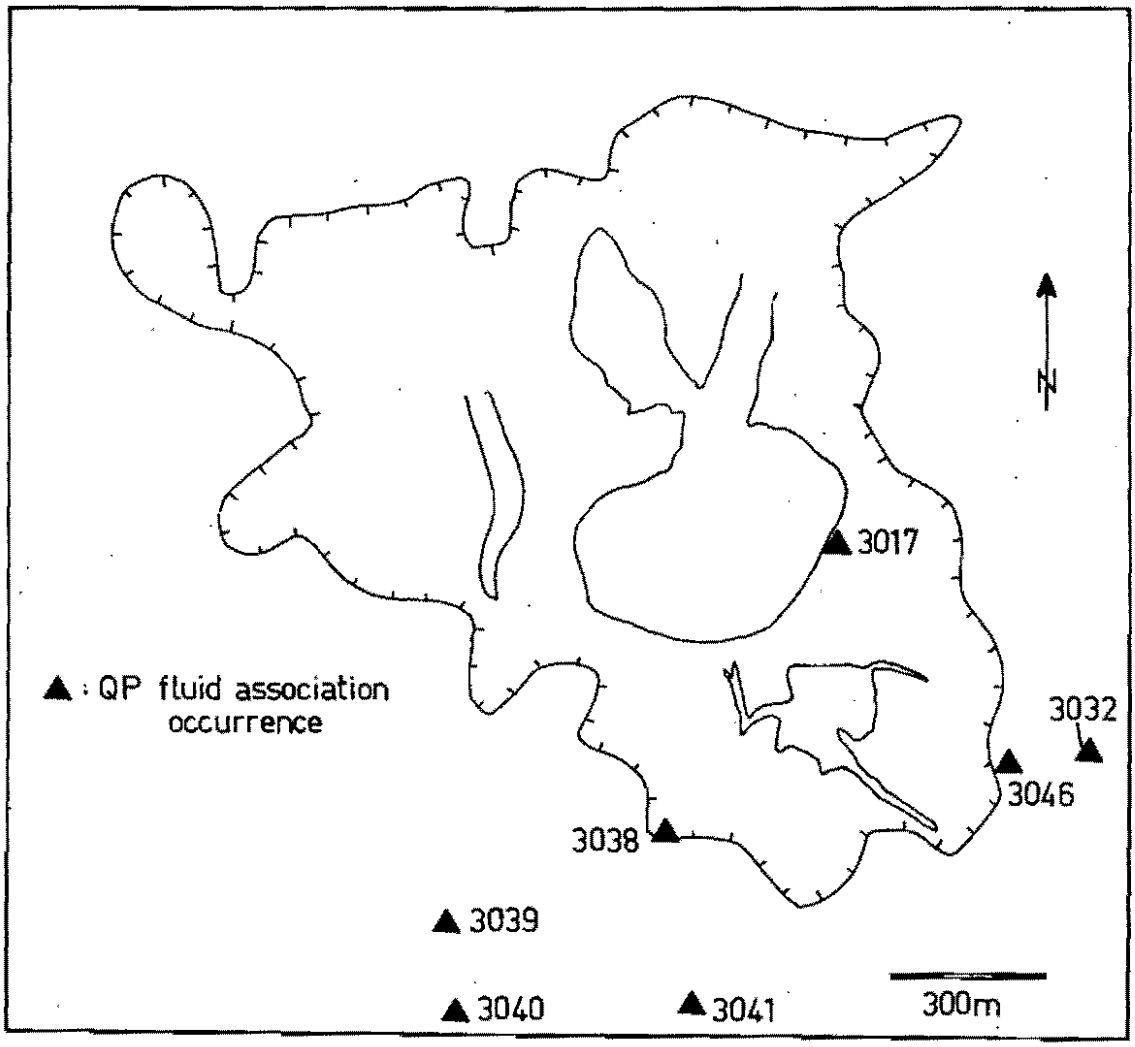
N
3017
▲ : QP fluid association occurrence
3032
3046
3038
3039
3040
3041
300m

of a special association of types I and II inclusions exhibiting various homogenisation phenomena at temperatures largely over 360°C. These phenomena include the following, which are characteristic of fluids homogenising at or near the critical point (see Yermakov, 1965, p.364 ff.). For type I inclusions:

1. T_h > 360°C, bubble diminishes rapidly just before homogenisation to liquid.
2. Homogenisation at the critical point.
3. Liquid boils just before homogenisation to gas.

and for type II inclusions:

4. Homogenisation to gas, largely at 360 - 420°C; liquid diminishes rapidly just before homogenisation.

In addition, there are type I inclusions with homogenisation temperatures up to 520°C. These homogenise by a gradual decrease in the volume of the bubble.

The veins which contain such inclusions (fluids termed the QP association from here on) were found only in specimens 103017, 103032, 103038, 103039, 103040, 103041 and 103046 (fig. 6-4). These have been interpreted as forming an arc encircling the Leucocratic Quartz Diorite (Eastoe, 1978), but an alternative interpretation should also be considered. This considers 103039, 103040 and possibly 103041 to belong to another group, possibly an earlier halo. In Chapter 9, reasons for favouring this alternative interpretation are discussed. Type I inclusions of lower homogenisation temperatures and type III inclusions are usually also present in veins bearing QP association inclusions. In 103017, type III inclusions bearing hematite are found in those parts of the quartz unaffected by the dense swarms of healed fractures with QP association inclusions. Solid inclusions of hematite have been observed

in the quartz, much of which was therefore probably deposited by salt-rich liquid. Type III inclusions in the rest of the quartz could have been destroyed during the intense fracturing. The QP association fluids may be associated with a later generation of lustrous pyrite crystals and quartz with very small, primary type II (?) inclusions along the growth zones. The later minerals were deposited on to a pre-existing vein, probably a quartz-Cu,Fe sulphide vein.

Salinity. Relatively few type I inclusions were large enough for freezing experiments. The points plotted in fig. 6-5 are individual (T_h,T_f) pairs distinguished according to specimen and to vein type (as suggested in Chapter 2, the "quartz-pyrite" classification may comprise three vein types: veins from outside the deposit, those bearing QP association fluids and others from within the deposit but bearing no QP association fluids).

Quartz-pyrite veins from outside the deposit contain mainly waters with T_f ranges of 0 to $-2^{\circ}C$ and $< -16^{\circ}C$, i.e. 0 - 3% and > 20% eq. NaCl respectively (fig. 6-5, square symbols). Certain inclusions have T_f values below $-21.1^{\circ}C$; these may contain salts other than NaCl. Specimen 103015 (within the deposit, but without QP fluids) gave T_f readings grouped around $-4^{\circ}C$ (~ 7% eq. NaCl). QP association inclusions which homogenised to liquid gave T_f readings in the range $-5^{\circ}C$ to $-20^{\circ}C$ and lower (8 to >22% eq. NaCl). For inclusions which homogenised at the critical point, there are conflicting indications of salinity. A T_c-range of 370 - $420^{\circ}C$ implies salinities of 0 - 4% eq. NaCl, but T_f readings on two such inclusions (in 103017 and 103040) were $-15^{\circ}C$ and $-22 \pm 3^{\circ}C$, implying very much higher salinities in terms of the system NaCl-H_2O. While small amounts of divalent ion in solution may radically affect the freezing properties of such solutions, the critical point data of Marshall & Jones (1974) suggest that divalent ions will have only a small

effect on critical phenomena. Salinity estimates based on T_c are therefore regarded as more reliable than those based on T_f. Inclusions homogenising to gas at $T_h < 400^{\circ}C$ must contain less than 3% eq. NaCl (Sourirajan & Kennedy, 1962).

Temperatures. T_h histograms are presented in fig. 6-6. The quartz-pyrite veins from outside the deposit all contain inclusions which homogenised at $T_h < 320^{\circ}C$. Only 103045 contains a significant number of inclusions homogenising at higher temperatures. 103015 from the pit contains primary inclusions homogenising at 300 - 330°C. For these, for the T_h readings for veins from outside the deposit and probably for the lower-temperature inclusions from 103017 and 103032 (for which there are no salinity estimates), the pressure corrections are given in Table 5-1.

The temperatures of formation of the QP association are best discussed in the light of the arguments presented in Chapter 9. The temperatures of critical and near-critical phenomena are at worst minimum estimates of the formation temperatures of the fluid inclusions concerned, but they may well be true estimates. The liquids of higher salinity and higher T_h (as in 103017) formed at higher temperatures. The histogram for 103017 indicates many T_h readings in the range 400 - 460°C, and a "tail" of higher values stretching off beyond 500°C. This "tail" suggests that the liquids may have been boiling, and thus that the more common T_h readings below 460°C may be true formation temperatures. The decrepitation temperatures of QP association inclusions in 103017 are 560 - 570°C.

Relationship with type I inclusions from quartz-Cu,Fe sulphide veins. The broken line in fig. 6-5 encompasses the field of T_h, T_f data for quartz-Cu,Fe sulphide veins (from fig. 5-1). Except for four inclusions from 103043 with $T_f < -24^{\circ}C$, all (T_h, T_f) points for veins outside the

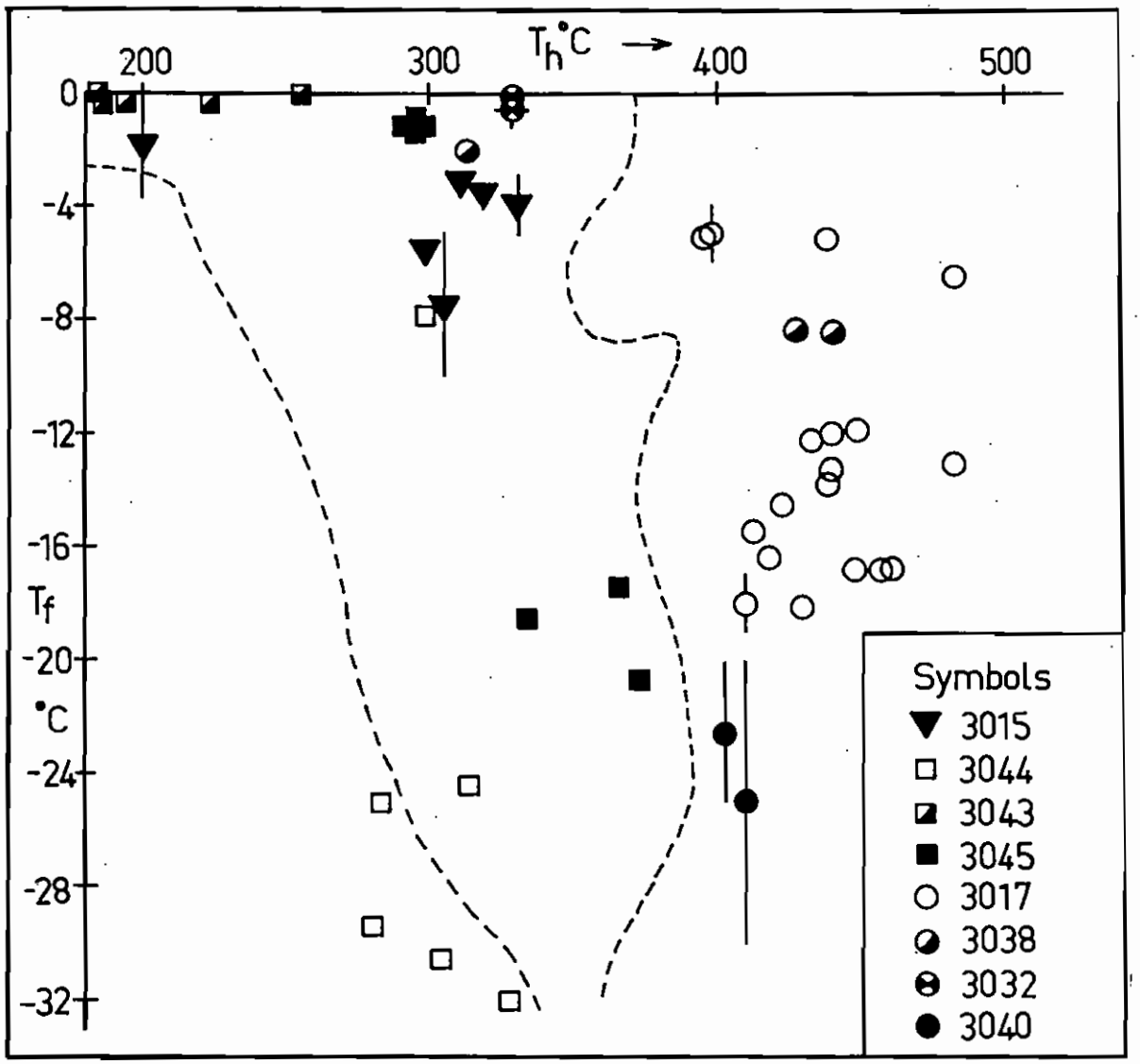

Fig. 6-5 T_h data vs. T_f data for type I inclusions from quartz-pyrite veins. Each symbol corresponds to a single specimen; the specimen numbers in the legend are prefixed by 10 in the University of Tasmania catalogue. Bars give the uncertainty of data. The dashed line encompasses the field of data from type I inclusions in quartz-Cu,Fe sulphide veins.

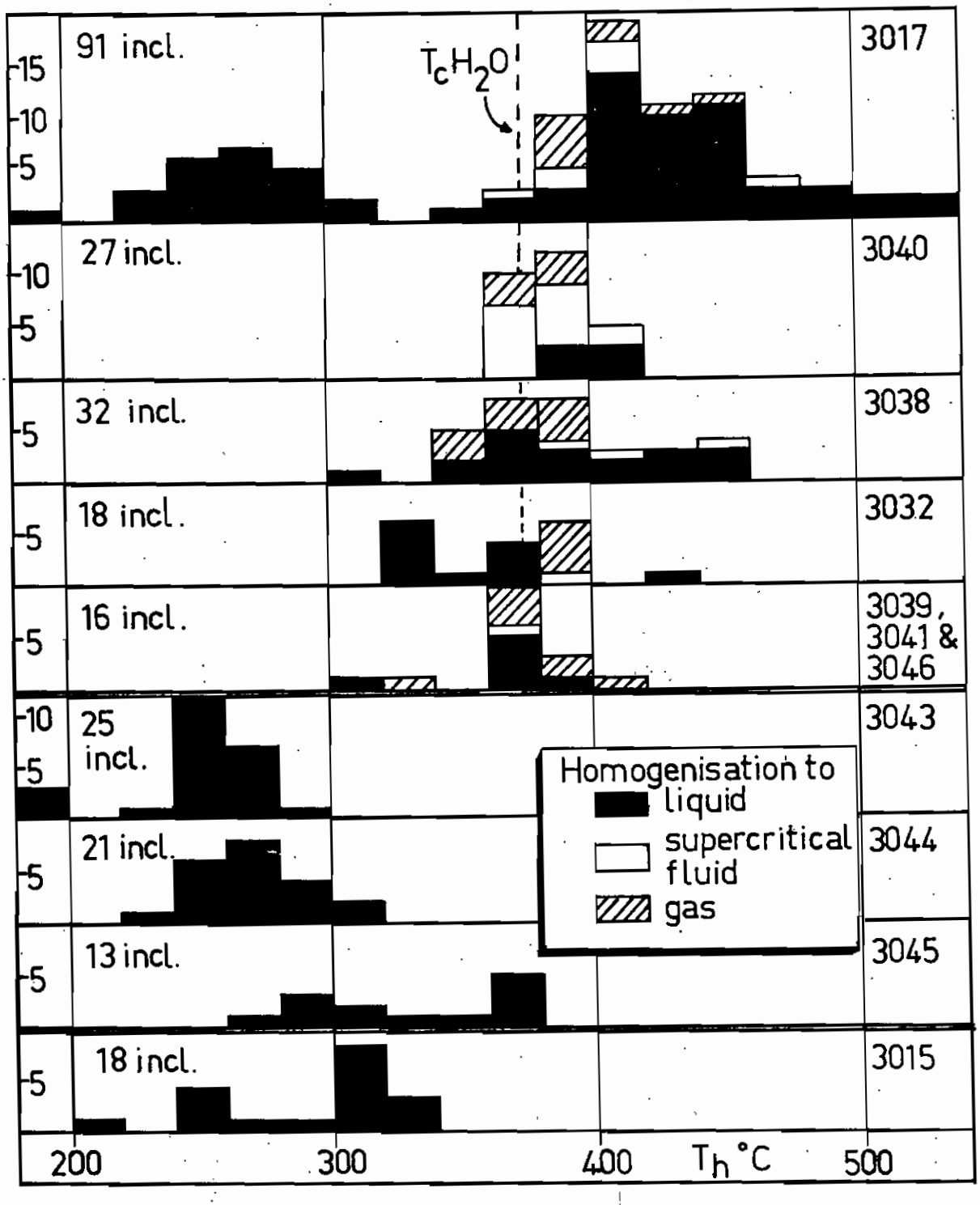

Fig. 6-6 Histograms of T_h data for type I inclusions (and a few type II) from quartz-pyrite veins. The top five histograms are for specimens bearing QP association fluid inclusions (see text). The critical temperature of water is indicated. 3043-3045 are specimens from outside the ore-zone, and 3015 from within the ore-zone. Specimen numbers are prefixed by 10 in the University of Tasmania catalogue.

deposit and for 103015 within the deposit also lie in this field. The QP fluid association plots outside the field, on the high temperature side, but differs from the fluids in other type I inclusions only in temperature. Therefore the QP association could be the result of heating of fluids like those preserved in type I inclusions in quartz-Cu,Fe sulphide veins. The higher salinities (and T_h measurements) in QP association fluids may have resulted from the boiling of less-saline waters.

PYRITE ± BLEACHED SELVAGE

Although this vein-type appears to be free of gangue minerals at hand specimen scale, a thin section of 103470 revealed small quartz crystals projecting into the seam of pyrite from the margin. A little of the quartz is enclosed by the pyrite. The quartz contains fluid inclusions, the larger and more visible of which are mostly type II inclusions. There are also much less abundant type I inclusions and some intermediate between types I and II. No type III inclusions were observed. Some very small primary inclusions associated with a growth zone of the quartz were difficult to classify, but the larger ones seem to be type II inclusions. The deposition of the quartz (and pyrite) was probably associated with a vapour phase, and possibly also with a boiling liquid of low to moderate salinity. No heating or freezing measurements were made.

SPHALERITE-PYRITE VEINS

A specimen of quartz associated with pyrite and small quantities of sphalerite, chalcopyrite and galena, 103042, contained type I inclusions suitable for study. The inclusions were of indeterminate habit, but no other type of inclusion was found in the specimen. The T_h mode was 310°C and salinities range between 0 and 2% eq. NaCl (fig. 6-7). A pressure correction of about 15°C (Potter, 1978) is implied for a pressure of 300 bars. The formation temperature of 330°C is to be compared with sulphur isotope temperatures of 270 - 310°C for other pyrite-sphalerite veins (see Chapter 11). The T_h,T_f plot for 103042 indicates fluids indistinguishable from those most frequently represented in the type I inclusions in quartz-Cu,Fe sulphide veins (fig. 5-1).

QUARTZ HEALING BRECCIATED SPHALERITE

Type I inclusions from 103048 were indeterminate in habit, and gave T_h readings in the range 200 - 320°C. T_f readings were mainly between 0 and -2°C, giving a pressure correction of about 15°C. These fluids, too, compare closely with the fluids in type I inclusions in quartz-Cu,Fe sulphide veins.

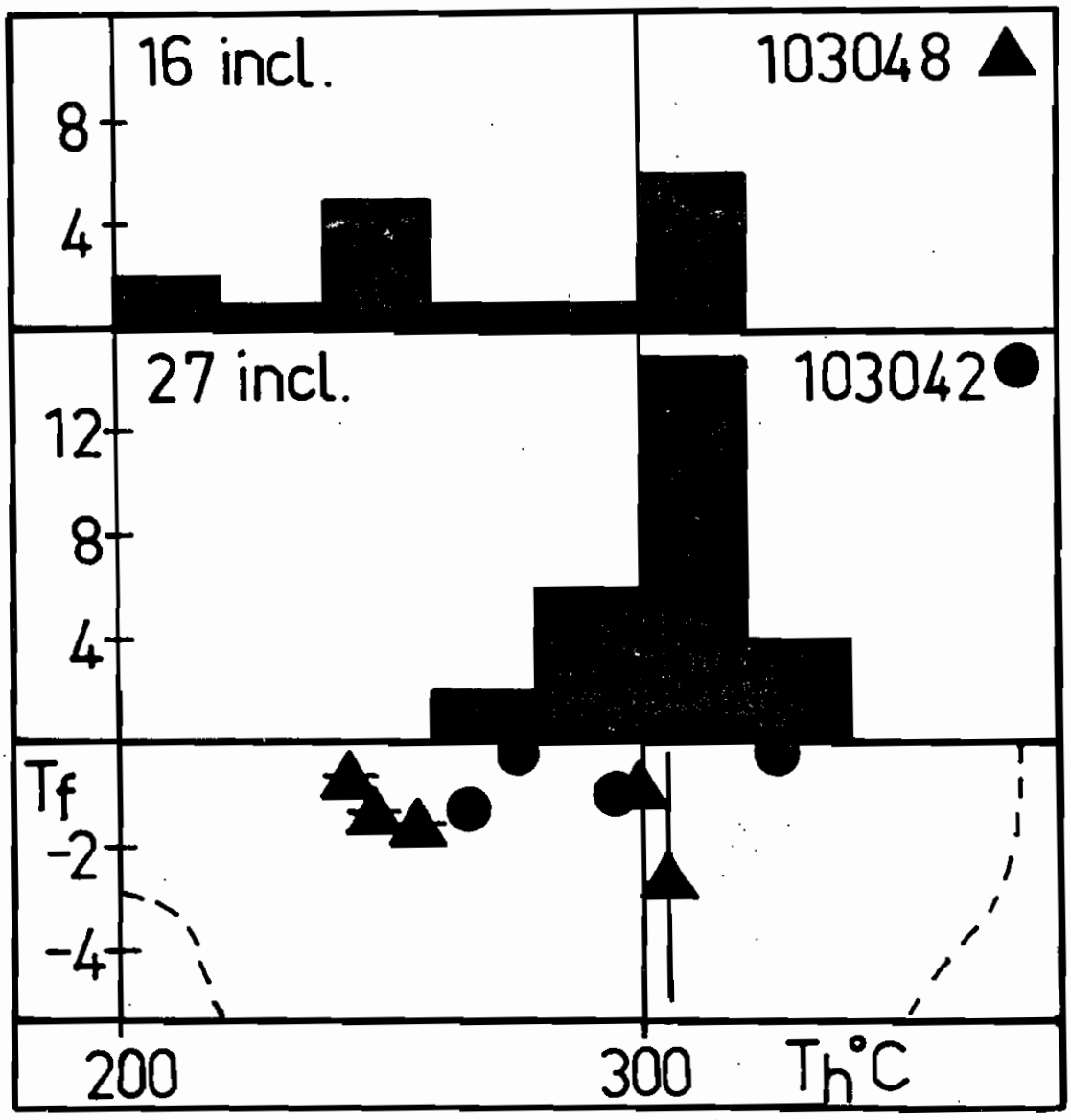

Fig. 6-7 T_h histogram and T_h vs. T_f for 103048 (quartz healing brecciated sphalerite) and 103042 (a quartz-pyrite-clay vein with minor sphalerite, chalcopyrite and galena).

CHAPTER SEVEN: PRESSURE ESTIMATES

Three methods of estimating the pressure during mineralisation are available from the fluid inclusion data. The first applies to the QP fluid association (see Chapter 6); the second and third apply to the salt-rich liquids and their vapours.

QP ASSOCIATION

A fluid inclusion which homogenises at T_c must have been trapped at $P \geq P_c$ and $T \geq T_c$. In 103017 the mode of T_c is 410°C, and in 103040 the mode is 400°C (see fig. 6-6). These correspond respectively to P_c values of 280 and 270 bars in the system $NaCl-H_2O$ (Sourirajan & Kennedy, 1962). These are minimum pressure estimates, on the assumption that there are no other substances present in sufficient quantity to change the critical properties of the fluids (experiments with a crushing stage revealed little, if any, CO_2 in these specimens). Similar pressure estimates apply to the other specimens in which there were homogenisations at the critical point.

TYPE II INCLUSIONS

The data obtained from type II inclusions have been discussed in Chapter 5 (see fig. 5-4). When type II inclusions homogenise, the temperature and pressure in the inclusions must be less than T_c and P_c of the vapour they contain. In 103026, which appears to have formed near 400°C on the basis of type III inclusion data, the type II inclusions with small liquid rims homogenise at temperatures less than 400°C. The 400°C formation temperature must apply to the type II inclusions if the salt-rich

liquid was in equilibrium with the vapour. Assuming the system NaCl-H_2O to be an adequate representation of the vapour, the P_c at 400°C is 290 bars. A similar estimate may apply for 103029, where the formation temperature of the vapour is less certain. These are maximum possible pressures of formation. In veins formed at higher temperatures, much higher maximum pressure estimates may apply. Consistent with this, the homogenisation temperatures of type II inclusions in 103012 and 103022 were observed to be higher, generally >420°C (but not measured precisely) in inclusions with small liquid rims.

TYPE III INCLUSIONS

If the salt-rich liquids in type III inclusions are adequately represented by the system NaCl-KCl-H_2O, the data of Ravich & Borovaya (1949) can be used to estimate the vapour pressures of the boiling liquids. A few such liquids at Panguna saturated or close to saturation in NaCl contained about 3 parts NaCl to 1 of KCl by weight; such a liquid has a vapour pressure greater than 200 bars between 450 and 600°C (fig. 7-1). An upper limit of 300 bars has been interpolated in a part of Ravich & Borovaya's diagram where the data are sparse. At higher temperatures the pressure diminishes, approaching 50 bars at 700°C. The most concentrated liquids at Panguna have about 4 parts NaCl to 1 of KCl by weight; this permits pressures a little higher than in the 3:1 case (by 10 - 20 bars at saturation). The most dilute liquids contain about 2 parts NaCl to 1 of KCl, and these would have a vapour pressure between 200 and 250 bars (values again interpolated).

The salt-rich liquids could deviate from the conditions of the experiments of Ravich & Borovaya because of the presence of other salts (probably lowering the vapour pressure) or volatiles other than water

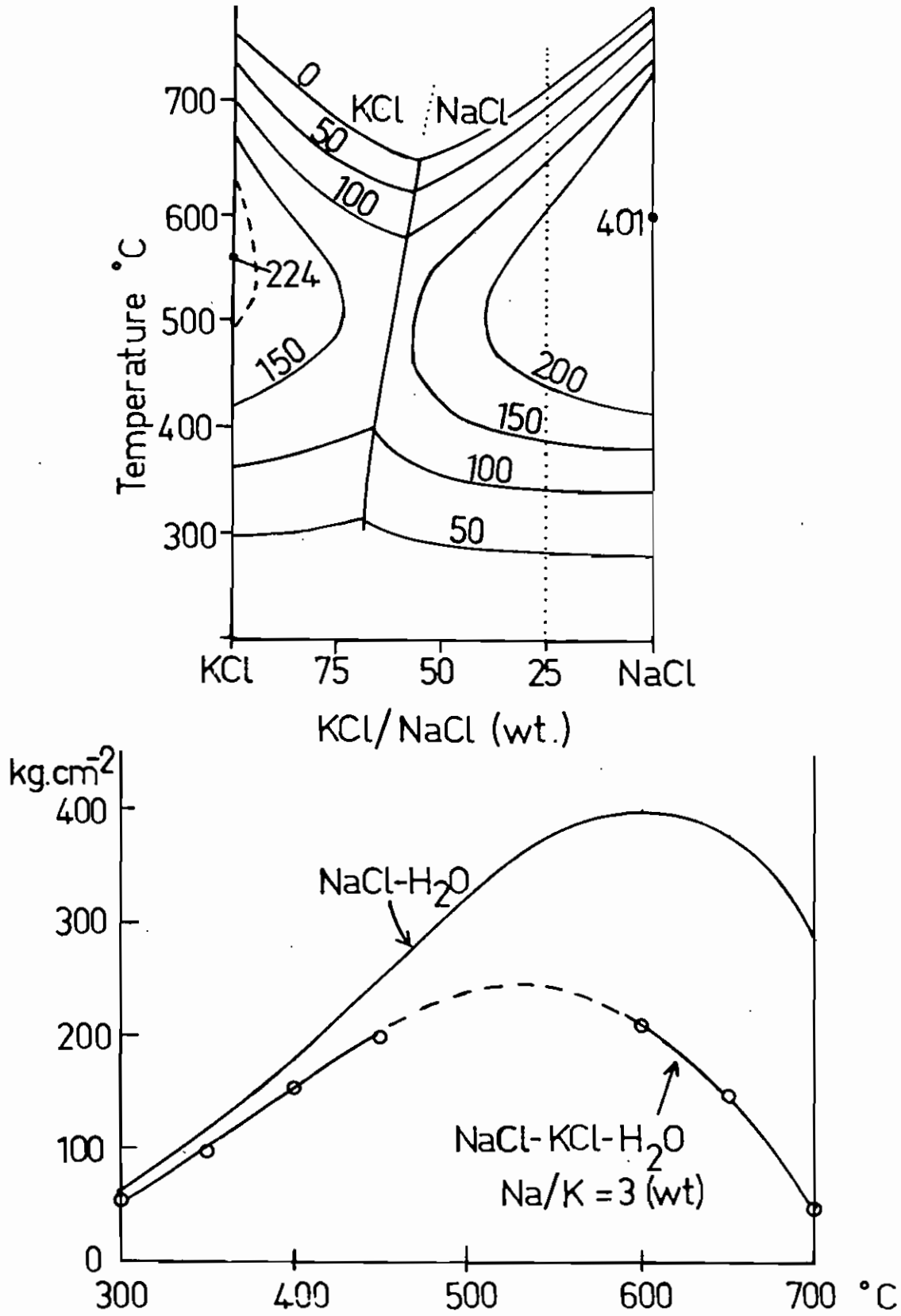

Fig. 7-1 Vapour pressures in the system NaCl-KCl-H_2O. The upper figure gives vapour pressure isobars in kg/cm^2 for saturated liquids with KCl/NaCl ratios as indicated on the abscissa, and at temperatures from 300 to 700°C. The lower diagram gives vapour pressure curves for two liquids of fixed KCl/NaCl ratio. After Ravich & Borovaya (1949). One bar ≈ 1 kg cm^{-2}.

(raising it), if the liquids were unsaturated with respect to NaCl (raising the vapour pressure) and also if they were supersaturated (lowering it). Unsaturation is most likely in the case of the most dilute and certain more concentrated liquids (see Chapter 5). Saturation or supersaturation appears to be the case for the rest. Therefore the best pressure estimate by this method is 200 - 300 bars for the liquids which appear to be saturated in NaCl.

SUMMARY

QP association fluids, the specimens in which most of the type II inclusion data were collected and the lower-temperature saturated salt-rich liquids are all associated with the edge of copper mineralisation (see Chapters 5 and 6). Therefore all of the considerations above are consistent with a pressure of 270 - 290 bars near the edge of the deposit. Within the deposit, the pressure may have been lower where those salt-rich liquids thought to have been supersaturated were present, or higher where there were higher-temperature saturated or unsaturated salt-rich liquids. These matters will be examined again in Chapter 9.

CHAPTER EIGHT: THE HISTORY OF THE DEPOSIT

The vein classification (Table 3-1) does not include any subdivision of quartz-Cu,Fe sulphide veins beyond distinguishing veins with a central sulphide seam from those with disseminated sulphide only near the Leucocratic Quartz Diorite. However, there are other indications that more than one phase of quartz-Cu,Fe sulphide veining took place. Such veins intersect each intrusive body in the deposit, yet the relationships between the intrusives and copper mineralisation (and silicate alteration) differ widely (Fountain, 1972). The Leucocratic Quartz Diorite and the southern part of the Kaverong Quartz Diorite are strongly mineralised and are largely altered to potassic assemblages. The Biotite Granodiorite is weakly mineralised (except in the marginal Intrusive Breccias) and is altered largely to phyllic and argillic assemblages. The Biuro Granodiorite is very weakly mineralised and relatively unaltered. The two pyrite haloes delineated in this study give a further indication of multiple veining phases.

Adding the fluid inclusion data to the intersection relationships between veins and intrusives (the only useful field criteria for classifying quartz-Cu,Fe sulphide veins) allows an improved interpretation. Areas of high salinity or high temperature (or both) are considered as possible centres of mineralisation and suggest a centre in and near the Leucocratic Quartz Diorite (Phase B) and another along the west edge of the Biotite Granodiorite (Phase C). Data from veins thought to be associated with these centres have been excluded from the map. The residual fluid inclusion data (fig. 8-1) have been termed Phase A. In the following discussion of their relationships, the three phases are best treated in the order C, B, A.

PHASE C

The centre along the west edge of the Biotite Granodiorite is defined by specimens 103001, 103004, 103005, 103006, 103012, 103013, 103014 and 103022. It is younger than the Biuro Granodiorite because 103013 and 103014 cut that intrusion. It is, hence, younger than other mineralisation in the vicinity, since the Biuro Granodiorite intersects all other mineralisation and alteration patterns around it (Fountain, 1972). The specimens listed belong to the core area of a phase of mineralisation (phase C) which probably also includes all other quartz-Cu,Fe sulphide veins cutting the Biotite Granodiorite and its minor phases. The edge of phase C has not been located, except perhaps to the east where low salinities occur within the orebody (specimens 103007, 103008, 103017 and 103021). So the minimum extent of phase C includes the Biotite Granodiorite and the Biuro Granodiorite, and part of the area between them (fig. 8-1).

PHASE B

The centre in and near the Leucocratic Quartz Diorite is marked by a concentration of quartz veins (fig. 3-1) and high copper grades (Baldwin *et al.*, 1978), as well as by high T_h data from specimens 103031 and 103047. It is encircled by a halo of pyrite veins and possibly by another halo of quartz-pyrite veins bearing the QP-fluid association (specimens 103017, 103020, 103032, 103040, 103046; see fig. 8-1). This phase (B) may itself have comprised two stages because there are two generations of quartz-Cu,Fe sulphide veins. High salinities and temperatures at the southern margin of the orebody (102636, 103029, 103030) belong to a separate centre about 100 m from the nearest Leucocratic Quartz Diorite contact. This centre, too, may belong to phase B.

RELATIONSHIP OF B AND C

Since they affected different parts of the orebody, it cannot be shown that phases B and C took place simultaneously or otherwise, but the mode of occurrence of the pebble dykes suggests that phases B and C waned concurrently. The pebble dykes mapped by mine geologists are parallel, and occur only in two discrete groups (fig. 2-3). One group cuts the centre of phase B mineralisation and the other cuts the centre of phase C. It is suggested that all of the pebble dykes formed in a single episode of violent boiling, as low salinity waters inundated the waning mineralisation centres along newly-created, deeply-penetrating, NE-NNE fractures. Phase B, if it comprised two stages, may have been active both before and during phase C activity.

PHASE A

If mineralisation belonging to phases B and C is excluded (i.e. veins enclosed by the haloes about the Leucocratic Quartz Diorite, and those which cut the Biotite Granodiorite or the Biuro Granodiorite or the area between them), the asymmetric element of the salinity and temperature distributions remains (fig. 8-1). This is called phase A. Since only a minimum extent could be established for phase C it is possible that phase C data remain in fig. 8-1. However, the sparseness of phase C veining, even at the implied centre of this phase, and the simplicity of the proposed phase A pattern, suggest that few if any are left. There is a broad field of veins with T_sNaCl from 450°C to 490°C, bounded to the south and southwest by a zone of lower salinities, i.e. a zone of dilution by groundwater. There is also a fall in temperature from more than 700°C in the north to 350 - 430°C along the same zone to the south and southwest. Phase A has a pyritic halo (fig. 4, Baumer &

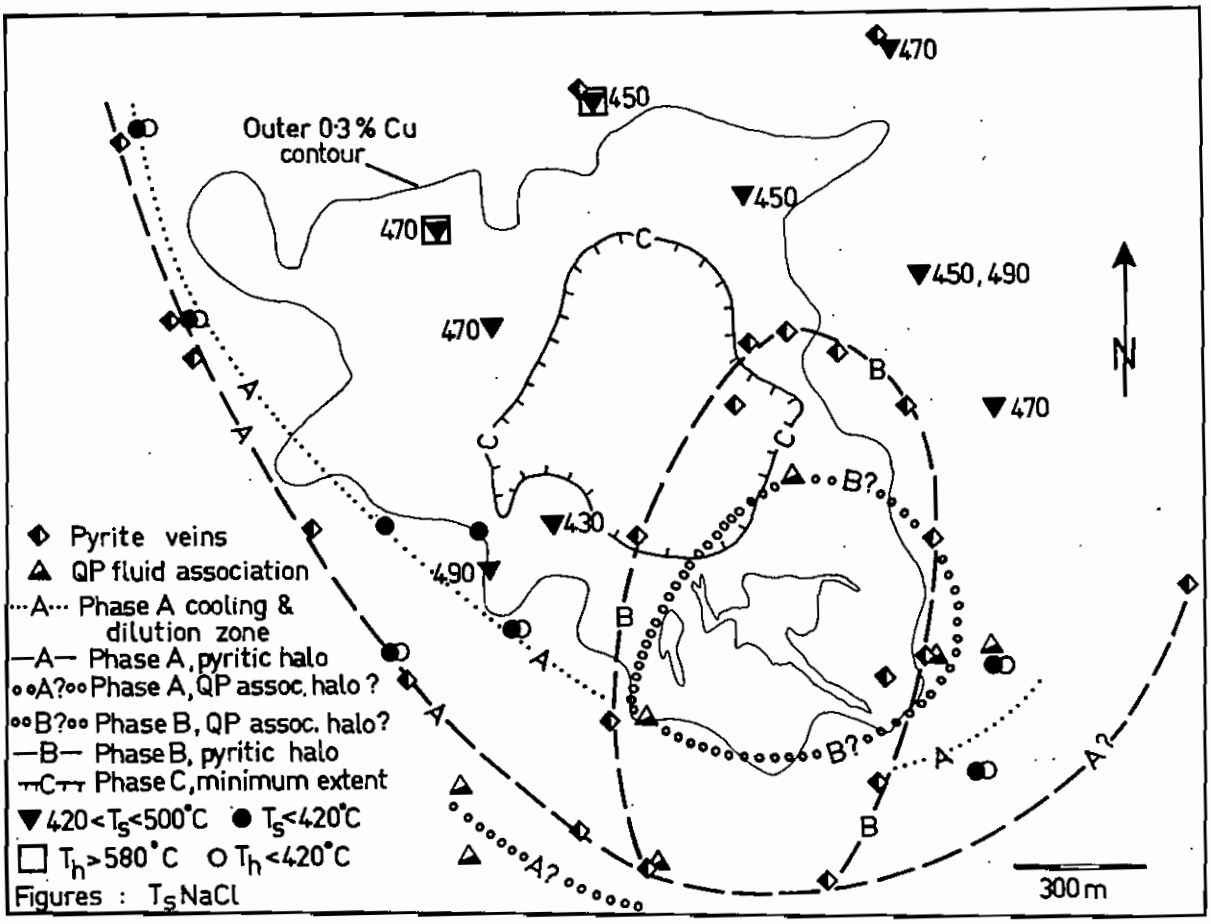

Fig. 8-1 Map of phase A fluid distribution. The fluid inclusion data enclosed by the phase B haloes and the minimum extent of phase C have been excluded. The contact of the Leucocratic Quartz Diorite and the outer 0.3% Cu contour are as in fig. 2-3.

Fraser, 1975) slightly beyond and parallel to the zone along which dilution occurred. This is shown separately in fig. 8-1. There could also be a QP association halo similar to the one suggested for phase B. Three quartz-pyrite specimens (103039, 103040, 103041) with QP association fluid inclusions occur beyond the ore-zone and may be part of a halo running parallel to the zone in which salt-rich liquid was cooled and diluted. Other parts of the proposed halo were not accessible for sampling. Previously (Eastoe, 1978), all of the specimens with QP association fluids were ascribed to a single halo encircling the Leucocratic Quartz Diorite.

The asymmetric temperature and salinity distributions of phase A (with respect to the 0.3% Cu contour) are consistent with the formation of phase A while the southern part of the Kaverong Quartz Diorite was hot. According to data from specimens 102676 and 102998, the temperatures were sub-magmatic (700°C or greater).

Two hypotheses relating phase A to the intrusive sequence arise. The first is that phase A was related to the emplacement of the Kaverong Quartz Diorite and predated the Biotite Granodiorite. This hypothesis is favoured by the association of the biotitisation of the southern margin of the Kaverong Quartz Diorite (to give the Biotite Diorite) with copper mineralisation. Such biotitisation continues beyond the economic deposit and is not spatially related to the Biotite Granodiorite which appears to be unaffected by it. The phase A zone of cooling and dilution, and the pyrite halo, are parallel to the margin of the Biotite Diorite (in particular, in tracing the form of the southeastward projection, most of which has been displaced by the Biotite Granodiorite). The second hypothesis relates phase A to the intrusion of the Biotite Granodiorite while the Kaverong Quartz Diorite was still hot.

The central position of the Biotite Granodiorite with respect to copper mineralisation and the presence in its melt of boiling, salt-rich liquid (demonstrated by primary type II and III fluid inclusions in quartz phenocrysts) favour the second hypothesis. Yet there do not appear to be any fluid inclusion data centred on the Biotite Granodiorite. For this reason, and because of the Biotite Diorite-copper association, the first hypothesis is preferred here.

The evolution of salt-rich liquid from the Biotite Granodiorite must have had some effect, as yet not accounted for, on the surrounding rocks. The only mineralisation obviously associated with the Biotite Granodiorite seems to be the sanidine-biotite-quartz-chalcopyrite matrix in parts of the Intrusive Breccias. The mineralisation is sharply bounded at the breccia-country rock contacts, suggesting that fluid transport was mainly upwards through the steeply-dipping breccia bodies rather than outwards at this stage (fig. 8-2). Ford (1976) suggested that the Biotite Granodiorite stock reached a level higher than the roof zones of the Kaverong Quartz Diorite and the Leucocratic Quartz Diorite. If this is so, mineralisation associated with the Biotite Granodiorite may have taken place above the exposed orebody, or may not have occurred at all because of unsuitable physical conditions at higher levels.

CONDITIONS DURING PHASE B

The symmetry of the pyrite halo around the Leucocratic Quartz Diorite implies that the temperature distribution had changed between phases A and B. By analogy with phase A, where the pyrite halo was probably associated with the dilution and cooling of salt-rich liquid, the presence of a closed pyritic halo indicates that cooling and dilution of the salt-rich liquid took place around the whole cell of phase B mineralisation, and that groundwater had already inundated the ore-zone.

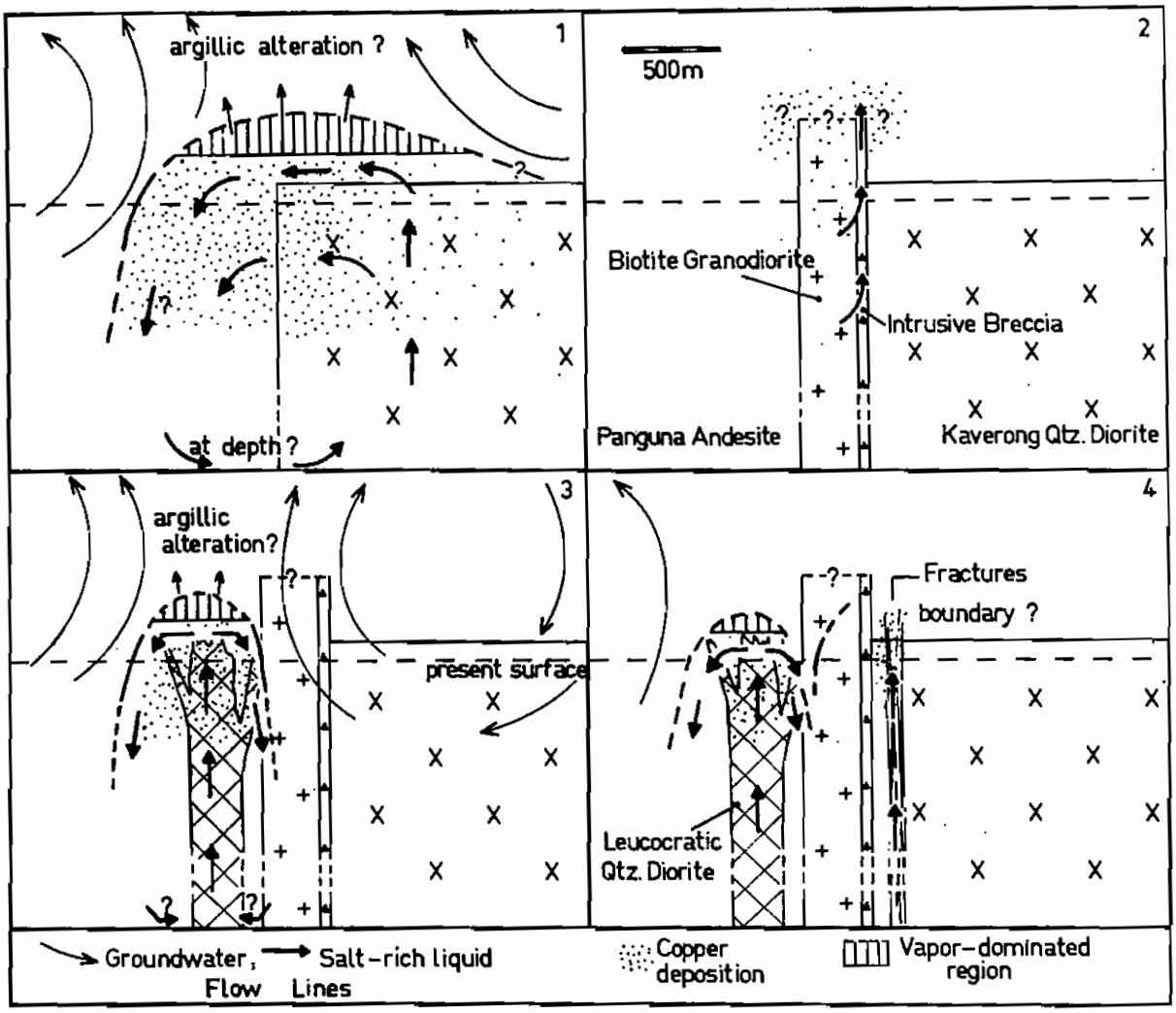

Fig. 8-2 Four proposed stages in the evolution of the Panguna deposit. The sketches are of a vertical section through the centre of the Leucocratic Quartz Diorite and oriented NNW.

1. Phase A.
2. Intrusion of the Biotite Granodiorite.
3. Phase B.
4. Phase C (phase B probably continuing).

The horizontal scale is approximate and the vertical scale is not specified. The forms of the intrusions are simplified, and the Intrusive Breccia at the contact of the Biotite Granodiorite has been projected onto the section. The present surface is approximated by a horizontal broken line.

Phase B therefore occurred well after the waning of phase A and the cooling of the entire system, including the Biotite Granodiorite (because this is cut by the phase B pyrite halo). Page & McDougall (1972) detected a difference of 0.5 - 1.5 m.y. between the K-Ar ages of fresh Kaverong Quartz Diorite and the younger hydrothermal alteration of the smaller porphyry stocks, and this is sufficient time for the proposed change in thermal regime.

EVENTS PRIOR TO PHASE A

It has already been noted (Chapter 3) that a phase of amphibole-magnetite-quartz veining preceded all quartz-Cu,Fe sulphide veining. The alteration accompanying the amphibole-magnetite-quartz veining is pervasive in the Panguna Andesite out to the propylitic alteration zone. West of the deposit, however, three quartz-Cu,Fe sulphide veins (103003, 103025, 103026) have outer selvages containing plentiful biotite. A little amphibole, possibly igneous, remains and is rimmed by biotite in 103026, but other ferromagnesian minerals have been entirely replaced. Plagioclase phenocrysts are rimmed and veined with biotite, and much of the groundmass consists of fine-grained biotite; the texture is one of replacement. In 103003 and 103025 the textures are hornfelsic. In 103003, plentiful randomly-oriented plates of biotite occur between plagioclase phenocrysts. 103025 is a fine-grained hornfels consisting largely of biotite and quartz. It is possible that at least two of these specimens preserve a contact-metamorphic biotite hornfels which predates the amphibole-magnetite-quartz event and survives only beyond the edge of amphibole alteration. This biotite does not appear to be associated with the quartz-Cu,Fe sulphide veins. The inner selvages of 103003, 103025 and 103026 consist of albite ± chlorite ± sericite. Only in veins closer

to the orebody is secondary biotite visibly associated with quartz-Cu,Fe sulphide veins. Biotite hornfels is characteristic of the British Columbian porphyry copper deposits, where it is occasionally confused with potassic alteration (Sutherland Brown, 1976b). The outer boundary of the hornfels commonly coincides roughly with the pyritic zone in the British Columbian deposits; this seems likely at Panguna, too, on the evidence of the three specimens. If there was an early biotite hornfels at Panguna, then it has been very effectively masked by the subsequent amphibole alteration. None of the specimens with alteration amphibole (103049, 103466, 103467) gives any indication that amphibole has replaced pre-existing biotite.

SUMMARY

Mineralisation appears to have taken place at intervals throughout the intrusive cycle. There was a hiatus between an early group of phenomena (the Kaverong Quartz Diorite, phase A and possibly the Biotite Granodiorite) and a later group (the Leucocratic Quartz Diorite, the Biuro Granodiorite, phases B and C, and the pebble dykes). During the hiatus, groundwater invaded the ore-zone. The sequence of events suggested by the arguments in this section is shown in Table 8-1.

The interpretation here differs in one major respect from that of Baldwin *et al.* (1978) who suggest that the Biotite Granodiorite, while not itself the progenitor of significant copper mineralisation, remobilised and assimilated phase A copper and upgraded the ore in the zone adjacent to its contact. They do not recognise a phase of mineralisation corresponding to the phase C of this study. The upgrading along the Biotite Granodiorite contact may be a broader manifestation of the contact-controlled escape of volatiles (in parts more spectacularly

evidenced as mineralised breccias). Otherwise, the fluids responsible for the upgrading have not been identified in this study. The veins which cut the Biotite and Biuro Granodiorites must be ascribed to another event, however minor in economic importance. Both this study and that of Baldwin *et al.* (1978) agree that the relatively low-grade Biotite and Biuro Granodiorites are not a low-grade core in the sense of Lowell & Guilbert (1970); rather they intersect pre-existing mineralisation.

Table 8-1

THE SEQUENCE OF EVENTS AT PANGUNA

IGNEOUS EVENTS		HYDROTHERMAL/PNEUMATOLYTIC EVENTS	AGE
Nautango Andesite			1.6 m.y.
		Pebble Dykes Pyrite-clay veining Sphalerite-pyrite veining Quartz-pyrite veining Groundwater inundation	
Biuro Granodiorite Leucocratic Quartz Diorite	order?	PHASE C - quartz-Cu, Fe sulphide-anhydrite veining + PHASE B (2 stages) - quartz-Cu, Fe sulphide-anhydrite veining + quartz-pyrite veining + pyrite veining.	3.4±0.3 m.y.
		Groundwater inundation	
Quartz-feldspar porphyries Intrusive Breccias Biotite Granodiorite		Intrusive Breccia matrix	
		PHASE A - quartz-Cu, Fe sulphide-anhydrite veining + pyrite veining Amphibole-magnetite-quartz veining and alteration.	
Kaverong Quartz Diorite (and contact metamorphism)			4.5±0.5 m.y.
Kieta Volcanics			?Oligocene - lower Miocene

K-Ar dates from Page & McDougall (1972).

CHAPTER NINE: FLUID SYSTEMS AND PORPHYRY COPPER FORMATION

THE WATER IN TYPE I INCLUSIONS

Low-salinity waters, unsaturated in NaCl at room temperature, have been present throughout the evolution of the orebody at Panguna, either immediately outside the ore-zone or pervading the whole area. The evidence for this is as follows:

(i) The dilution of salt-rich liquid near the edge of copper mineralisation;

(ii) The presence of secondary type I inclusions in all quartz-Cu,Fe sulphide veins and quartz phenocrysts. These cover the entire temperature range between copper mineralisation and about 150°C.

(iii) The presence, both inside and outside the ore-zone, of veins (mainly quartz-pyrite) containing only type I inclusions.

The waters in type I inclusions cannot readily be identified as meteoric or otherwise. Ford & Green (1977) suggested that the isotopic data for phyllic and argillic alteration products of the Biotite Granodiorite would be consistent with equilibrium with magmatic water at 500°C, or with meteoric water, ^{18}O-shifted in the propylitic zone, at 300°C (see Chapter 1). Combining this with textural evidence, they recognised the possibility of two generations of sericite-bearing alteration assemblages. This study has confirmed the availability of fluids at both temperatures in the Biotite Granodiorite. In specimen 103015, phyllic alteration is associated with water of low salinity. The younger generation of quartz in this vein (from the chlorite-sericite zone of the Biotite Granodiorite) encloses pyrite, chlorite and type I fluid inclusions, some of which are primary. The pressure-corrected

temperature is 320 - 350°C and the salinity is near 5% eq. NaCl. If isotopic and fluid inclusion data are considered together, this observation demonstrates that some of the phyllic alteration was due to low salinity meteoric water. Other sericite occurrences in the Biotite Granodiorite are clearly associated with quartz-Cu,Fe sulphide veins, and by implication, with magmatic waters.

It seems reasonable to suppose that all other low-salinity water in the deposit was also meteoric. Such water was present in the ore-zone only between and after pulses of salt-rich liquid, apparently flooding the ore-zone from outside. The variable salinities of type I inclusions from within the ore-zone (salinities are commonly far above the 0 - 3% eq. NaCl commonest in type I inclusions and probably representing uncontaminated groundwater) must have been due to the mixing of salt-rich liquid with the encroaching groundwater. The waning of the salt-rich liquid system and the inward movement of groundwater appears to have been of short duration compared with the period of copper mineralisation. The phase A salt-rich liquid boundary, for example, is relatively sharp, not smeared out. But because the fluids were distributed in fractures, pockets of salt-rich liquid could easily have remained to be mixed later with groundwater. This is consistent with the diminishing range of salinity in type I inclusions with decreasing T_h (fig. 5-1); as time progressed, and groundwater cooled the deposit, so less salt remained.

The pressure at the edge of the ore-zone was 270 - 290 bars (Chapter 7), the pressure of groundwater surrounding it. Cathles (1977) showed that the heating of water around an intrusion has little effect on the pressure distribution. Assuming that groundwater filled fractures all the way to the surface (there is no way of proving this), the depth of cover was about 3 km at the time of copper mineralisation.

The convection of groundwater, driven by heat from the cooling intrusion, is the model which best fits the phenomena described in this section. There is no evidence, however, that copper mineralisation is connected with this type of fluid system. The other mechanisms discussed in Chapter 1 will now be considered in the light of the data from Panguna.

THE ORTHOMAGMATIC MODEL AND THE VAPOUR-PLUME MODEL

At least some of the boiling salt-rich liquid in the deposit was of magmatic origin. This assertion is supported by the occurrence of primary type II and III inclusions in quartz phenocrysts of the Biotite Granodiorite, and by the continuity of properties between salt-rich liquids in veins and those in the phenocrysts. In particular, all K/Na ratios of salt-rich liquids lie on a single trend, and the temperatures of certain veins approach magmatic temperatures. That the salt-rich liquids were boiling wherever they occurred, and that they were associated with copper deposition, are interpretations which have been discussed in earlier chapters. Either the orthomagmatic model (the derivation of salt-rich liquid direct from silicate liquid by exsolution) or the vapour-plume model (Henley & McNabb, 1978 , i.e. the derivation of salt-rich liquid indirectly by condensation from magmatic vapour) might be consistent with these observations.

Quantities of salt-rich liquid. Both mechanisms are capable of supplying a large amount of salt-rich liquid. This can be shown by the following rough calculations:

Consider 1 kg of magma exsolving volatiles. The experiments of Ryabchikov (1975), as well as the fluid inclusions in quartz phenocrysts show that under the conditions of crystallisation of high-level

calc-alkaline intrusions, two non-silicate fluids, vapour and salt-rich liquid, coexist with silicate liquid and crystals. Ryabchikov estimates that the magma will exsolve 1 - 2% by weight of water and that this water will contain a mole fraction of chlorine equal to 0.02 ± 0.01. Taking the mean in each case, the bulk composition of the non-silicate fluids will be 15 g H_2O + 1.0 g NaCl (assuming all chlorine is in the form of NaCl). The compositions of coexisting liquids and gases under various conditions in the system NaCl-H_2O are taken from Sourirajan & Kennedy (1962) and these can be used to work out the distribution of NaCl between vapour and liquid (both generated direct by exsolution). The results of three calculations are set out in Table 9-1.

Table 9-1

T, °C	P, bars	NaCl:H_2O (weight)*		Distribution of NaCl (% of total NaCl)	
		in liquid	in gas	in liquid	in gas
700	500	75:25	2:98	71	29
700	1000	60:40	4:96	40	60
700	1100	50:50	7:93	56	44

* from Sourirajan & Kennedy (1962).

The calculations are rough, not least because the liquid compositions are taken from a part of Sourirajan & Kennedy's diagram where there are very large interpolations. Also, 800°C would be a better magmatic temperature estimate, but data are not available above 700°C. At 800°C, the vapours should contain more of the NaCl, so that the calculations above serve to demonstrate that a significant amount of the NaCl exsolved by the magma will be carried away as vapour.

Condensation over the first hundred degrees of cooling of the vapour will remove about 99% of the salt from the vapour at 500 bars (see fig. 19 of Sourirajan & Kennedy, 1962, reproduced here as fig. 9-1); on cooling from magmatic temperatures to 600°C (the temperature of minimum NaCl solubility in the vapour at 400 - 600 bars) virtually all of the salt is removed. At 800 bars, the solubility minimum is at 650°C, and cooling will still remove most of the salts from the vapour. This is the lithostatic pressure corresponding to a hydrostatic pressure of 300 bars; if formed at 800 bars or higher, the vapour will undergo a rapid temperature and pressure decrease on moving towards groundwater and will condense out most of its salt as salt-rich liquid. Comparable amounts of salt-rich liquid can thus be formed by the two mechanisms.

K/Na ratios. The condensate as a whole will clearly preserve the K/Na ratio of the vapour, and since the temperature fall to 600°C will probably occur over a short distance above the intrusion, the condensate is unlikely to be separated into fractions differing in K/Na. This should provide a test for distinguishing the two types of salt-rich liquid, because preliminary calculations by Lagache & Weisbrod (1977) indicate that KCl and NaCl fractionate between liquid and vapour to different extents. The vapour has a lower K/Na than the liquid for fluids in equilibrium with two alkali feldspars. For instance, at 640°C and 900 bars, the molar K/Na ratios are 0.28 for the liquid and 0.18 for the vapour. Although not buffered in the same way by feldspars, the orthomagmatic fluids at Panguna should undergo similar fractionation because fluid properties, not those of the solid phases, control the difference between liquid and vapour. If orthomagmatic and condensate salt-rich liquids are separated, then two different trends of K/Na ratios ought to be present, probably in different places. At Panguna, only one K/Na trend has been detected; this trend applies to three separate phases of

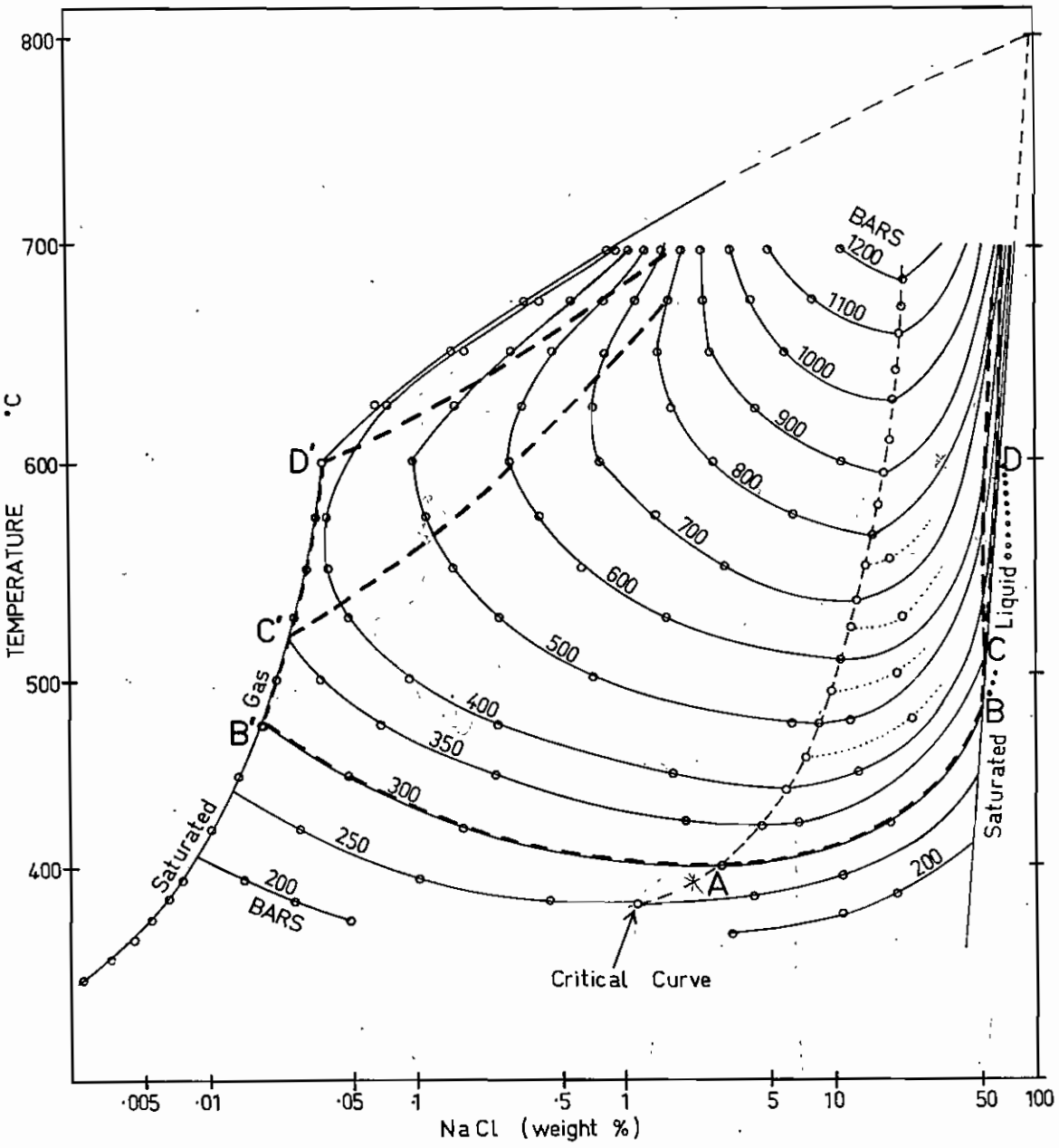

Fig. 9-1 Isobars of the two-phase region in the system $NaCl-H_2O$, from Sourirajan & Kennedy (1962). Each isobar gives the compositions of coexisting vapour and liquid at various temperatures. Possible paths of fluid-evolution at Panguna are shown, and are discussed in the text. The part of the path representing supersaturated salt-rich liquid is shown in dots between B and D.

evolution of salt-rich liquid (see fig. 5-10) and also includes orthomagmatic salt-rich liquid from the Biotite Granodiorite. It may be concluded that only one sort of salt-rich liquid was present at near-magmatic temperatures, and that the source was orthomagmatic. The single exception to the trend, 103029, might be explained as condensate salt-rich liquid, since the K/Na ratio is low relative to other salt-rich liquids.

It seems much more likely, however, that the temperature gradient above the part of the intrusion exsolving volatiles, or the subsolidus part where boiling takes place, is very steep. Most of the condensation which must occur over the first hundred degrees of cooling will take place where the condensate cannot really remain separate from the orthomagmatic salt-rich liquid. Because of its density, the salt-rich condensate will descend, eventually mixing with and becoming indistinguishable from the orthomagmatic salt-rich liquid. In this case, the vapour plume model becomes a giant reflux condenser.

Whether salt-rich condensate was being separated, or refluxed and mixed with orthomagmatic salt-rich liquid, cannot be determined from the fluid inclusion evidence from Panguna. The single trend of K/Na data does, nonetheless, rule out any significant deposition of quartz-Cu,Fe sulphide veins from a separate condensate.

FLUID EVOLUTION ACROSS THE TWO-PHASE REGION

Predictions. No matter what the mechanism of generation of the two fluid phases associated with the ore-zone, be it boiling or condensation, the fluid evolution across the two-phase region can be considered in a way similar to the treatment given by Henley & McNabb (1978). Those authors examined the changes across an isobaric section at 500 bars, at which pressure it is possible to vary the compositions of two unsaturated

$NaCl-H_2O$ fluids in equilibrium from the critical point up to magmatic temperatures. The 500 bar isobar in fig. 9-1 is the locus of the fluid compositions. The two-phase region characteristic of porphyry copper deposits would thus be bounded by a surface defined by the critical temperatures and pressures of the fluid system, and the fluids within the two-phase zone would converge towards a common composition as the boundary surface was approached.

It has already been noted (Chapter 6) that fluids with homogenisation properties indicating that they are near the critical point at 400°C are characteristic of a set of quartz-pyrite veins and (Chapter 8) that these veins may be parts of outer haloes to phase A and phase B mineralisation. The pressure at the edge, in this case, is about 300 bars according to inclusions which homogenise at the critical point. It will now be supposed that these fluids were, in fact, on the boundary surfaces of the respective two-phase regions. Using phase data for the $NaCl-H_2O$ system (Sourirajan & Kennedy, 1962), here shown as fig. 9-1, the evolution of composition of the two fluids across a horizontal section of the two-phase region will be examined for the case with a boundary pressure of 300 bars.

The critical boundary is represented by point A on the 300 bar isobar. In the two-phase region adjacent to the boundary, the fluid evolution in a horizontal section will be isobaric, the compositions diverging from A towards B and B'. These fluids are unsaturated in NaCl.

At B and B', the liquid and vapour become saturated in NaCl. This happens at a temperature near 475°C. If the temperature is raised still further (on moving still further into the two-phase region), the isobaric evolution of coexisting vapour and liquid is no longer possible under equilibrium conditions. Several paths are possible, differing in the temperature at which the fluids depart from the saturation curves.

Any path which follows the saturation curves to temperatures over 600°C is not possible because of the maximum in the vapour pressure of saturated NaCl-H_2O at 600°C (Keevil, 1942). A boiling, saturated liquid moving away from a hot source would have to increase its vapour pressure as its temperature fell towards 600°C. This, in fact, would not occur; while the salt-rich liquid would still move outwards, in liquids above 600°C, the pressure would increase to the value of the maximum vapour pressure and the liquids would cease to boil. They would therefore be unable to cool. Toulmin & Clark (1967) have shown that expansion and mixing with groundwater are the only significant means of cooling fluid in a large, established hydrothermal system. Mixing with groundwater cannot be feasible at the centre of the system (see below for a discussion of where such mixing occurs); this leaves only expansion, which for a sub-critical, incompressible liquid implies boiling.

Permissible paths may leave the saturation curves if the fluids become unsaturated at temperatures below 600°C - such paths leave the curves at C, C' and D, D' in fig. 9-1. These paths permit two fluids to coexist at pressures and temperatures which decrease monotonically together. They have been drawn to approach lithostatic pressure, 800 bars, as magmatic temperatures are approached. Since only unsaturated fluids can coexist at the magmatic pressure of 800 bars or greater (see fig. 9-1) this will be the ultimate direction of the departure from saturation.

At submagmatic temperatures, however, supersaturation may permit more complex phenomena. Since the vapour pressures of supersaturated NaCl-H_2O liquids are not known, it is difficult to predict anything other than general limits to the behaviour of the fluids. The vapour pressures of supersaturated liquids will certainly be less than those of saturated liquids. Pressures may, as we shall see below, fall below the boundary

pressure, 300 bars. Ostensibly, the possibility of supersaturation makes it possible to circumvent the pressure barrier imposed on saturated liquids, so that a liquid boiled to saturation and then supersaturation at a temperature over 600°C could continue boiling and cooling to lower temperatures. In practice, however, the link (i.e. boiling) between cooling and increase in concentration, combined with any regularities in the vapour pressures of the supersaturated liquids, might severely limit the range of possible paths. A possible indication of the operation of such a constraint will be discussed below.

Comparison of predictions and observation. In Chapters 5 and 6, various homogenisation phenomena of type III inclusions were described. It was found that there were certain regularities: in particular that the threshold of saturation was crossed twice; that $T_h > T_s$NaCl for the highest and lowest temperature salt-rich liquids (i.e. these were unsaturated); and that T_sNaCl < T_h for an intermediate range of fluids. Fig. 9-2 is a selection of histograms taken from earlier figures and typifying these varieties of behaviour. The distribution of the various behaviour types is shown on a map of the deposit in fig. 9-3.

The low-temperature group of unsaturated fluids comprises fluids with T_h up to 460°C and salinity up to 20% eq. NaCl, and also the most dilute of the salt-rich liquids. For the latter, T_h is usually near 400°C. The group of salt-rich liquids with $T_h \simeq T_s$NaCl in the range 400 - 430°C also probably belong to the unsaturated group because of the metastability phenomenon (Chapter 5) which raises T_h during series of heating runs.

The liquids for which T_sNaCl > T_h cover the whole upper salinity range from 430 to 580°C. These have been interpreted as supersaturated liquids (Chapter 5), some supersaturated by several tens of degrees. They occur in the temperature range in which saturation is suggested by

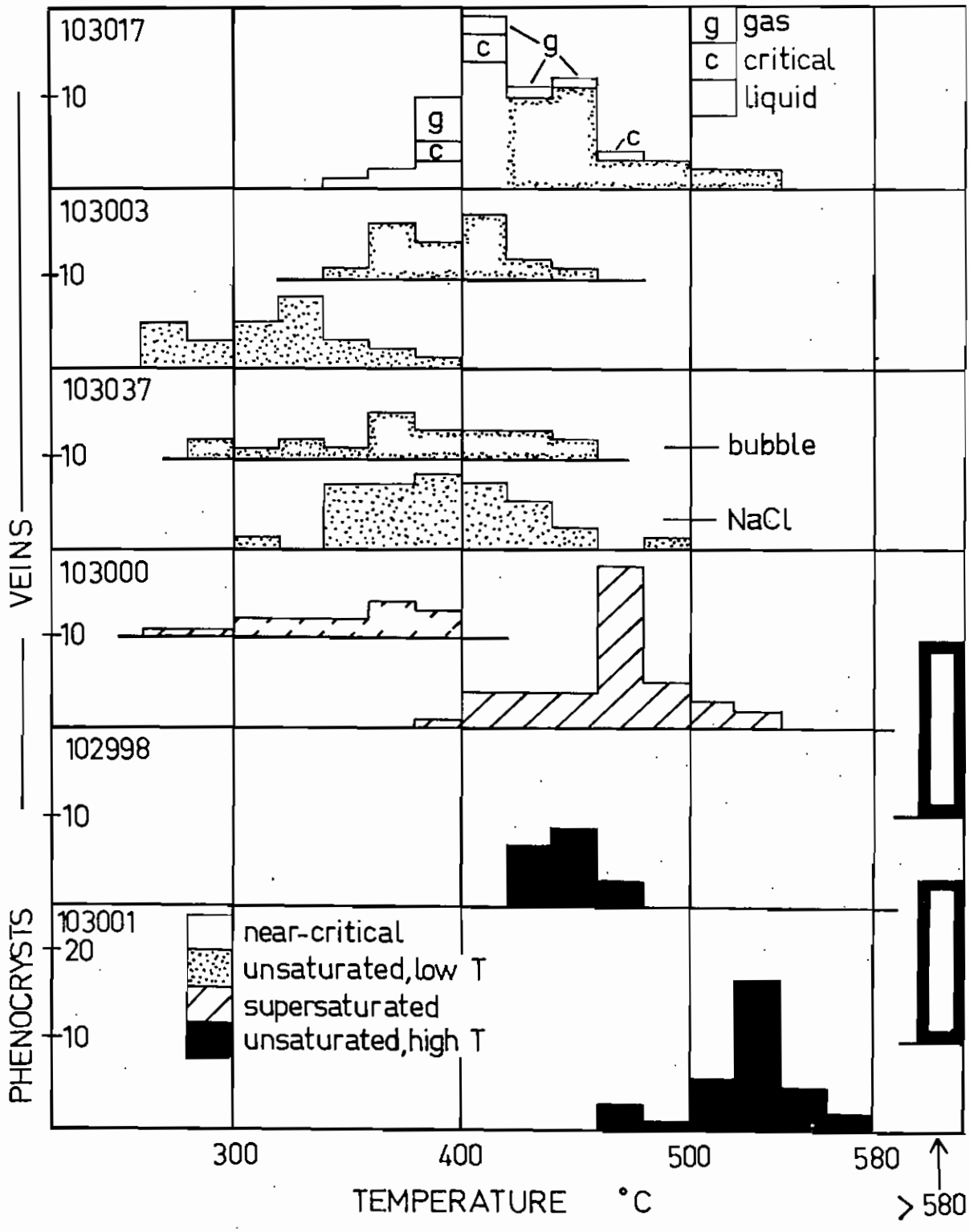

Fig. 9-2 A selection of histograms of fluid inclusion data (from figs. 5-7, 6-2 and 6-6), chosen to illustrate the various types of phase behaviour in salt-water liquids.

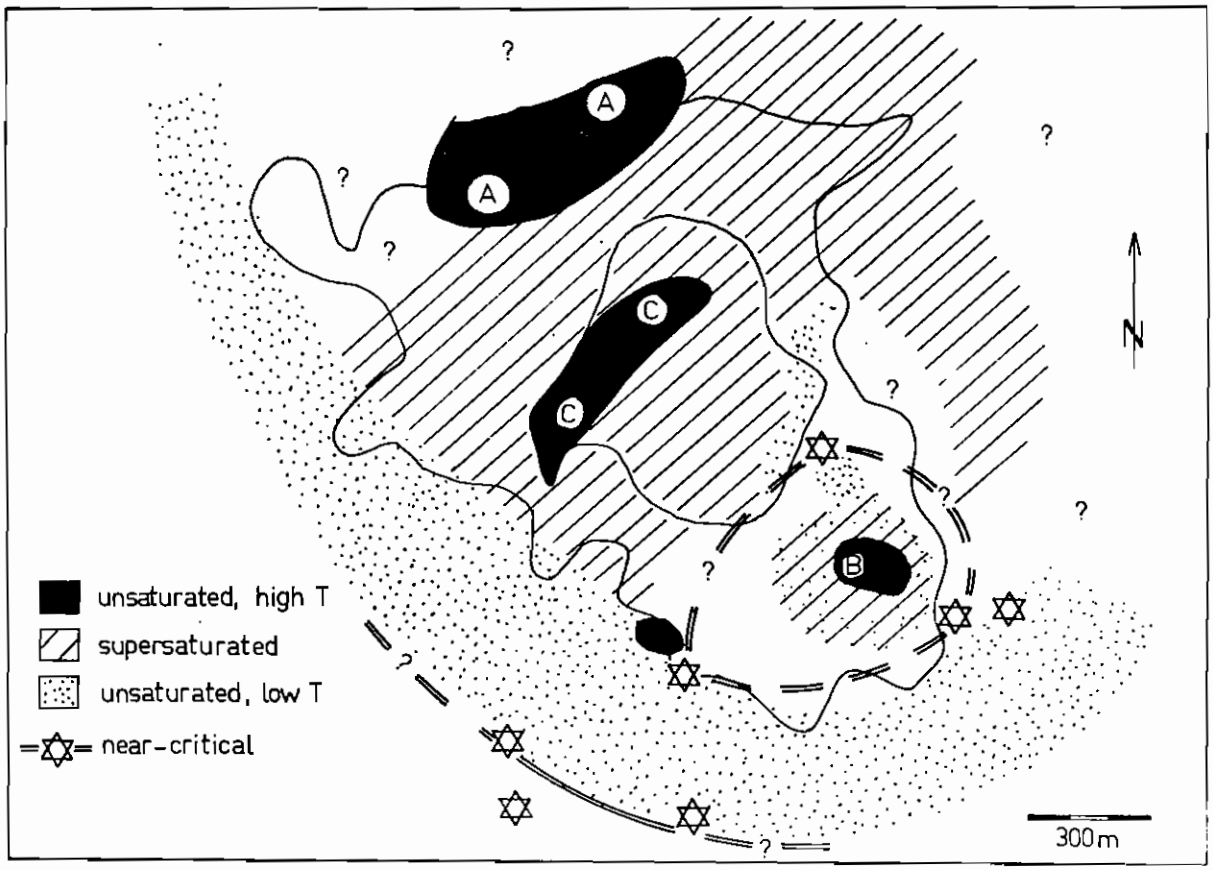

Fig. 9-3 Distribution of the various types of phase-behaviour in salt-water liquids. Letters refer to phases A, B and C of Chapter 8. The outer 0.3% Cu contour is shown as in fig. 2-3, and the minimum extent of phase C as in fig. 8-2.

phase data for NaCl-H_2O. The only alternative explanation of this behaviour would require a different pressure-temperature path for the salt-rich liquids, so that the ones with T_sNaCl > T_h are trapped, then become saturated in halite, then boil (rather than being trapped after becoming saturated and then supersaturated without precipitating NaCl, while boiling). This does not seem consistent with the presence, without exception, of vapour inclusions in veins where type III inclusions behave in this way. The supersaturation hypothesis is thus preferred here.

The precise lower temperature limit of supersaturation is masked by the metastability effect, but is probably a little higher than 430°C where the crossover of homogenisation order occurs. The threshold appears to be the same for all phases of mineralisation. The precise upper limit is also difficult to fix because no specimen pinpointing a high-temperature crossover of T_h and T_sNaCl has been found. The crossover is implied by the presence of unsaturated liquids at temperatures over 580°C. These unsaturated liquids occur in phases A, B and C and are notably abundant in phenocrysts from the Biotite Granodiorite.

In a supersaturated liquid, T_sNaCl must be an upper limit on the temperature of formation. In phases A and B, where the highest T_sNaCl mode is 500°C, there is therefore a temperature gap of at least 80°C unrepresented by fluid inclusions. The salinities and K/Na ratios are, nonetheless, continuous between supersaturated and unsaturated liquids. In phase C, salinities range up to 580°C. The most concentrated liquids (in 103022, 103001) are highly supersaturated, while unsaturated liquids from the same phase have T_sNaCl = 500 - 520°C. This suggests that the higher salinities are the result of concentration by boiling of the liquids of lower salinity. Since saturation must therefore have occurred at a temperature nearer to 500 - 520°C, there is again a temperature gap

unrepresented by fluid inclusions. The lowest of the few T_h measurements done on high-temperature unsaturated liquids is about 600°C in 103031; this may fix the upper end of the temperature gap, at least for that specimen. Within the temperature gap lies the high-temperature crossover point of T_h and T_sNaCl. The high-temperature unsaturated liquids have T_sNaCl in the range 500 ± 30°C, and the supersaturated liquids diverge from this range. This suggests that the saturation point or points occur in the range 500 ± 30°C; there is no ostensible reason to suppose that a single crossover temperature applied to all phases of salt-rich liquid.

Despite the uncertainties in the temperature determinations, the observed phase properties of the boiling salt-rich liquids at Panguna closely match what was predicted from the NaCl-H_2O phase digram. The sequence of homogenisation behaviour fits well, given the added complication of metastable supersaturation, and the ranges predicted for the upper and lower saturation points are quite reasonable. It must be remembered that the comparison of the experimental work of Sourirajan & Kennedy (1962) with the observations at Panguna rested on the assumption that the critical fluids of the QP association composed external haloes to the two-fluid-phase regions in which the deposit formed. This led to the pressure estimate at the edge. The match so obtained between experiment and nature strongly suggests that the assumption is valid.

The hydrothermal system at Sar Cheshmeh. The only previous set of results with which this model can be compared are those of Etminan (1977) from Sar Cheshmeh (see Chapter 1). Etminan found boiling liquids of lower salinity (unsaturated at room temperature) around the zone of salt-rich liquid corresponding to the main phase of mineralisation. He did not, however, report the presence of a critical-point boundary, and he did not give a map of the salinity distribution within the zone of salt-rich liquid. Both homogenisation orders are reported: $T_h > T_s$NaCl is

characteristic of fluids found in the intrusive breccia and a later phase of dykes. Overall, Etminan's report is not sufficiently detailed to show whether the same sort of fluid evolution occurred at Panguna and Sar Cheshmeh, but the data on main-phase fluids suggest that a detailed study could obtain such information.

CONDITIONS IMPOSED BY THE REAL SYSTEM

The presence of KCl. An assumption, tacit until now, has been that the NaCl-H_2O system is an adequate physical approximation of the porphyry copper fluid system. The real salt-rich liquid contains about 15% KCl. The close correspondence of real and predicted fluid behaviour described in the previous section suggests that this assumption, too, is valid, in any case from the point of view of temperatures. Vapour pressures are much reduced relative to the NaCl-H_2O system when KCl is added (Ravich & Borovaya, 1949). According to those data (fig. 7-1 of this thesis) the vapour pressures of boiling NaCl-KCl-H_2O liquids saturated in NaCl could not exceed 300, perhaps 250 bars. Within the zone of supersaturation, then, there was probably a zone of pressure lower than hydrostatic pressure outside the deposit (270 - 280 bars , the critical point estimates), unless other volatiles exerted sufficient partial pressures, possibly 10% of the total pressure, over the salt-rich liquids. It is known that there was very little CO_2 in the fluids; other possibilities will be considered in Chapter 10.

The temperature at the maximum vapour pressure of saturated salt-rich liquids varies between 600°C (NaCl-H_2O) and about 500°C (the mixture with KCl:NaCl of about 3:2 by weight). Other mixtures have intermediate values (Ravich & Borovaya, 1949). The position of the maximum vapour pressure is difficult to judge accurately, even where Ravich & Borovaya have drawn

curves (see fig. 7-1); it is necessary to extrapolate for Panguna liquids so that at best the temperature can only be estimated at 550 ± 50°C. It has been explained above that this would be a maximum limit for T_sNaCl if saturated liquids only were involved. At Panguna, supersaturated liquids were present, some of them concentrated by boiling, yet T_sNaCl does not exceed 580°C. The correspondence between the observed maximum value of T_sNaCl and the temperature of the maximum vapour pressure may be fortuitous, or it may indicate that they are related for supersaturated liquids just as they would be for saturated liquids.

The role of groundwater. In theory, it would be possible to modify the compositions of two coexisting fluids along the paths in fig. 9-1 while maintaining a constant bulk composition. In natural situations, the great density contrast between the two fluids will bring about their separation in an open, fractured medium. Volatiles, mainly water, will be removed, driving the denser fluid towards saturation and supersaturation in NaCl as has been described. The observed return to unsaturation at lower temperatures cannot, therefore, be brought about without a diluent from outside the ore-zone, in this case groundwater.

The change from salt-rich liquid (giving inclusions saturated in NaCl at room temperature) to groundwater (giving unsaturated inclusions) occurs in the range AB of fig. 9-1. Here, there is a large change in liquid salinity for a relatively small change in temperature. The change should therefore be confined to a narrow zone. Any smoothing of the transition will take place by the outward diffusion of salts or the inward diffusion of water. This should not broaden the boundary zone significantly; Turner *et al.* (1970) have shown experimentally that two convecting liquids with a large density contrast will remain physically separate across a sharp interface essentially unaffected by diffusion even when horizontal. So most of the lateral salinity change due to mixing

with groundwater will occur in a relatively narrow zone, such as has been observed in phase A at Panguna. By implication, most of the motion in the liquids must be vertical.

THE RELATIONSHIP OF FLUID DISTRIBUTION WITH METAL AND ALTERATION ZONING

The association of potassium silicate alteration with salt-rich liquid, and of groundwater with propylitic alteration, is well-established at Panguna. Few other absolutely consistent relationships are apparent, comparing fig. 2-4 and fig. 9-3, but this is doubtless due to the complexity of superposition in much of the deposit. Southwest of the deposit, there appears to have been no superposition of salt-rich liquids after phase A. There, the critical-point boundary thought to belong to phase A corresponds with a segment of the phase A pyritic halo (see fig. 2-4). It also corresponds with the appearance of chabazite in veins (fig. 3-13). Fountain (1972) shows wallrock biotite alteration continuing out to this halo. The boundary of supersaturated salt-rich liquid (essentially the same as the boundary of all salt-rich liquid) corresponds with the southwestern part of the outer 0.3% Cu contour, and a decline in the density of quartz veining (fig. 3-1). Between these two boundaries, this study has shown that propylitic alteration appears, either pervasively (103035) or as a thin inner selvage (103025, 103026). The same relationship between fluids and copper grades has not been observed to the north and east of the area affected by phase A. This is because the margin of the orebody was hot to the north, but the reason is not evident in the case of the eastern side. Probably, the fluid boundary was not located because the area concerned could not be sampled. Three of the four sphalerite occurrences with chalcopyrite (fig. 3-7) are in the low-temperature, unsaturated zone of fig. 9-3. This suggests that groundwater may have been the source of the zinc. Consistent with that

suggestion, Ford (1976) reported a halo of Pb-Zn trace enrichment in the propylitic zone southwest of the deposit. There may also be a vague enrichment of trace Cu in the same halo. Low salinity waters at temperatures near 300°C deposited veins bearing sphalerite, tennantite and galena within the ore zone and outside it. Again, in 103017, pyrite probably associated with QP association fluids occurs with minor marcasite, chalcopyrite, sphalerite and very minor tennantite. Given the low salinities of some of the salt-rich liquids in 102594, a groundwater origin could be possible for the unusual metals - As, Pb, Zn, Sn, Co and Ni - found with the bornite in that specimen.

Thus there are indications that groundwater could have contributed to the accumulation of metals (including Cu) in the Panguna deposit. The influence of groundwater, however, was confined to the zones of dilution of salt-rich liquid - relatively narrow in phase A. This, and the presence of Cu,Fe sulphide with salt-rich liquid in quartz phenocrysts, indicates that most of the copper, in phase A at least, was of magmatic origin. For the later phases, new and remobilised copper cannot be distinguished. In phase B, for instance, groundwater may have deposited, or re-deposited, Cu, Fe and Mo as the discontinuous sulphide veinlets which seem to compose a halo to the Leucocratic Quartz Diorite, largely beyond the halo of thin pyrite veins (fig. 3-15). The centres of phases B and C certainly correspond with the highest grades in the deposit (as shown by Baumer & Fraser, 1975); this implies that the intensification of mineralisation in later phases, either by the introduction of new material or by the reworking of old, was significant in raising copper grades.

TEMPERATURES AND PRESSURES IN THE TWO-PHASE REGION

Temperatures. There was a single source of heat - the magma that supplied the salt-rich liquid - during each phase of copper mineralisation. Therefore fluid temperatures should decline away from the hot centre, probably in steps governed by the distribution of the various zones of fluid. No outward increases in temperature would be expected. The temperature at the critical-point boundary was about 400°C. This calls into question the T_h data for certain veins thought to have formed from supersaturated salt-rich liquid, namely those with $T_h < T_s$NaCl and $T_h < 400^{\circ}$C. It appears that T_h gives too low an estimate of the formation temperature in these cases, possibly because of the metastability effect discussed in Chapter 5. The temperatures of these supersaturated liquids are bracketed by 400°C and by T_sNaCl which is generally 500°C or less.

Pressures. At the critical-point boundary, the pressure was 270 - 290 bars, assumed to be the hydrostatic pressure of groundwater surrounding the two-phase region. At magmatic temperatures inside the two-phase region, and possibly at a point below the level of the ore-zone, fluids were under lithostatic pressure (>800 bars). Between the two pressure regimes, the pressure need not have decreased monotonically. It has already been suggested that the vapour pressures of superstaurated salt-rich liquids were less than the pressure at the critical-point boundary. Fig. 9-4 shows the pressure variation across a horizontal section of the deposit as a function of temperature, and relative to the vapour pressure curve of a saturated salt-rich liquid approximating the Panguna liquids in composition (the curve is from Ravich & Borovaya, 1949). The letters A, B and C correspond with the lettering of fig. 9-1. Point C has been put at 500°C; as explained above, this is thought to have

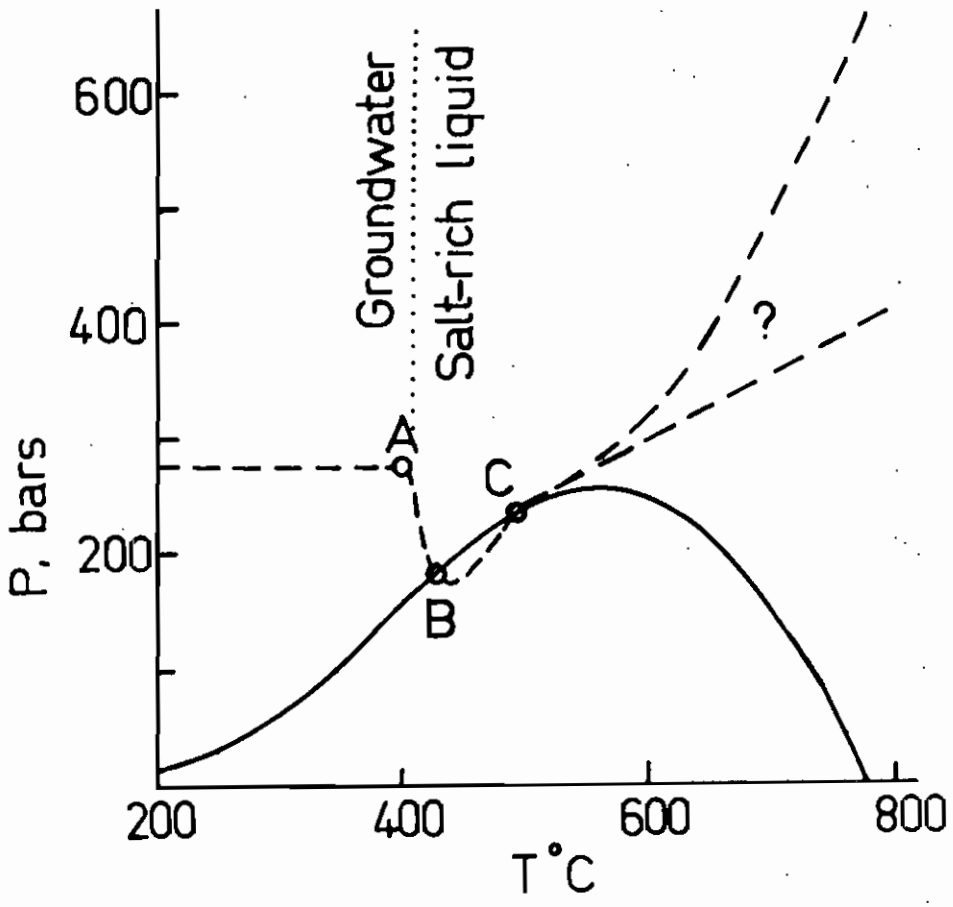

Fig. 9-4 Variation of vapour pressures (dashed line) in the two-phase region as a function of temperature, and relative to the vapour pressure curve (solid line) of a saturated salt-rich liquid (after Ravich & Borovaya, 1949). The lettering corresponds with that used in fig. 9-1.

been the higher temperature of saturation in NaCl. At temperatures over 500°C, pressure and temperature probably increased together, but exactly how is not known. Because of the relationship between temperature and distance from the heat-source (previous paragraph) the abscissa corresponds in a non-proportional way with the distance from the hot centre.

The pressure regime described so far would occur in the two-phase region once it had reached a steady state. None of the evidence from fluid inclusions relates to the conditions during the establishment of such a system, in particular to the phenomena leading to the formation of the fracture-systems that control copper mineralisation. Higher fluid pressures (over 800 bars at the level being considered) would be required. The emplacement of the stocks was probably accompanied by the explosive release of volatiles, a phenomenon quite distinct from, but perhaps the precursor of, those fluid phenomena accompanying copper mineralisation.

K/Na RATIOS IN THE SALT-RICH LIQUIDS

Any adequate model for the fluid interaction at Panguna must be able to account for the linear increase in K/Na ratios with decreasing salinity (see fig. 5-12). From the discussions above, it emerges that the K/Na phenomenon and salinity are not related to temperature monotonically, even though low salinities and high K/Na generally correspond with lower temperatures. Therefore a satisfactory explanation must deal primarily with the salinity dependence of K/Na, and the constancy of the KCl concentration over the whole range of salinity. Five processes may be relevant.

(i) K/Na fractionation during boiling. Lagache & Weisbrod (1977) have predicted that K/Na (gas) will be less than K/Na (liquid) in systems buffered by two alkali feldspars, e.g. at 400 bars and 500°C,

K/Na (gas) = 0.69 K/Na (liquid). Even without the feldspar constraint, boiling should enrich the residual liquid in K relative to Na, and should also increase the KCl content and the total salinity if it occurs to a significant extent. Thus it cannot explain the low K/Na ratios of the supersaturated liquids with T_sNaCl > 550°C. Supersaturated liquids at lower T_sNaCl should also have K/Na increased by boiling, yet their K/Na ratios do not differ from the ratios of unsaturated liquids of similar salinity.

(ii) The precipitation of halite. Solid inclusions which might be halite have been seen in vein quartz (Chapter 4), but these did not give a positive reaction to a test for NaCl. In any case, the precipitation of halite could not explain the change in K/Na over the whole range, specifically for all unsaturated liquids. Nor could it account for the low K/Na ratios in liquids supersaturated to T_sNaCl > 550°C by boiling.

(iii) K/Na fractionation due to differential diffusion. Turner *et al.* (1970) have shown that at low temperatures, K ions have a slightly higher flux per unit concentration gradient than Na ions at an interface separating two fluids of different density. At higher temperatures, the difference in flux per unit gradient would be expected to diminish. Therefore differential diffusion will reduce the K/Na ratio of salt-rich liquid near the boundary, but perhaps imperceptibly at high temperatures. This mechanism cannot affect liquids away from the boundary with groundwater.

(iv) Mixing of two liquids. The dilution of salt-rich liquid, particularly along the boundary with groundwater, appears to generate much of the observed variation in salinity. The linear trend of salt-rich liquid compositions in fig. 5-12 strongly suggests that they can all be derived by mixing two end-member liquids. One end-member is the

salt-rich liquid derived from the magma. The evolution of several phases of salt-rich liquid from closely-related magmas might reasonably be expected to yield just one such isochemical end-member. The other must be derived from around the ore-zone, and must have about 15% KCl and up to 30% NaCl (the most dilute salt-rich liquids on the linear trend have a total salinity of 45%). It must be generated by a mechanism than can be repeated for each phase of mineralisation.

Groundwater at the critical point boundary has 2 - 3% eq. NaCl; similar or more saline waters are found in veins outside the mine area. The groundwater is boiled between the critical point boundary and the boundary where salt-rich liquid becomes predominant, according to the fluid evolution model proposed so far. Some of the QP association fluids have salinities near 20% eq. NaCl. It seems likely, then, that groundwater was being concentrated by boiling in a zone enveloping the ore-zone, eventually yielding salt-rich liquid. Since the groundwater was in equilibrium with propylitic alteration assemblages (in which Na is fixed in albite, but little or no K is fixed) for some distance around the deposit in each phase of mineralisation, it could have been relatively rich in potassium. The lack of a suitable buffering reaction argues against chemical control; besides, the groundwater immediately adjacent to phase B and C salt-rich liquids must have been altering phase A potassic assemblages to some extent, a chemical environment quite different from that experienced by phase A groundwaters. A reproducible control might have to be physical rather than chemical. Turner *et al.* (1970) state that density difference is capable of keeping two liquids separate across a sharp boundary, so that similarity in density is a requirement for effective mixing. It may be that the inferred groundwater-derived end-member composition has a density at which mixing with the magmatic salt-rich liquid becomes rapid enough to dominate composition

change due to boiling, alteration and other effects. Condensate salt-rich liquid could not have been the diluent because as explained earlier in the chapter, it would initially have a lower K/Na than the ortho-magmatic salt-rich liquid.

One lower temperature, lower salinity inclusion relatively rich in KCl was found in 103047. It has a K/Na ratio of 0.64 (atomic). It belongs to a group of secondary inclusions which appear to have necked down, and which now give heterogeneous data (T_sNaCl = 294 - 363°C, 6 readings; T_h = 298 - 331°C, 4 readings). Thus the high K/Na ratio may be spurious. The fluid also contains too much KCl to be a sample of the diluent.

The mixing mechanism cannot account for the concordance of K/Na values from the highly supersaturated liquids with the general trend. A close examination of the graph of T_sKCl vs. T_sNaCl (fig. 5-10) reveals that there may indeed be a slightly different trend for T_sNaCl > 500 - 520°C. The difference is not perceptible in the triangular diagram (fig. 5-12) for the small salinity range involved.

(v) Rock-fluid interaction. Various studies, e.g. Orville (1963), Ryabchikov (1975) and Lagache & Weisbrod (1977) have examined the relationship between the K/Na ratio of salt-water fluids in equilibrium with alkali feldspars or with calc-alkaline assemblages and temperature, pressure and salinity. All have shown a temperature dependence; K/Na decreases with falling temperature. In addition, Lagache & Weisbrod have shown that there is a pressure dependence based on the unmixing of gas and liquid at lower pressures, but that there is neither a salinity nor a pressure dependence for the liquid phase K/Na. This already suggests that the K/Na variation at Panguna is not primarily a chemical phenomenon. There is no strict temperature dependence of K/Na; rather, liquids with similar salinities, but different temperatures have similar K/Na ratios.

The KCl content, if buffered by some chemical reaction, should not remain constant (as it in fact does) over the whole temperature range.

The decrease in K/Na with decreasing temperature in feldspar-buffered systems is the opposite of what happens in general (if not absolutely strictly) at Panguna. There is no reason why the K/Na ratios at Panguna should be subject to that constraint, for the liquid was apparently not in equilibrium with two feldspars at any stage. In the magma, there are plagioclase phenocrysts, but no alkali feldspar phenocrysts. In the ore-zone, plagioclase is destroyed and alkali feldspar is formed beside quartz-Cu,Fe sulphide veins. Optical investigation of the selvage feldspars of veins near the groundwater to salt-rich liquid boundary revealed plentiful albite. Microprobe investigation revealed a potassic feldspar as well, but the relationship of the two feldspars is not clear. Certainly, the K/Na ratios for these veins are quite inconsistent with the published data for feldspar-buffered systems near 400°C.

An exchange of alkalis between wallrock and liquid must nonetheless have occurred. The effect must have been subordinate to, and opposite to, that of mixing on the alkali composition of the liquid. The veins in which liquids are thought to have been supersaturated to T_sNaCl $\geq$ 550°C by boiling and in isolation from mixing effects have well-developed inner selvages of sanidine. The formation of this sanidine would deplete the liquid in K and enrich it in Na, decreasing the K/Na ratio as observed.

Summary, implications and comparison with other deposits. Given a magmatic supply of salt-rich liquid with T_sNaCl = 500 ± 30°C and characteristic K/Na, no single mechanism is able to explain the K/Na variation of liquids evolving to both higher and lower salinities. In the direction of lower salinity, mixing with another salt-rich liquid seems best able to account for observations, if a reproducible salt-rich liquid can be generated around the ore-zone. Where mixing does not occur, i.e.

in the direction of higher salinity, alkali exchange with the wallrock would explain the trend. The boiling of groundwater has been suggested as a source for the non-magmatic salt-rich liquid, and this is quite possible according to the physical model explained earlier.

It is interesting to examine K/Na data from other deposits. Those few gleaned from recent publications (Roedder, 1971; Moore & Nash, 1974; Etminan, 1978) and a personal communication (Wilkins, 1978, for the Ok Tedi deposit) have been plotted as T_sKCl vs. T_sNaCl with the Panguna trend for comparison in fig. 9-5. As a group, Sar Cheshmeh, Frieda and Ok Tedi overlap the Panguna trend for $300^{\circ}C < T_s NaCl < 500^{\circ}C$; individual deposits, however, cover only parts of that range. For these, a mixing process like that at Panguna is plausible. The only real departure from the Panguna trend seems to be in the case of Bingham, and even this is not a large departure. On the other hand, Cloke *et al.* (in press) reported that salt-rich liquids from the Granisle and Bell porphyry copper deposits, British Columbia and from a Pb-Zn skarn at Naica, Mexico, plot along lines indicating evolution of composition by precipitation of halite. The physics of such systems must be quite different from what has been inferred at Panguna. There may thus be two - or more - distinct physical types of hydrothermal system responsible for porphyry copper formation, these reflecting differences in the physical situations, e.g. availability of groundwater.

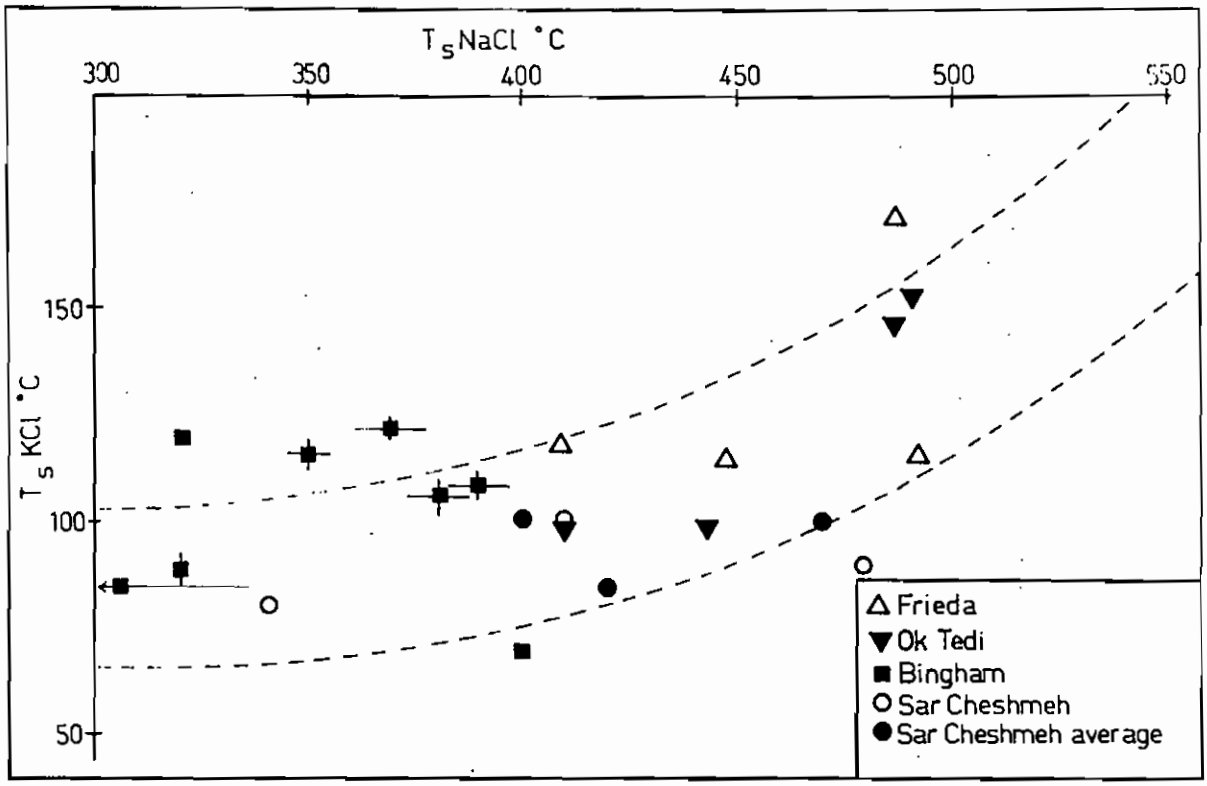

Fig. 9-5 T_SKCl vs. T_SNaCl for other porphyry copper deposits. The dashed lines give the trend of Panguna data (see fig. 5-10). Data sources: Frieda (this study, see appendix); Ok Tedi (Wilkins, pers. comm.; the T_SNaCl data are based on single heating runs); Bingham (Moore & Nash, 1974); Sar Cheshmeh (Etminan, 1977).

ADDING THE VERTICAL DIMENSION

The differences in density of the salt-rich liquids, the vapours and the groundwaters imply that fluid evolution in the vertical dimension will be as important to an understanding of porphyry copper formation as the changes that occur across a horizontal section. The vertical extent of sampling at Panguna was insufficient to give any indication of what happens above and below the essentially-horizontal section of the mine as it was in 1974. The horizontal section of the fluid system is the only available constraint for the following discussion of changes above and below.

Vertical and horizontal flow. The likelihood of mainly vertical fluid motion has been discussed above. The vapour, with a density of 0.3 g/cm^3 or less, would rise vertically on both sides of the boundary between salt-rich liquid and groundwater. Salt-rich liquid (1.2 - 1.5 g/cm^3) would sink relative to groundwater (0.8 - 0.9 g/cm^3, Potter & Brown, 1977), while groundwater adjacent to the ore-zone would be buoyant relative to both salt-rich liquid and surrounding, cooler groundwater. All groundwater adjacent to the two-phase region of the porphyry copper system was probably moving towards (from below), and upwards beside, the two-phase region in a convecting flow regime extending through a volume of rock much greater (both vertically and horizontally) than that of the eventual ore-deposit (see fig. 9-6). The mixing of groundwater and salt-rich liquid was a second-order effect superimposed on the vertical movements.

The sinking of the salt-rich liquid might be expected to carry copper mineralisation to some depth around the source intrusion. James (1971) has described deep mineralisation at Bingham as ragged skirts draped around the central pluton at depth and joining as a hood through the top of the pluton (not over it). This means that the top of the

pluton was already solid, and that the magmatic fluids were being derived at depth. At Panguna, phase A mineralisation about the Kaverong Quartz Diorite seems to have had a hot, relatively barren "centre" in the unbiotitised part of the intrusion. The biotitised part (the Biotite Diorite) was certainly solid, but at temperatures over 700°C during mineralisation. So phase A mineralisation could be a portion of an asymmetric shell to the Kaverong Quartz Diorite, or may be part of a hood passing into the intrusion. The asymmetry of the fluid distribution makes the distinction difficult. In the case of phase B, the mineralisation is a hood passing through the top of the Leucocratic Quartz Diorite, which seems too small to have provided fluid without tapping magma at depth. Part of the veining occurred before the stock had solidified and part after; veins of an early set become increasingly indistinguishable from wallrock with distance from the contact towards the centre of the stock, while a later set cuts across the whole stock. Phase C mineralisation took place in solid rocks, and bears no obvious relationship to an intrusion. In phases B and C and possibly A there has been a transfer of salt-rich liquid vertically upwards through solid rock. Despite the density of salt-rich liquid, this will occur for the following reasons:

(i) the buoyancy of salt-rich liquid, vapour or a single-phase aqueous fluid (whichever is appropriate to the pressure regime at depth) relative to silicate liquid (density > 2 g/cm^3) will favour the accumulation of all non-silicate fluids at the highest still-liquid part of the magma. Also, it may only be in the highest parts of the magma chamber that the temperature and pressure conditions are suitable for the exsolution of non-silicate fluids.

(ii) Once a stock has penetrated and fractured the country rock permeated elsewhere at the same level by groundwater, and has itself partly

solidified and become fractured, it will become a conduit for non-silicate fluids from below. Even the dense salt-rich liquid will be pumped up the stock by the difference between hydrostatic pressure at the top and lithostatic pressure (plus any tectonic overpressure) in the magma where the exsolved fluids are accumulating. Each hundred bars of pressure difference could support a column of about 770 m of liquid of density 1.3 g/cm^3. At Panguna the difference was greater than 500 bars.

At some level in the stock, and not in general at the top (James, 1971), the salt-rich liquid ceases to rise and moves horizontally into the country rock before turning down. The reasons for this are not completely clear, but it could be connected with a sudden change of pressure regime. A column of salt-rich liquid could not be supported because of its density in rock permeated elsewhere by groundwater. Therefore the salt-rich liquid would spread horizontally at the change in regime from lithostatic to hydrostatic. The change appears to occur near the top of the intrusion. At this level, the cooling of magmatic vapour would also be important, and large quantities of salt-rich condensate would be generated. This liquid would either descend and then spread horizontally at its confluence with orthomagmatic salt-rich liquid, or be entrained in convecting groundwater.

The top of the system. James (1971) suggested that copper mineralisation also occurred in a stockwork immediately above the zone of lateral spreading of salt-rich liquid. Higher in the system, according to Sillitoe (1973), pyrite or marcasite, gypsum and sulphur would be deposited, and fumaroles might be the surface expression of the system. Observations on the ore-zone at Panguna suggest that the convection of groundwater heated by the intrusion and the rising of vapour into a plume over the ore-zone and the intrusion are the fluid phenomena which dominate the top of the system. The interaction of groundwater and vapour would

depend on the size of the system and on fluid velocities. For example, rapidly-rising vapour might entrain groundwater and as a result be cooled and condensed before rising very far above the ore-zone. The mixed fluid would be very reactive as a result of inheriting HCl, SO_2 or other volatiles from the vapour. The presence of fumaroles at the surface would not require the persistence of vapour from the deposit to the surface. In some of Cathles' (1977) calculated models, groundwater boils in a discrete two-phase region within 1 km of the surface.

There would be no salt rich condensate in the plume at temperatures lower than the solubility minimum of NaCl in the vapour (450 - 475°C at 250 - 300 bars; Sourirajan & Kennedy, 1962). It is possible, however, that salt-rich liquid could be generated higher in the system by the boiling of groundwater (as at the level of the ore-zone).

The type of critical-point boundary proposed at Panguna has a lower limiting pressure of 221 bars (P_cH_2O). In fact, the limit might be higher because groundwater is seldom free of dissolved salts. In a hydrostatic pressure regime, a pressure of 221 bars corresponds with a depth of about 2.4 km. The critical-point boundary could thus persist at most 600 m above the section examined. It need not have closed over the ore-zone because the upward transport of vapour may dominate other fluid phenomena in the centre of the system at these levels.

The system below the exposed ore-zone. The sinking of salt-rich liquid from the ore-zone has already been discussed. Salt-rich liquids were boiling in all parts of the exposed ore-zone, and in order for boiling to continue at depth in a salt-rich liquid of constant salinity, the local geothermal gradient would have to exceed about 25°C/100 bars (rough estimate from Sourirajan & Kennedy, 1962, fig. 19). Increases in salinity due to boiling would necessitate larger gradients. In an area subject to magmatic activity, abnormally large geothermal gradients are

to be expected, and thus it is likely that boiling could continue below the ore-zone. It also seems probable that the sinking salt-rich liquid would eventually be recycled in a convecting cell.

Other fluid phenomena at depth would depend on whether groundwater persists below the exposed ore-zone. In the initial discussion of the horizontal spreading of the salt-rich liquid, it was suggested that such spreading might occur at the boundary between hydrostatic and lithostatic pressure regimes, i.e. at the lower limit of groundwater. If, however, groundwater did continue below the section studied, the interaction with salt-rich liquid would take on a different character. The critical-point boundary would move to higher temperatures and salinities with increasing depth and pressure - e.g. at 400 bars it would be at 440°C and 6% eq. NaCl and at 500 bars, 475°C and 9% eq. NaCl. Groundwater would be subject to convection over a vertical distance of several km, and any regular increase in groundwater salinity with depth is therefore unlikely. Rather, the higher salinities at the critical-point boundary would be due to mixing with salt-rich liquid, i.e. the critical-point boundary, or the onset of boiling, would occur within the zone of mixing. It appears, then, that no groundwater salt would be involved in the interaction of groundwater and salt-rich liquid, and this would lead to a different K/Na variation in the salt-rich liquids.

Summary. The fluid phenomena which have been deduced for the Panguna deposit could occur only within a narrow range of pressures and corresponding depths, although the entire hydrothermal system extended over a larger vertical range. This qualitative examination suggests that the change of pressure regime from lithostatic to hydrostatic was important in determining the level at which mineralisation took place.

COMPARISON OF PANGUNA WITH PREVIOUSLY-SUGGESTED FLUID MODELS

In Chapter 1, current ideas on the fluid-intrusion interactions responsible for porphyry copper formation were reviewed. These can now be evaluated against the proposed hydrothermal system at Panguna.

An orthomagmatic model, by which salt-rich liquid and vapour are exsolved by a cooling, crystallising magma, is certainly consistent with part of the observation at Panguna. An additional source of salt-rich liquid is required and the physics of the system suggest that it is groundwater concentrated by boiling. The boiling of groundwater under other circumstances has also been suggested (Chapter 8) as an explanation of the pebble dykes. So despite their relative disfavour to date, boiling groundwater models seem to account for important features of the Panguna deposit. The mechanism of condensing a salt-rich liquid from magmatic vapour should also operate, but it does not contribute to the mineralisation in the way that Henley & McNabb (1978) have proposed. Lastly, the simple convection of groundwater cools the deposit once the source of magmatic salt-rich liquid wanes. None of the mechanisms, then, can be ruled out as irrelevant to the formation and evolution of the Panguna deposit.

Fig. 9-6 is a summary of the ideas discussed so far in the form of a hypothetical vertical section through a porphyry copper system.

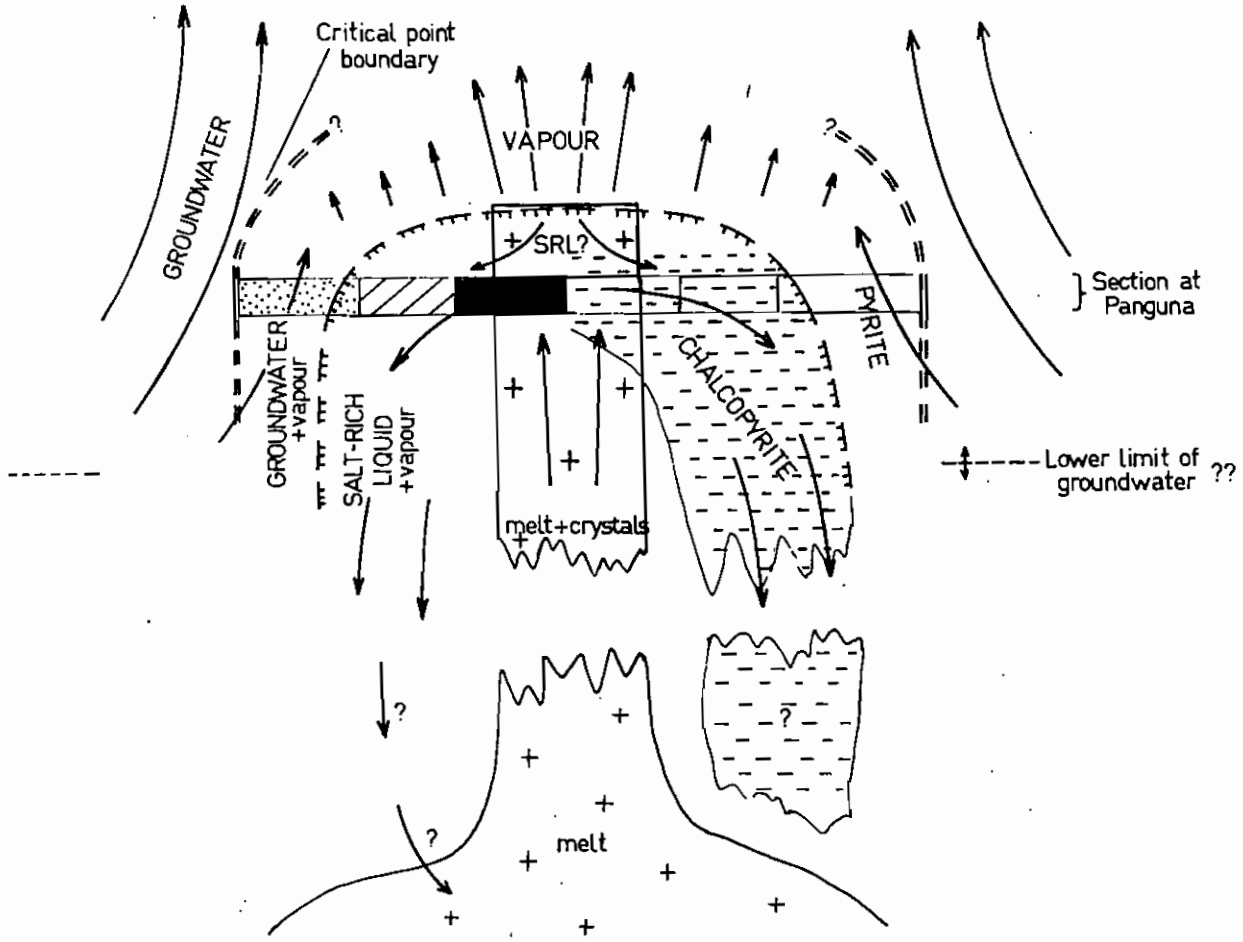

Fig. 9-6 Diagrammatic vertical section of a porphyry copper deposit associated with a stock (+ pattern) showing fluid circulation, phase-behaviour of salt-water liquids (patterns as in fig. 9-4) and estimated pressure and temperature gradients (top). Copper mineralisation is shown as - pattern.

CHAPTER TEN: CHEMICAL CONSIDERATIONS

The variety of mineralisation styles at Panguna presents a multitude of chemical problems. Here, it is intended to examine only phenomena associated with the primary deposition of copper at temperatures over 400°C.

The fluid system consists of salt-rich liquid and vapour at equilibrium, both phases being at equilibrium at a given point with certain crystalline phases. Whereas the liquid cools and evolves in equilibrium with the solids, the vapour is continually removed from the system and can only be considered to be at equilibrium with the solids at its point of origin. The system tends to lose volatiles throughout mineralisation. Neither fluid can be dealt with in terms of aqueous electrolyte chemistry. Because alkali chlorides and water are present in comparable quantities in the liquid, the alkali chlorides cannot be solvated as in more dilute solutions. The alkali chlorides tend to associated in the temperature range being considered (Montoya & Hemley, 1975). They are, in effect, solvents; solute-solvent interactions are just as likely to involve them as to involve water. Solvation of ions does not occur in the vapour either, associated species being the rule.

Since the temperatures involved range from 400°C up to magmatic temperatures, the discussion is inevitably speculative. Thermodynamic data are not available for some substances at these temperatures and are suspect for others, while fugacity and activity coefficients are in many instances unknown. The following conventions and assumptions are adopted:-

1. The standard states of solids and liquids are the pure substances in their most stable form at T and 1 atm pressure, and for gases, the ideal gas at T and 1 atm. This is the convention adopted in the tables of

Robie & Waldbaum (1968) and JANAF (1971). The former have been used here as a source of data for solid phases and the common gases, and the latter for the gaseous metallic oxides and halides unless otherwise stated.

2. Pressures are therefore expressed in atmospheres and temperatures in Kelvin. This is despite the choice of units earlier in this work. It is easier to relate bars and degrees Celsius to the literature on the physical properties of the systems, and atmospheres and Kelvin to the thermodynamic data. Since two significant figure accuracy is probably more than sufficient in the following calculations, the bar and the atmosphere will be considered as equal, and earlier results in bars will be transposed direct into atmospheres.

3. No pressure correction is applied to the equilibrium constant k. In equilibria involving condensed phases, the pressure dependence of the equilibrium constant is expressed

$$\Delta \log k_{P_2-P_1} = -2.303 \frac{\Delta V_s}{RT} (P_2-P_1)$$

where ΔV_s is the change in molar volume of all condensed species in the particular equilibrium. In this case, P_1 is the standard state pressure, 1 atm. In order that the correction be negligible, say $|\Delta \log k| \leq 0.1$,

$$|\Delta V_s| \leq 1.5 \text{ cal/atm at } P_2 = 300 \text{ atm}, \quad T = 700 \text{ K}$$

$$|\Delta V_s| \leq 0.9 \text{ cal/atm at } P_2 = 800 \text{ atm}, \quad T = 1100\text{K}.$$

ΔV_s data are not available for all substances of interest, especially chalcopyrite and bornite but in the following relevant reactions, ΔV_s can be evaluated:-

$3Fe_2O_3 = 2Fe_3O_4 + \frac{1}{2}O_2$ $\quad \Delta V_s = -0.04$ cal/atm

$2FeS_2 + 3/2O_2 = Fe_2O_3 + 2S_2$ $\quad -0.42$

$3FeS_2 + 2O_2 = Fe_3O_4 + 3S_2$ $\quad -0.65$

$ZnS + 2O_2 = ZnSO_4$ $\Delta V_s = -0.42$ cal/atm

$PbS + 2O_2 = PbSO_4$ -0.40

$CaSO_4 + TiO_2 + SiO_2 = CaTiSiO_5 + \frac{1}{2}O_2 + 3/2S_2$ -0.76

It will be assumed that the pressure correction is negligible for all other reactions.

The notation used in this section is tabulated in the Introduction Chapter.

THE BUFFERING OF K/Na IN SALT-RICH LIQUIDS

In Chapter 9, it was suggested that the K/Na ratios of the salt-rich liquids were the product of the mixing of two salt-rich liquids, one derived from the magma and the other from groundwater by boiling. The consistency of the trend over three phases of mineralisation suggests that the alkali ratios in both end members were externally controlled.

The intrusive suite at Panguna is low in potassium. Ford (1976) gave average K_2O contents of 1.72% for the Kaverong Quartz Diorite, and 1.42% for the Biuro Granodiorite, compared with 3.07% for average granodiorite (Taylor, 1969). The Panguna intrusives crystallised phenocrysts of quartz and plagioclase, but not of alkali feldspar. Equilibrium between the salt-rich liquid and the plagioclase, which generally contains less than 0.5% K_2O (Ford, 1976) could result in low K/Na ratios in the liquid. It is possible to do a rough calculation to test this.

Na and K are exchanged between plagioclase and liquid by the following reaction:

$$KAlSi_3O_{8(pl)} + NaCl_{(liq)} = NaAlSi_3O_{8(pl)} + KCl_{(liq)} \quad \ldots 10.1$$

Ryabchikov (1975) gives activity coefficients for the orthoclase component in plagioclase, and the activity of the albite component, but they must

be read from small diagrams and so are not available in very precise form.

Values of $k_{10.1}$, the equilibrium constant, are available for temperatures up to 923 K (Hemley, cited in Brimhall, 1977).

$$k_{10.1} = \frac{X_A \gamma_A}{X_O \gamma_O} \cdot \frac{a_{KCl}}{a_{NaCl}}$$

(subscripts A for albite component, O for orthoclase). The activities of KCl and NaCl are for the salt-rich liquid; to relate these to mole fractions, it will be assumed that the ratio of activity coefficients is 1. Montoya & Hemley (1975) used such an assumption, but for much less concentrated solutions of salts. Thus

$$\frac{a_{KCl}}{a_{NaCl}} = \frac{m_{KCl}}{m_{NaCl}} = k_{10.1} \cdot \frac{a_O}{a_A}$$

The constant $k_{10.1}$ increases as a function of temperature over the range 773 - 923 K, and has a value of 0.44 at 923 K. A rough linear extrapolation based on the three data points indicates a value of about 0.6 at 1073 K.

The mole fractions of albite and orthoclase in plagioclase have been taken from Ford (1976) who analysed cores and rims of phenocrysts from the four main intrusions at Panguna. These are plotted, X_O vs. X_A as mole percentages, in fig. 10-1. Where core and rim analyses are available for the same phenocryst they are joined by a straight line. The ratio a_O/a_A has been contoured on the same axes; this was calculated from Ryabchikov's data for 1073 K.

There is commonly a large change in composition between core and rim in a phenocryst. In those few phenocrysts across which Ford did analytical traverses, most of the change takes place in the rim only,

Fig. 10-1 Compositions of plagioclase phenocrysts in the Panguna intrusive rocks. Mole % $KAlSi_3O_8$ is plotted against mole % $NaAlSi_3O_8$ (data from Ford, 1976). Both core and rim compositions are plotted, and are joined where available for single phenocrysts. The lowest diagram is a contour plot of the ratio a_{or}/a_{ab} at 1073 K (see text for explanation), with the fields of rim compositions for each of the four intrusions (symbols shown beside names in other diagrams) superimposed.

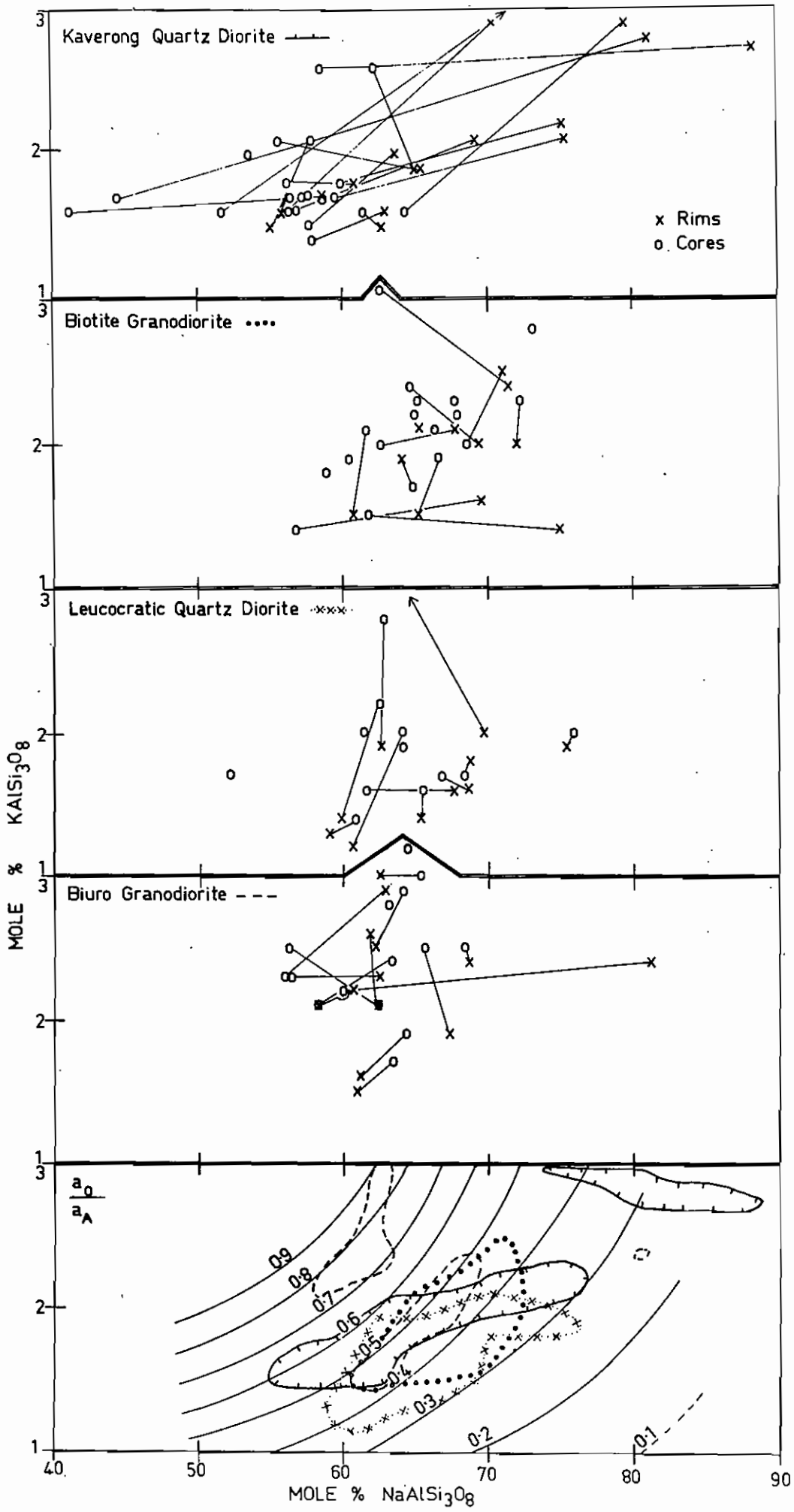
Kaverong Quartz Diorite
x Rims
o Cores
Biotite Granodiorite
Leucocratic Quartz Diorite
Biuro Granodiorite
MOLE % KAlSi3O8
MOLE % NaAlSi3O8
aO/aA
0·9
0·8
0·7
0·6
0·5
0·4
0·3
0·2
0·1
40
50
60
70
80
90
1
2
3

i.e. this zone represents an event which occurred late in the crystallisation of the phenocrysts. Strong albitisation, by as much as 37 mole %, accompanied by an increase in the K content, is characteristic of the Kaverong Quartz Diorite. In the Leucocratic Quartz Diorite, a reduction in K content and relatively little change in Na is typical. Changes intermediate between these types are found in the other intrusions. Comparing the changes with the a_O/a_A curves, it is seen that all major changes in composition are in the direction of increasing a_O/a_A. Other phenocrysts indicate very little change in the ratio, except for two in the Biuro Granodiorite where there is a definite decrease.

The rim event was probably the exsolution of volatiles from the magmas. Later alteration seems unlikely; in the Kaverong Quartz Diorite, where there is considerable variation in the style of subsequent alteration, the rim compositions bear no relationship to Ford's descriptions of the alteration in each specimen. The fields of rim compositions are superimposed on the a_O/a_A contours in fig. 10-1. The fluid composition is obtained thence with the constant $k_{10.1}$. If $k_{10.1}$ at 1073 K is estimated to be 0.6 - 0.7, a fluid with $m_{KCl}/m_{NaCl} \simeq 0.25$ (a likely value for a primary magmatic fluid with $T_s NaCl \simeq 500^oC$) is possible for $a_O/a_A <$ about 0.4. For those, or lower values of $k_{10.1}$ at 1073 K, equilibrium between liquid with the low K/Na values found at Panguna is possible for many of the phenocrysts in the Kaverong Quartz Diorite, the Biotite Granodiorite and the Leucocratic Quartz Diorite, but only for one from the Biuro Granodiorite. For higher K/Na in the primary salt-rich liquid, the upper limit on a_O/a_A is a little higher. The results seem consistent with the field and petrographic interpretation that the Biuro Granodiorite did not exsolve important quantities of mineralising fluids, whereas the others did.

THE FUGACITIES OF OXYGEN AND SULPHUR DURING COPPER MINERALISATION

The mineral assemblages at Panguna include many species useful for fixing the fugacities of oxygen and sulphur. Most of these, however, occur in low-temperature veins, and diagrams like those of Holland (1965) are useful only at temperatures below 800 K. These parameters are vital to an understanding of the processes taking place in the magma at temperatures much higher than 800 K. Other constraints must be invoked if they are to be evaluated.

Oxygen fugacity. Coarsely-bladed, primary hematite in quartz-Cu,Fe sulphide veins, and hematite replacing magnetite in vein selvages have been described in Chapter 3, and by Lawrence & Savage (1975). Hematite as a daughter mineral and as solid inclusions is typical of many of these veins, especially the high-temperature ones, but is also completely absent from other veins. Yet others bear magnetite (Lawrence & Savage, 1975) or have selvages containing unaltered magnetite intergrown with chalcopyrite or bornite. Therefore the oxygen fugacity appears to have remained near the hematite-magnetite (HM) buffer

$$2Fe_3O_4 + \tfrac{1}{2}O_2 = 3Fe_2O_3 \qquad \ldots 10.2$$

(possibly a little higher on average).

The various estimates of the oxygen fugacity at the HM buffer differ among themselves by at least one log unit, indicating the likely limitations of the thermochemical data being used here. The data used for the HM buffer reaction in figs. 10-2 and 10-3 have been taken from Haas & Robie (1973), and other data are from Robie & Waldbaum (1968). The data are consistent with the coexistence of sphalerite and hematite up to and beyond 850 K, but galena will not coexist with hematite above about 780 K. The occurrence of galena, bornite and hematite in 102594 (formed between 700 and 800 K) brackets the oxygen fugacity for that specimen tightly near the HM value.

Chalcopyrite and hematite usually occur together. At first sight, this might fix an upper limit to the oxygen fugacity at temperatures below 820 K where the tetragonal polymorph of $CuFeS_2$ becomes unstable (Yund & Kullerud, 1966). The chalcopyrite-bornite-hematite equilibrium

$$5CuFeS_2 + S_2 = Cu_5FeS_4 + 4FeS_2 \quad \ldots 10.3$$

has been plotted using Barton's unpublished data (Barton & Skinner, in press), and the other boundaries of the chalcopyrite fields in fig. 10-2 are based on this, e.g. the boundary representing

$$5CuFeS_2 + 3O_2 = Cu_5FeS_4 + 2Fe_2O_3 + 3S_2 \quad \ldots 10.4$$

has slope 1 and passes through the point at which hematite, pyrite, chalcopyrite and bornite coexist. The unreliability of the data have already been stressed, however. The apparent convergence of the oxygen fugacities at HM and at the hematite-pyrite-chalcopyrite-bornite point with rising temperature suggests that high $CuFeS_2$ polymorphs and hematite might not be able to coexist at higher temperatures. No watertight conclusions can be drawn from the thermochemical data, which become even less reliable for the Cu,Fe sulphides above 820 K. Certainly, observation at Panguna suggests the opposite; that hematite and $CuFeS_2$ do coexist over the whole temperature range. However, it is not certain that the Cu,Fe sulphides now seen in veins formed above 820 K have retained their original compositions. Chalcopyrite, and less frequently bornite, are present yet the broad range of compositions of the cubic Intermediate Solid Solution, the high-temperature equivalent of chalcopyrite (Yund & Kullerud, 1966) implies that other exsolution products such as talnakhite, mooihoekite and haycockite ought to be present. Etch and microprobe investigations (etch methods from Cabri & Hall, 1972) have failed to reveal any of these; Barton (pers. comm, 1977) has commented that the sulphides may have undergone later additions of sulphur during the long hydrothermal history of Panguna.

Fig. 10-2 Equilibria relevant to Panguna mineralisation, shown on log f_{S_2} vs. log f_{O_2} plots for temperatures of 700, 800 and 850 K. The field of chalcopyrite is stippled. RAQ/S refers to the rutile-anhydrite-quartz-sphene equilibrium (equation 10.6). Standard state pressure of all substances = 1 atm.

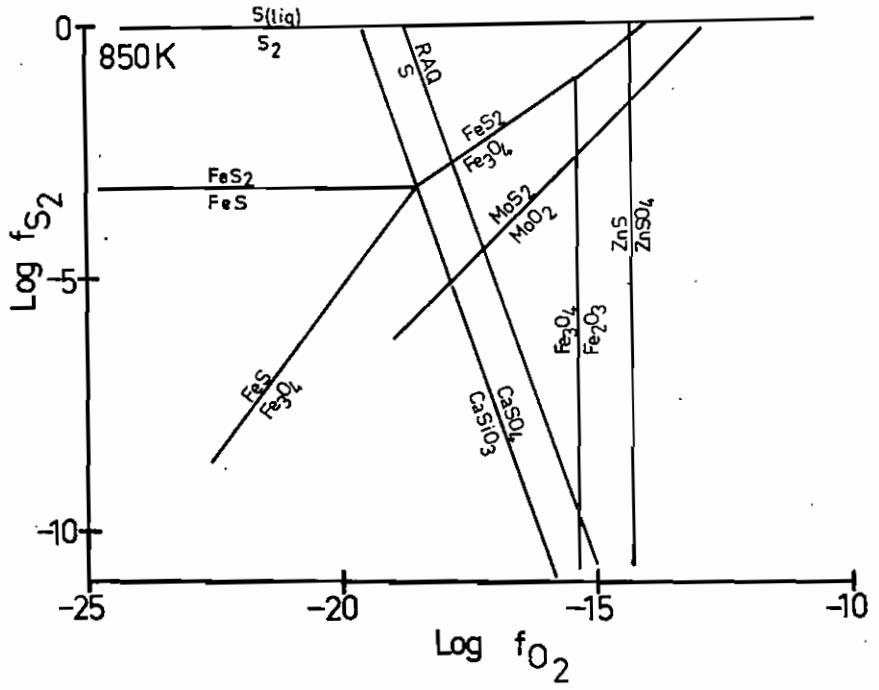
850 K
S(liq)
S2
RAQ
S
FeS2
Fe3O4
FeS2
FeS
MoS2
MoO2
ZnS
ZnSO4
Fe3O4
Fe2O3
FeS
Fe3O4
CaSO4
CaSiO3
0
-5
-10
Log fS2
-25
-20
-15
-10
Log fO2

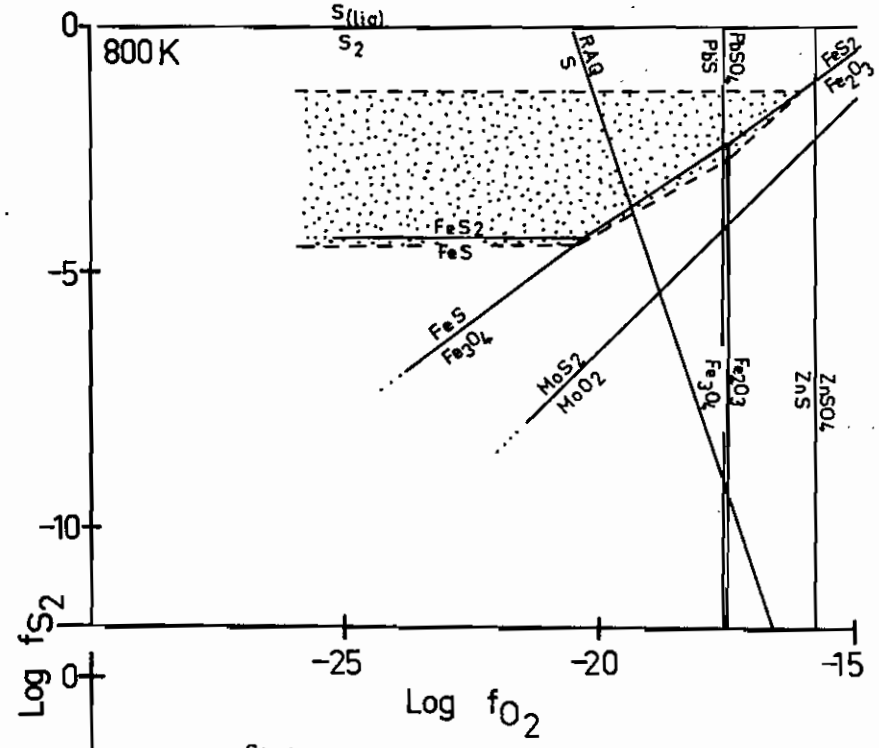
800 K
S(liq)
S2
RAQ
S
PbS
PbSO4
FeS2
Fe2O3
FeS2
FeS
FeS
Fe3O4
MoS2
MoO2
Fe3O4
Fe2O3
ZnS
ZnSO4
0
-5
-10
Log fS2
-25
-20
-15
Log fO2

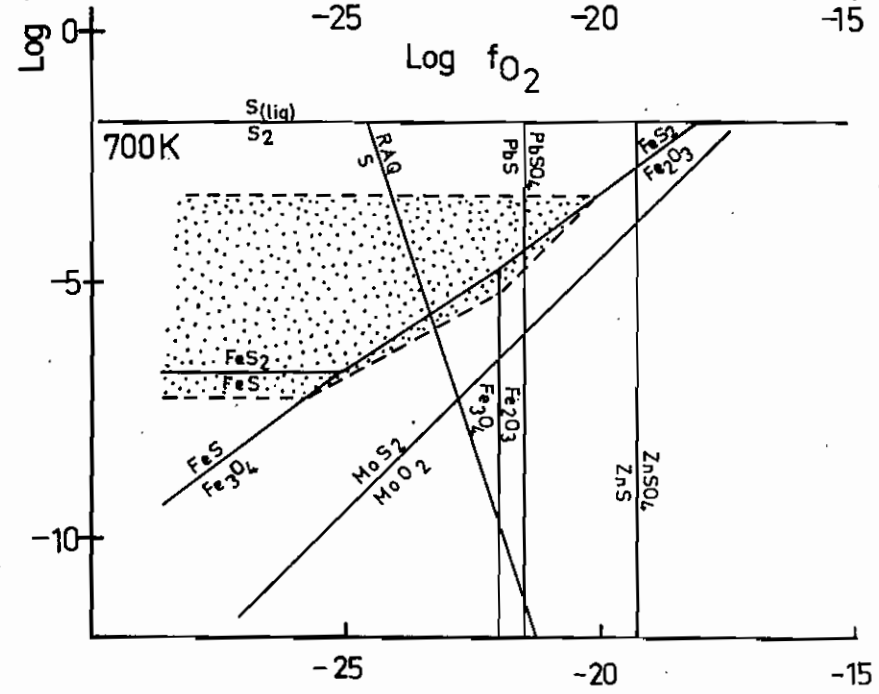
700 K
S(liq)
S2
RAQ
S
PbS
PbSO4
FeS2
Fe2O3
FeS2
FeS
FeS
Fe3O4
MoS2
MoO2
Fe3O4
Fe2O3
ZnS
ZnSO4
0
-5
-10
-25
-20
-15

Sulphur fugacity. The sulphur condensation reaction

$$S_2 = 2S_{(liq)} \quad \ldots 10.5$$

sets an absolute upper limit to the sulphur fugacity because no native sulphur is known in the deposit. The narrow range over which hematite and chalcopyrite coexist below 820 K would bracket the sulphur fugacity closely if it were reliable. It is nonetheless consistent with the broader limits set by the equilibria:

$$TiO_2 + CaSO_4 + SiO_2 = CaTiSiO_5 + \tfrac{1}{2}S_2 + 3/2O_2 \quad \ldots 10.6$$

(represented as RAQ/S in figs. 10-2 and 10-3), and

$$MoS_2 + O_2 = MoO_2 + S_2 \quad \ldots 10.7$$

(data for 10.7 from Holland, 1965). Rutile, anhydrite, quartz and molybdenite are characteristically found with chalcopyrite in veins with included hematite. Molybdenite has not been found in veins formed above 850 K, although Holland's data for reaction 10.7 suggest that the co-existence of molybdenite with rutile, quartz, anhydrite and hematite is possible at higher temperatures. Rutile is abundant in the selvages of anhydrite - quartz-Cu,Fe sulphide veins formed above 900 K (e.g. 102998, 102675 and 103012). If the whole assemblage is at equilibrium, then reaction 10.6 sets the only useful lower limit to the sulphur fugacity at high temperatures. The gaseous equilibrium

$$\tfrac{1}{2}S_2 + O_2 = SO_2 \quad \ldots 10.8$$

can be used to set an upper limit at high temperatures in conjunction with the constraint $P_{SO_2} \leq P_{total}$. Let us assume for the moment that $P_{SO_2} \leq 0.1\ P_{total}$ (justification will be given in the section below on sulphur gas species), i.e. P_{SO_2} is no greater than the values given in Table 10-1. To find the fugacity of SO_2, the Lewis & Randall approximation for gas mixtures is used;

viz. "the fugacity of each constituent is equal to its mole fraction multiplied by the fugacity it would exhibit as a pure gas, at the same temperature and the same total pressure."

(Denbigh, 1971)

In this case,

$$f_{SO_2} = \gamma_{SO_2} \cdot P_{tot.} \cdot X_{SO_2} = 0.1\, \gamma_{SO_2} \cdot P_{tot.}$$

Using the equilibrium constants in Table 10-1 and fugacity coefficients from Newton (1935), the limiting fugacities of S_2 and SO_2 have been calculated (Table 10-1) and are plotted in fig. 10-3.

The limits at temperatures over 900 K do not appear to overlap any estimated high-temperature continuation (for Intermediate Solid Solution) of the $CuFeS_2$ fields from lower temperatures unless oxygen fugacities fall well within the magnetite field. The absence of magnetite from many high-temperature vein selvages and replacement textures in others argue strongly against adjusting the oxygen fugacity to fit. The blame might better be placed on the thermochemical data, and the uncertainty as to what happens at high temperatures.

Qualitatively, it is seen that the sulphur fugacity must increase with decreasing temperature to a maximum value near 800 K, and then decrease with continued cooling.

At 800 K, the fugacity of SO_2 for chalcopyrite-hematite-magnetite equilibrium is 11 atm, and the total fluid pressure is about 300 atm. At a log oxygen fugacity 1 unit above HM, the fugacity of SO_2 becomes 316 atm, corresponding to a pressure close to the total fluid pressure. Thus, at 800 K the oxygen fugacity must be very close to the value at the HM buffer as accepted here. This conclusion might be substantially changed by relatively small changes in the thermochemical data.

Table 10-1

FUGACITIES OF S_2 AND SO_2.

A. Maximum f_{S_2}, given $P_{SO_2} = 0.1\ P_{tot.}$ ($X_{SO_2} = 0.1$)

T K	P_{SO_2} atm.	γ_{SO_2}	$f_{SO_2} = X_{SO_2} \cdot \gamma_{SO_2} \cdot P_{tot.}$	log f_{SO_2}	log $k_{10.8}$	log f_{O_2} (HM)	log $\frac{f_{SO_2}}{f_{S_2}^{1/2}}$	log f_{S_2}
1100	80	1.11	89	2.0	13.4	-8.8	4.6	-5.5
1000	50	1.00	50	1.7	15.1	-11.0	4.1	-4.8
900	40	0.94	38	1.6	17.2	-13.8	3.4	-3.6

$$\log \frac{f_{SO_2}}{f_{S_2}^{1/2}} = \log k_{10.8} + \log f_{O_2}$$

B. Minimum f_{SO_2}, given minimum f_{S_2} (at rutile-anhydrite-quartz-sphene boundary, f_{O_2} = HM).

T K	log f_{S_2} (f_{O_2}=HM)	log $\frac{f_{SO_2}}{f_{S_2}^{1/2}}$	log f_{SO_2}	f_{SO_2} atm.
1100	-8.7	4.7	0.35	2.2
1000	-9.4	4.1	-0.60	0.25
900	-9.6	3.4	-1.40	4.0×10^{-2}

C. Range of f_{SO_2} and f_{S_2} (from A and B, above).

T	log f_{SO_2}	log f_{S_2}
1100	1.2 ± 0.8	-7.1 ± 1.7
1000	0.6 ± 1.0	-7.1 ± 2.3
900	0.1 ± 1.5	-6.6 ± 3.0

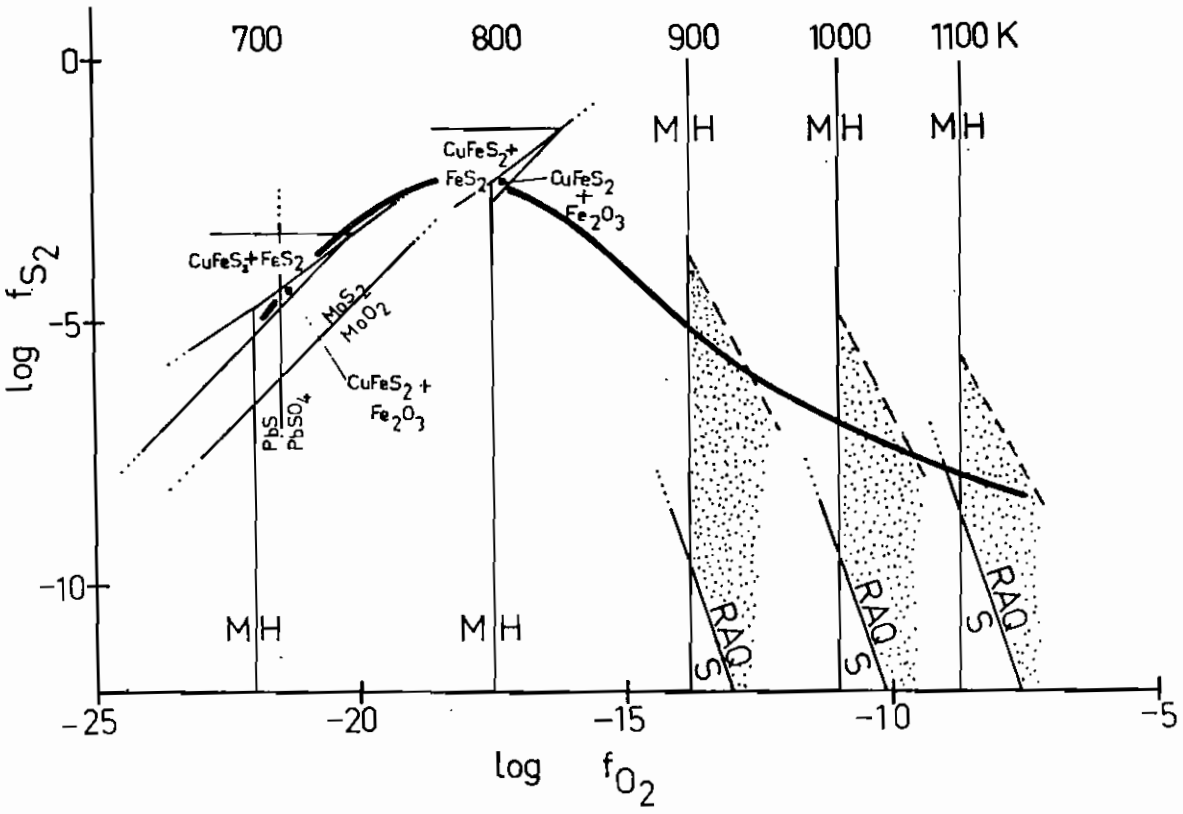

Fig. 10-3 A likely log f_{S_2} - log f_{O_2} path, as a function of temperature. See text for an explanation of assumptions. The stippled areas are the f_{O_2} - f_{S_2} fields at 900, 1000 and 1100 K, limited by the constraints:- hematite-magnetite equilibrium (M/H); rutile-anhydrite-quartz-sphene equilibrium (RAQ/S); P_{SO_2} = 0.1 P_{tot}. (dashed line, position calculated from γ_{SO_2}, f_{O_2} and data for equilibrium 10.8). There is no upper limit for f_{O_2}.

THE CHEMISTRY OF THE VAPOUR PHASE

State of water. Increasing pressure favours the polymerisation of H_2O in the vapour phase (Hastie, 1975, p.75 ff.). At pressures of 300 - 800 atm and temperatures near 1000 K the dimer predominates. The fugacity coefficient, as tabulated for example by Anderson (1967), corrects for this source of non-ideality so that the thermochemical data for monomeric water can be used. Mole fractions, however, ought to be calculated taking polymerisation into account. For the calculations which follow, the pressures and fugacities of water listed in Table 10-2 will be used, assuming $P_{H_2O} = P_{tot.}$. This assumption will be re-examined in the section on sulphur species, below.

Fugacity of HCl. Ryabchikov (1975) has suggested the following reaction to evaluate the fugacity of HCl in magmatic fluids

$$2NaCl_{(liq)} + H_2O_{(gas)} = Na_2O_{(xl)} + 2HCl \qquad \ldots 10.9$$

He estimated the activity of NaCl in the salt-rich liquid to be 0.35 ± 0.06; at Panguna the approach of salt-rich liquids to saturation near 700 K may mean that the activity approaches 1. Otherwise, Ryabchikov's estimate can be used. The error in this is much less than that involved in the estimation of the activity of Na_2O, which Ryabchikov does by setting limits based on granitoid mineralogy (presence of quartz and feldspars, absence of corundum at one extreme and of wollastonite at the other, fixing $a_{Al_2O_3}$ within limits and thence a_{Na_2O} by a reaction involving the decomposition of albite to its constituent oxides).

At 1000 K, equilibrium with a granitoid assemblage implies a HCl fugacity of 0.4 to 4.0 atm (Table 10-3). At the lower temperatures, the calculations will not correspond exactly with the situation in porphyry coppers; although quartz and one feldspar are present, the activities of the feldspar components will differ from those used by Ryabchikov. The estimates are therefore probably only general indications.

Table 10-2

FUGACITY OF WATER

T, K	$P_{tot.}$, atm.	γ_{H_2O}	f_{H_2O}, atm.	log f_{H_2O}
700	300	0.77	230	2.4
800	300	0.82	245	2.4
900	300	0.88	264	2.4
1000	500	0.88	440	2.6
1100	800	0.84	670	2.8

Table 10-3

FUGACITY OF HCl

T, K	log $k_{10.9}$	log f_{H_2O}	log a_{NaCl}	log a_{Na_2O}	log f_{HCl}
700	-27.3	2.4	0.0	-23±1	-1.0±0.5
800	-23.4	2.4	-.69±.16	-21±1	-0.7±0.6
850	-21.8	2.4	-.69±.16	-19.5±1	-0.7±0.6
1000	-17.9	2.6	-.69±.16	-16.8±0.8	0.1±0.5

$$\log f_{HCl} = \tfrac{1}{2}(\log k + \log f_{H_2O} + 2\log a_{NaCl} - \log a_{Na_2O})$$

Table 10-4

DIMERISATION OF NaCl

T, K	log $k_{10.10}$	$P_{tot.}$, atm.	P_{NaCl}, atm.	$P_{Na_2Cl_2}$, atm.
700	8.27	0.36	4.4×10^{-5}	0.36
800	6.42	0.05	1.4×10^{-4}	0.05
850	5.70	0.05	3.2×10^{-4}	0.05
900	4.98	0.09	1.0×10^{-3}	0.09
1000	3.82	1.57	1.6×10^{-2}	1.55

Fugacity of NaCl. For each set of pressure-temperature conditions, the composition of the vapour in the NaCl-H_2O system can be estimated from the fluid evolution paths discussed in the previous chapter, in conjunction with the data of Sourirajan & Kennedy (1962). The species present will depend on equilibrium in the following sets of gaseous reactions:

$$2NaCl = Na_2Cl_2 \quad \ldots 10.10$$

$$NaCl + H_2O = NaOH + HCl \quad \ldots 10.11$$

$$2NaCl + 2H_2O = Na_2(OH)_2 + 2HCl \quad \ldots 10.12$$

$$NaCl + 2H_2O = NaCl.2H_2O \quad \ldots 10.13$$

$$NaOH + H_2O = NaOH.H_2O \quad \ldots 10.14$$

(10.13 and 10.14: suggested by Hastie (1975))

Thermochemical data are available in JANAF (1971) for all except the hydrate species. Considering initially only reaction 10.10, i.e. a vapour containing only sodium chloride at a total partial pressure P_t, P_t is calculated from the NaCl content of the vapour (wt. % is converted to mole fraction and thence to pressure), with water dimeric. Whether NaCl is mainly dimeric or monomeric does not, as shall be seen, change the final solution because the factor of 2 by which P_t would vary as a result is relatively insignificant in the solution of the two equations

$$P_{NaCl} + P_{Na_2Cl_2} = P_t$$

$$P_{Na_2Cl_2}/P^2_{NaCl} = k_{10.10} \text{ (assuming } P_i = f_i)$$

The P_t values in Table 10-4 assume the predominance of dimers, but the same qualitative result, the predominance of dimers, can be obtained assuming mainly the monomer in the mole fraction calculation.

From thermochemical data for reactions 10.11 and 10.12, and the previously-established fugacities of HCl, the following are obtained:

at 1000 K,

$$\log \frac{f_{NaOH}}{f_{NaCl}} = -3.5 \pm 0.5; \quad \log \frac{f_{Na_2(OH)_2}}{f^2_{NaCl}} = -3.7 \pm 1.0$$

and at 850 K,

$$\log \frac{f_{NaOH}}{f_{NaCl}} = -4.2 \pm 0.7; \quad \log \frac{f_{Na_2(OH)_2}}{f^2_{NaCl}} = -2.9 \pm 1.4$$

For $\log f_{NaCl} < 0$, as it is here (considering the predominance of the dimer) NaOH is a minor species, but $Na_2(OH)_2$ may predominate over NaCl and possibly also over Na_2Cl_2. Hastie (1975) has explained that the change in slope of the solubility curve of NaCl in water vapour (see fig. 9-1) implies different chemical mechanisms of solution above and below 873 K and that these are consistent with reaction 10.14 above 873 K, and reaction 10.13 below 873 K. In the absence of the required thermochemical data, no firm conclusions can be drawn on the likely fugacity of NaCl. It is evident that NaCl will be a minor species, dominated by Na_2Cl_2, and possibly by the hydrated species. The values of P_{NaCl} in Table 10-4 will be diminshed by the formation of hydrates. The values in Table 10-4 will be used as maximum estimates of P_{NaCl} and f_{NaCl}.

Sulphur species. At temperatures over 673 K, only H_2S, S_2 and SO_2 need be considered among all the possible sulphur-bearing species in hydrothermal fluids (Barnes & Czamanske, 1967; Ohmoto & Rye, in press). S_2 is usually considered only because its fugacity is a useful chemical parameter.

In a system containing only H_2O and sulphur species, the constraints are

$$X_{SO_2} + X_{H_2S} + X_{H_2O} = 1$$

$$\tfrac{1}{2}S_2 + O_2 = SO_2 \qquad \ldots 10.8$$

$$H_2S + 3/2O_2 = H_2O + SO_2 \qquad \ldots 10.15$$

It has been shown in a previous section that the fugacity of sulphur cannot be limited without making assumptions about the fugacity of SO_2. Here, we shall begin by examining the relative fugacities of H_2O and H_2S, assuming only that H_2O is a major constituent (and not, for the moment, that $f_{H_2O} = \gamma_{H_2O}.P_{tot.}$) and setting a high limit for P_{SO_2}. The relationship of f_{H_2O} and $P_{tot.}$ will then be re-examined, and, finally, the ratio f_{SO_2}/f_{H_2S} will be calculated.

The ratio f_{H_2O}/f_{H_2S} depends on f_{S_2} and f_{O_2} in the following way:

$$\log \frac{f_{H_2O}}{f_{H_2S}} = \log k_{10.15} + 3/2 \log f_{O_2} - \log f_{SO_2}$$

In Table 10-5, this ratio is calculated assuming a mole fraction of 1 for SO_2 in the vapour. For lower mole fractions (an order of magnitude lower would be reasonable), higher H_2O/H_2S ratios are obtained. Thus only at 700 K might H_2S become important relative to water in the vapour and this is unlikely, because the mole fraction of SO_2 will be very small at 700 K. The fugacity ratio corresponds approximately with the pressure ratio because the ratio of fugacity coefficients is near 1. Except perhaps at 700 K, then, H_2S can be neglected relative to H_2O so that, to a sufficient approximation,

$$X_{SO_2} + X_{H_2O} = 1$$

Equation 10.8 can be used as a constraint only at 700 and 800 K where mineral equilibria provide upper and lower limits. At 900 - 1100 K,

Table 10-5

SULPHUR SPECIES EQUILIBRIA

1. $\frac{1}{2}S_2 + O_2 = SO_2$ $\quad \log k_{10.8} = \log f_{SO_2} - \log f_{O_2} - \frac{1}{2} \log f_{S_2}$

T	$\log k_{10.8}$	$\log f_{O_2}$		$\log f_{S_2}$		$\log f_{SO_2}$		
		HM	HM+1	HM	HM+1	HM	HM+1	
700	24.0	-22.0	-21.0	-5.0	-4.1	-0.5	0.9	f_{SO_2} derived from f_{S_2}, chalcopyrite-hematite assemblage.
800	19.8	-17.5	-16.5	-2.5	-1.7	1.1	2.5	
900	17.2	-13.8	-12.8	-6.6±3.0	-9.1±3.4	0.1±1.5	-0.2±1.8	f_{S_2} derived from pressure limits on SO_2 and rutile-anhydrite-quartz assemblage.
1000	15.1	-11.0	-10.0	-7.1±2.3	-9.6±2.8	0.6±1.0	0.3±1.4	
1100	13.4	-8.7	-7.7	-7.1±1.7	-9.6±2.1	1.2±0.8	0.9±1.1	

2. $H_2S + 3/2O_2 = H_2O + SO_2$ $\quad \log k_{10.15} = \log f_{H_2O} + \log f_{SO_2} - 3/2 \log f_{O_2} - \log f_{H_2S}$

T	$\log k_{10.15}$	$\log f_{O_2}$		$\log f_{SO_2}$ * if $X_{SO_2}=1$	$\log \frac{f_{H_2O}}{f_{H_2S}}$		$\frac{\gamma_{H_2S}}{\gamma_{H_2O}}$ †	$\log \frac{f_{SO_2}}{f_{H_2S}}$	$\log \frac{f_{SO_2}}{f_{H_2S}}$	$\log f_{H_2S}$	
		HM	HM+1		HM	HM+1		$P_{H_2O} = P_{tot.}$, HM	HM+1	HM	HM+1
700	34.6	-22.0	-21.0	2.4	-0.8	0.7	1.2	-0.8	0.7	0.3	0.2
800	29.8	-17.5	-16.5	2.4	1.2	2.7	1.2	1.2	2.7	-0.1	-0.2
850	27.9	-15.3	-14.3	2.4	2.6	4.1	1.2	2.6	4.1		
900	26.0	-13.8	-12.8	2.5	2.8	4.3	1.2	2.9	4.4	-2.8±1.5	-4.6±1.8
1000	23.0	-11.0	-10.0	2.7	3.8	5.3	1.2	3.9	5.4	-3.3±1.0	-5.1±1.4
1100	20.5	-8.7	-7.7	3.0	4.5	6.0	1.4	4.7	6.2	-3.5±0.8	-5.3±1.1

* coefficients from Newton (1935)

† coefficients from Ryzhenko & Volkov (1971) and Anderson (1967).

mineral equilibria provide only a lower limit to the sulphur fugacity, and an assumption must be made about the partial pressure of SO_2 in order to place an upper limit. If all of the volatiles exsolved by a magma go into a single fluid, the molar ratio SO_2:H_2O can be calculated from Ryabchikov's (1975) estimate, 1 - 2%, of the water lost by the magma, and one he quotes from Vinogradov for the sulphur content of such magmas, 0.04%. These are by weight, so that the molar ratio is 0.02 (H_2O as monomers) or 0.04 (dimers). Thus the limit $P_{SO_2} < 0.1\ P_{tot.}$ is adopted; if Vinogradov's estimate is low (it is difficult to see how the sulphur content of magmas which characteristically exsolve volatiles could be estimated) the fluid could carry away twice as much sulphur and still fall within the limit.

With this limit, it is possible to calculate the fugacity ratio SO_2:H_2S and thence the fugacity limits of H_2S. The partial pressure of $(H_2O)_n$ must be greater than $0.9\ P_{tot.}$ and the mole fraction of $H_2O \geq 0.9$. By the Lewis & Randall Rule,

$$f_{H_2O}(\text{pure}) \geq f_{H_2O}(\text{mixture}) \geq 0.9\ f_{H_2O}\ (\text{pure at same T \& P})$$

therefore, $0 \geq \log f_{H_2O}(\text{mixture}) - \log f_{H_2O}(\text{pure}) \geq -0.05$.

This correction may be regarded as negligible, and the fugacity ratio of SO_2 to H_2S calculated using $f_{H_2O}(\text{pure})$. The ratios, and the fugacity ranges of H_2S at the various temperatures are listed in Table 10-5, and plotted in fig. 10-4. In the figure, it is clearly shown that SO_2 is the principal sulphur species in the vapour in the porphyry copper environment. This need not be the case in the liquid, as will be seen in Chapter 11.

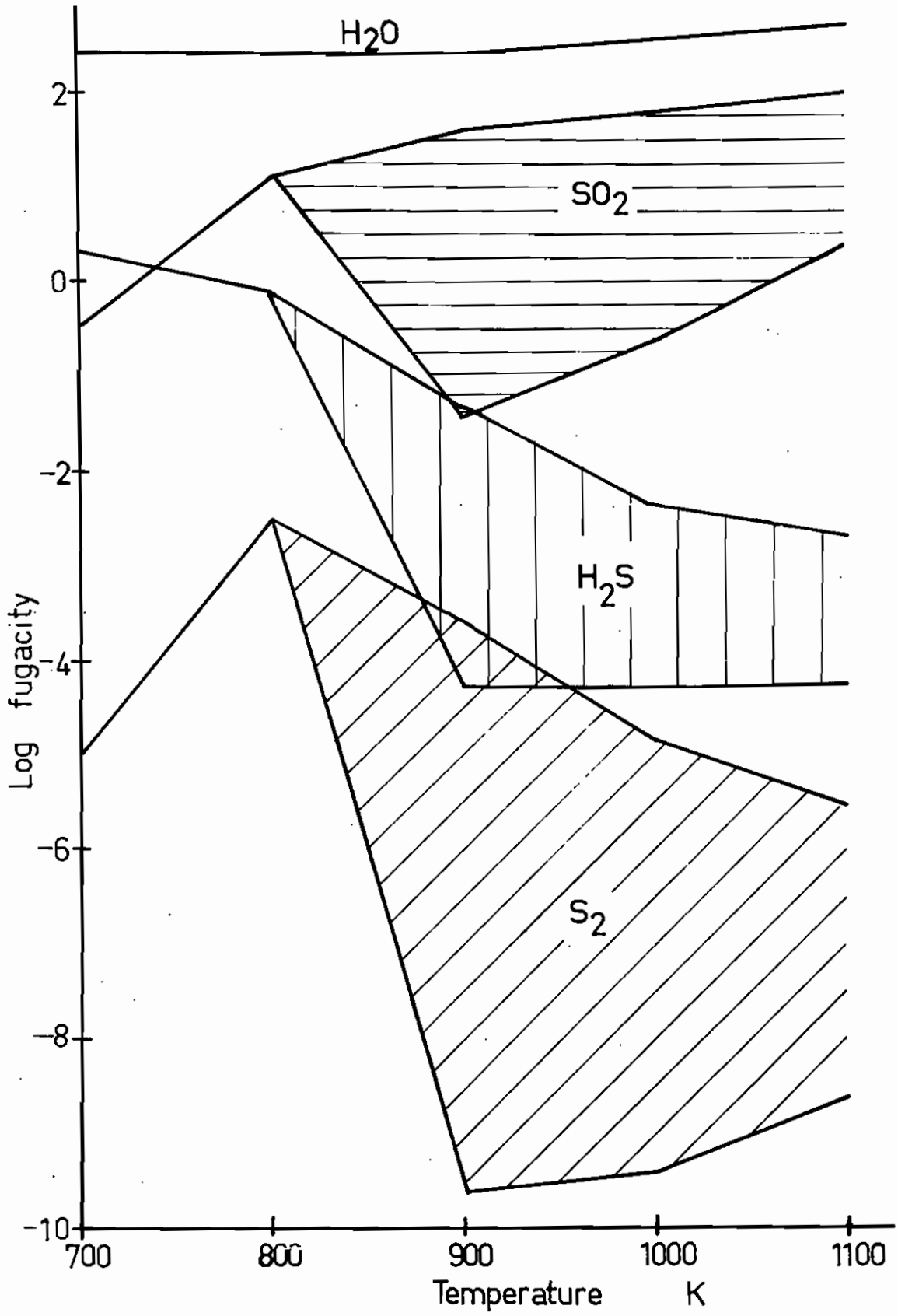

Fig. 10-4 Limits on the fugacities of H_2O, SO_2, H_2S and S_2 over the temperature range 700 - 1100 K at Panguna. Assumptions discussed in text.

BASE METAL TRANSPORT IN THE VAPOUR

The vapour in porphyry copper systems removes a large amount of water, and may remove significant amounts of other volatiles such as NaCl, SO_2, H_2S, HCl and volatile base-metal species. The Henley & McNabb (1978) vapour plume mechanism, for example, would require significant transport of copper in the vapour. The vapour, as suggested by Krauskopf (1964), may also play a part in the separation of the vase metals. The possibility of base-metal transport in vapour when fluid inclusions are decrepitated has been discussed in Chapter 4. The chemical-transport properties of the vapour in porphyry copper deposits will now be examined in the light of current thermochemical data. The approach is to be compared with that of Krauskopf (1964). It differs from Krauskopf's in that newer thermochemical data are available, and in the consideration of complex metal-bearing volatile species.

Enhanced volatility in salt mixtures. Some metal halides, particularly those of trivalent metals, are volatile at high temperatures. The mixing of halid salts gives rise to complex halide species. In a large number of mixed halide systems, the measured vapour pressures are higher than can be explained by the vapour pressures of the individual components. Commonly, then, the formation of complex halides in mixed halide systems enhances the volatility of the simple components. Reviews on this phenomenon include those of Schaefer (1976), Binnewies & Schaefer (1973) and Hastie (1975). Hastie's book includes a set of rules for the estimation of the thermochemical properties of many species, and a discussion of the possible application of the enhanced volatility notion to the problems of ore genesis.

The importance of enhanced halide volatility in chemical transport has been recognised, both in unapplied investigation (Schaefer, 1974) and

in metallurgy (the TORCO, or segregation process for the extraction of copper; Brittan, 1970; and Gross & Stuart, 1971).

Chloride volatility versus hydroxide volatility. Enhanced volatility is also characteristic of non-halide systems, in particular metal oxide - water systems and possibly sulphide systems (Hastie, 1975). Since water is the main constituent of porphyry-copper vapour, the relative importance of chloride and hydroxide volatility must be a first consideration. On p.68 ff. Hastie considers the ratio $P_{M(OH)_2}/P_{MCl_2}$ as a function of the ratio P_{HCl}/P_{H_2O}. From data available for certain cases in JANAF (1971), and from a consideration of the bond-dissociation energies involved, he deduces the following generalised thermochemical data for the reaction

$$MCl_2 + 2H_2O = M(OH)_2 + 2HCl \qquad \ldots 10.16$$

$$\Delta S \simeq -4 \pm 2 \text{ cal/deg.mole}, \quad T = 1000 - 2000 \text{ K}$$

$$\Delta H \simeq 28 \text{ kcal/mole.}$$

These are based on known thermodynamic data for reactions of type 10.16. Their negligible temperature dependence is characteristic of such vapour phase reactions (for the chloride-chloride reaction case, see below). Thus $\log k_{10.16} \simeq -7$ at 1000 K and -8 at 850 K, and

$$\frac{P_{MCl_2}}{P_{M(OH)_2}} = 10^7 \cdot \left(\frac{P_{HCl}}{P_{H_2O}} \right)^2 = 10^{2 \cdot 0 \pm 1 \cdot 0} \text{ at 1000K, and}$$

$$10^8 \cdot \left(\frac{P_{HCl}}{P_{H_2O}} \right)^2 = 10^{2 \cdot 0 \pm 1 \cdot 0} \text{ at 850 K.}$$

(using data from previous sections).

Chlorides of divalent metals appear to predominate over hydroxides, but by relatively small factors at the lower limit in each case. An uncertainty of an order of magnitude in $\log k_{10.16}$ would therefore mean that $P_{M(OH)_2} \leq P_{MCl_2}$. No similar considerations are available for the mono-

valent metals, although it has already been seen that $NaOH.H_2O$ may predominate over NaCl at temperatures over 873 K. For the trivalent metals it can be shown similarly that at 1000 K

$$\frac{P_{MCl}}{P_{M(OH)_3}} \simeq 10^{10} \cdot \left[\frac{P_{HCl}}{P_{H_2O}}\right]^3 = 10^{2\cdot5 \pm 1\cdot5}$$

The conclusions for divalent and trivalent metals are therefore similar. At 1000 K, hydroxides may be present at levels comparable to or less than the concentrations of simple chloride species. This does not rule out the possible predominance of complex chloride species over both. The importance of these will now be considered for Fe, Cu, Zn and Mo.

IRON SPECIES

Ferrous species. Chou & Eugster (1977) showed that $FeCl_2$ was the dominant iron-bearing species in supercritical chloride solutions at oxygen fugacities up to the hematite-magnetite buffer. The conditions of the experiments do not match those at Panguna; to investigate the effect of Panguna conditions, the following gaseous reaction is considered:

$$2FeCl_2 + 2HCl + \tfrac{1}{2}O_2 = 2FeCl_3 + H_2O \qquad \ldots 10.17$$

$$\log \frac{f_{FeCl_3}}{f_{FeCl_2}} = \tfrac{1}{2}(\log k_{10.17} - \log f_{H_2O} + \tfrac{1}{2}\log f_{O_2} + 2 \log f_{HCl})$$

Using the fugacities established in earlier sections,

At 1000 K, $\log k_{10.17} = 2.3$, and $\log \frac{f_{FeCl_3}}{f_{FeCl_2}} = -1.7 \pm 0.5$ at HM
or -1.4 ± 0.5 at HM+1

and at 850 K, $\log k_{10.17} = 3.6$, and $\log \frac{f_{FeCl_3}}{f_{FeCl_2}} = -2.1 \pm 0.6$ at HM
or -1.8 ± 0.6 at HM+1

Ferrous chloride predominates, then, and will be used as a base for the measurement of the iron content in vapour according to the reaction

$$\tfrac{1}{2}Fe_2O_3 + 2HCl + \tfrac{1}{2}O_2 = FeCl_2 + H_2O \quad \ldots 10.18$$

At 1000 K, $\log k_{10.18} = -6.1$ and $\log f_{FeCl_2} = -14.0 \pm 1.0$ at HM
or -13.5 ± 1.0 at HM+1.

At 850 K, $\log k_{10.18} = -7.2$ and $\log f_{FeCl_2} = -18.7 \pm 1.2$ at HM
or -18.2 ± 1.2 at HM+1.

Other ferrous species which could be considered are the dimer Fe_2Cl_4 and $NaFeCl_3$. The K-analogues of the Na-bearing complexes should behave similarly, and will not be considered here.

Thermochemical data for the reactions

$$2FeCl_2 = Fe_2Cl_4 \quad \ldots 10.19$$

$$NaCl + FeCl_2 = NaFeCl_3 \quad \ldots 10.20$$

can be estimated with the rules suggested by Hastie (1975, p.135 ff.). For reactions of the type A + B = C,

$$\Delta S = -30 \pm 5 \text{ cal/deg.mole.}$$

Hastie commented that ΔS for such homogeneous gaseous reactions is found to depend chiefly on the change in number of species. As a corollary, ΔS changes little with temperature, and the temperature dependence can be entirely neglected if only whole orders of magnitude are considered.

ΔH is given by a consideration of changes in the number and nature of chemical bonds, and for mixed complexes, by an additional, empirically-based measure of stability enhancement as a function of changes in the coulombic repulsion between metal atoms. For the coulombic effect, the change considered is that taking place on the reaction of two simple dimers to give two molecules of the complex species (see $NaFeCl_3$ example below).

For the cyclic Fe_2Cl_4 structure (Cl-Fe$\langle^{Cl}_{Cl}\rangle$Fe-Cl) the contribution of bond dissociation energy is the result of the substitution of four bridging Fe-Cl bonds for two terminal Fe-Cl bonds. Hastie has shown that the energy of a bridging bond in general is about 0.6 of the energy of a terminal bond linking the same types of atoms. In the case of Fe_2Cl_4 there is no coulombic repulsion effect, because both of the metal atoms are the same. The enthalpy change has a negligible temperature dependence (because it is due largely to changes in bond dissociation energies) if only whole orders of magnitude are dealt with.

It is found that $\Delta H = -0.4\ \overline{D}_{Fe-Cl}$, where $\overline{D}_{Fe-Cl}$ is the average bond dissociation energy of Fe-Cl bonds in $FeCl_2$, equal to 97.2 kcal/mole (Vedeneyev *et al.*, 1966). Thus $\Delta H = -38.9$ kcal/mole, and at 1000 K

$$\Delta G = \Delta H - T\Delta S = -9.6 \pm 5.0 \text{ kcal/mole.}$$

$$\log k_{10.19} = 2 \pm 1 = \log \frac{f_{Fe_2Cl_4}}{f_{FeCl_2}} - \log f_{FeCl_2}$$

$$\log \frac{f_{Fe_2Cl_4}}{f_{FeCl_2}} \simeq -12 \pm 2 \text{ at HM and at HM+1.}$$

Similarly, at 850 K,

$$\log \frac{f_{Fe_2Cl_4}}{f_{FeCl_2}} \simeq -16 \pm 2 \text{ at HM.}$$

Applying Hastie's rules to reaction 10.20, $\Delta S = -30 \pm 5$ cal/mole.deg and ΔH (bond) $= -0.2\ (D_{Na-Cl} + \overline{D}_{Fe-Cl}) = -38.9$ kcal/mole (data from Weast, 1975; and Vedeneyev, 1966).

To calculate the coulombic stabilisation, the reaction considered is

$$Na\langle^{Cl}_{Cl}\rangle Na + Cl-Fe\langle^{Cl}_{Cl}\rangle Fe-Cl = 2\ Na\langle^{Cl}_{Cl}\rangle Fe-Cl$$

Na and Fe are considered to be ions of charge +1 and +2 respectively, so that the change in electrostatic potential energy is

$$\Delta U = 2\left(\frac{1x2}{r_{Na}+r_{Fe}}\right) - \frac{2x2}{2r_{Fe}} - \frac{1x1}{2r_{Na}} \simeq -0.9\text{Å}^{-1} \text{ (arbitrary units)}$$

(r_i is the ionic radius of ion i, values from Weast, 1975). From fig. 3-6 of Hastie (1975), this corresponds with a stabilisation of $\Delta H \simeq -15$ kcal/mole.

So the total ΔH of reaction 10.20 is -53.9 kcal/mole. At 1000 K, $\Delta G = -23.9 \pm 5$, and $\log k_{10.20} = 5 \pm 1$;

$$\log \frac{f_{NaFeCl_3}}{f_{FeCl_2}} = 5 \pm 1 + \log f_{NaCl}$$

$$\leq 3 \pm 1 \quad \text{(if } \log f_{NaCl} \leq \log P_{NaCl} \text{ as in Table 10-4)}.$$

No better estimate is possible because of the uncertainty about f_{NaCl}; it can only be concluded that $NaFeCl_3$ could be the dominant species by a factor of 10^2 to 10^4.

At 850 K,

$$\log \frac{f_{NaFeCl_3}}{f_{FeCl_2}} \leq 4 \pm 1.$$

Ferric species. For the ferric species $NaFeCl_4$, there are thermochemical data in the literature. The gaseous reaction considered is:

$$NaCl + FeCl_3 = NaFeCl_4 \qquad \ldots 10.21$$

Galitskiy (1968) gives $\Delta G = -22.7$ kcal/mole at 1000 K, and -27.0 kcal/mole at 850 K.

At 1000 K, $\log k_{10.21} = 5.0 = \log \frac{f_{NaFeCl_4}}{f_{FeCl_3}} - \log f_{NaCl}$

and $\log \frac{f_{NaFeCl_4}}{f_{FeCl_3}} \leqslant 3.2$

At 850 K, $\log \frac{f_{NaFeCl_4}}{f_{FeCl_3}} \leq 1.5$

The dimerisation of $FeCl_3$ takes place by the gaseous reaction

$$2FeCl_3 = Fe_2Cl_6 \quad \ldots 10.22$$

At 1000 K, $\log k_{10.22} = 0.2$, so that

$$\log f_{Fe_2Cl_6} = \log k_{10.22} + 2 \log f_{FeCl_3} \simeq -31 \text{ at HM.}$$

Similarly at 850 K, Fe_2Cl_6 is unimportant.

Summarising, for all the ratios obtained above at 1000 K, $\log f_{H_2O} = 2.6$, $\log f_{HCl} = 0.1 \pm 0.5$, the fugacities of the iron-bearing species in the vapour are:

$\log f_{O_2}$	HM	HM+1
$\log f_{FeCl_2}$	-14.0 ± 1.0	-13.5 ± 1.0
$\log f_{FeCl_3}$	-15.7 ± 1.5	-14.9 ± 1.5
$\log f_{NaFeCl_3}$	$\leq -11 \pm 2$	$\leq -11 \pm 2$
$\log f_{NaFeCl_4}$	$\leq -12.5 \pm 1.5$	$\leq -11.7 \pm 1.5$
$\log f_{Fe_2Cl_4}$	-26 ± 3	-26 ± 3
$\log f_{Fe_2Cl_6}$	-31 ± 3	-30 ± 3

Evidently, iron transport in the vapour is of very minor significance, even if the volatility of hydroxide species approaches that of the chlorides.

COPPER SPECIES

There are no data for comparing the volatilities of the hydroxide and chloride species of monovalent copper, but it is possible to compare the various chloride species. Divalent chloride species are assumed not to exist at most of the temperatures of interest because $CuCl_2$ decomposes at 766 K (Barin & Knacke, 1973). CuCl, its polymers, $NaCuCl_2$, $NaCu_2Cl_3$, $CuFeCl_3$ and $CuFeCl_4$ will be considered.

For chalcopyrite-hematite equilibrium, the CuCl content of the vapour can be calculated for temperatures up to 820 K (the temperature at which the tetragonal polymorph of $CuFeS_2$ becomes unstable) within the limits of accuracy of the data.

$$CuFeS_2 + HCl + 2O_2 = \tfrac{1}{2}Fe_2O_3 + CuCl + \tfrac{1}{2}H_2O + S_2 \qquad \ldots 10.23$$

At 800 K, $\log k_{10.23} = -6.1$ (data for chalcopyrite from Barton & Skinner, in press) so that

$$\log f_{CuCl} = -\log k_{10.23} + 2 \log f_{O_2} - \log f_{HCl} - \log f_{S_2} - \tfrac{1}{2}\log f_{H_2O}$$
$$= -28.3 \text{ at HM and } -26.3 \text{ at HM+1.}$$

For the higher-temperature cubic polymorph, it is estimated that $G_f = -40 \pm 10$ kcal/mole at 1000 K (an extrapolation of Barton's data for the lower polymorph). In this case, $\log k_{10.23} = -6 \pm 2$ and $\log f_{CuCl} = -10 \pm 5$ at HM, assuming that the activity of $CuFeS_2$ in the solid solution is 1.

The polymers of CuCl. Except for the trimer (JANAF, 1971) the data are from Guido *et al.* (1972).

$$2CuCl = Cu_2Cl_2 \qquad \ldots 10.24$$

$\log k_{10.24} = 3.2 \pm 0.4$ at 1000 K and 5.5 ± 0.5 at 800 K.

$$\log f \frac{f_{Cu_2Cl_2}}{f_{CuCl}} = \log f_{CuCl} + \log k_{10.24}$$

$$-23 \text{ at 800 K, HM.}$$

At 1000 K, if $\log f_{CuCl} < -2.8$, $\log \frac{f_{Cu_2Cl_2}}{f_{CuCl}} < 0$.

$$3CuCl = Cu_3Cl_3 \qquad \ldots 10.25$$

$\log k_{10.25} = 20.4$ at 800 K and 13.6 at 1000 K.

$$\log \frac{f_{Cu_3Cl_3}}{f_{CuCl}} = \log k_{10.25} + 2 \log f_{CuCl} = -36 \text{ at 800 K and HM.}$$

At 1000 K, $\log \frac{f_{Cu_3Cl_3}}{f_{CuCl}} < 0$ if $\log f_{CuCl} < -6.8$

$$4CuCl = Cu_4Cl_4 \qquad \ldots 10.26$$

$\log k_{10.26} = 23.1 \pm 0.6$ at 800 K and 14.6 ± 0.6 at 1000 K.

$$\log \frac{f_{Cu_4Cl_4}}{f_{CuCl}} = \log k_{10.26} + 3 \log f_{CuCl} = -61 \text{ at 800 K and HM.}$$

At 1000 K, $\log \frac{f_{Cu_4Cl_4}}{f_{CuCl}} < 0$ if $\log f_{CuCl} < -4.7$

None of the polymers is significant beside CuCl at 800 K. The polymers could only be significant at 1000 K is log f_{CuCl} exceeded the limits indicated. None seems likely to be significant at Panguna, given the limits calculated roughly from reaction 10.23. Even the trimer can only become significant near the upper limit of f_{CuCl} estimated from equilibrium 10.23, from limits set deliberately very broad. At log f_{CuCl} > -6, log $f_{Cu_3Cl_3}$ > -4.4 and Cu transport in this form becomes important. In systems with higher f_{CuCl}, the trimer may predominate (e.g. the study of Gross & Stuart, 1971) or the tetramer may also be important (J.D. Williams, University of Tasmania, pers. comm., 1978).

Na-bearing species. Gross & Stuart (1971) found that the formation of the complexes $NaCuCl_2$ and $NaCu_2Cl_3$ "contributed a very considerable part" to copper transport at temperatures above 1000 K in the segregation process for copper extraction, but found no evidence of a Na_2CuCl_3 complex. They estimated equilibrium constants based on pressure ratios in torr; these will be used below with the pressures converted to atm. Again, the situation must be re-examined thoroughly for the conditions at Panguna. For the gaseous reaction

$$NaCl + CuCl = NaCuCl_2 \quad \ldots 10.27$$

$$\log k_{10.27} = \frac{-11900}{T} + 11.6 \pm 0.5$$

$$= -3.3 \pm 0.5 \text{ at 800 K (extrapolating) and } -0.3 \pm 0.5 \text{ at 1000 K.}$$

$$\log \frac{P_{NaCuCl_2}}{P_{CuCl}} = \log k_{10.27} + \log P_{NaCl}$$

$$\leq -6.8 \pm 0.5 \text{ at 800 K } (\log P_{NaCl} \leq -3.5)$$

$$\text{or} \leq -2.1 \pm 0.5 \text{ at 1000 K } (\log P_{NaCl} \leq -1.8).$$

The $NaCu_2Cl_3$ species is formed by the gaseous reaction

$$NaCl + 2CuCl = NaCu_2Cl_3 \quad \ldots 10.28$$

$$\text{for which } \log k_{10.28} = \frac{-25600}{T} + 25.3 \pm 1.0$$

$$= -6.7 \pm 1.0 \text{ at 800 K and } -0.3 \pm 1.0 \text{ at 1000 K.}$$

$$\log \frac{P_{NaCu_2Cl_3}}{P_{CuCl}} = \log k_{10.28} + \log P_{NaCl} = \log P_{CuCl}$$

$$\leq -38.5 \pm 1.0 \text{ at 800 K, HM, } \log P_{NaCl} \leq -3.5$$

$$\text{and} \leq -2.1 \pm 1.0 + \log P_{CuCl} \text{ at 1000 K; this is much}$$

less than $\log P_{NaCuCl_2}/P_{CuCl}$ at likely values of P_{CuCl}.
At the temperatures cited, neither complex is important compared with CuCl. $NaCuCl_2$ may become comparable with CuCl at a temperature greater than 1000 K, possibly at magmatic temperatures.

Fe-bearing species. These can be considered using rules given by Hastie (1975). For

$$CuCl + FeCl_2 = CuFeCl_3 \quad \ldots 10.29$$

$$\Delta S = -30 \pm 5 \text{ cal/deg.mole}$$

$$\Delta H \text{ (bond)} = -0.2 \ (D_{Cu-Cl} + \overline{D}_{Fe-Cl}) \qquad (\overline{D} \text{ for } FeCl_2)$$

$$= -36.4 \text{ kcal/mole.}$$

ΔH (coulombic repulsion) = -15 kcal/mole

Total ΔH = -41 kcal/mole.

Log $k_{10.29}$ = 2 ± 2 at 1000 K and 5 ± 1 at 800 K.

$$\log \frac{f_{CuFeCl_3}}{f_{CuCl}} = \log k_{10.29} + \log f_{FeCl_2}$$

$$= -16 \pm 2 \text{ at HM, 1000 K,}$$

or much less at HM, 800 K.

The species $CuFeCl_4$ can be treated similarly, but estimating the coulombic repulsion enthalpy term from Hastie's diagram engenders an uncertainty of ±10 kcal/mole.

$$CuCl + FeCl_3 = CuFeCl_4 \quad \ldots 10.30$$

ΔS = -30 ± 5 cal/deg.mole

ΔH (bond) = $-0.2\ (D_{Cu-Cl} + \overline{D}_{Fe-Cl}) = -35.8$ kcal/mole

($\overline{D}$ for $FeCl_3$)

ΔH (coulombic repulsion) = -20 ± 10 kcal/mole.

Log $k_{10.30}$ = 6 ± 4 at 1000 K and 8 ± 4 at 800 K.

$$\log \frac{f_{CuFeCl_4}}{f_{CuCl}} = \log k_{10.30} + \log f_{FeCl_3}$$

$$= -10 \pm 6 \text{ at 1000 K, HM, and less at 800 K.}$$

Neither of the iron-bearing species need therefore be considered. Dewing (1970) found no stable complexes of larger size formed between CuCl and $FeCl_3$ under the conditions of his experiments (673 - 1073 K, CuCl-$FeCl_3$ melt present).

Summary. Of the possible copper-bearing species considered, CuCl is the predominant one at 800 K, and probably also at 1000 K. Even at 1000 K, rough calculations suggest that there is only a very small amount of copper in the vapour.

ZINC SPECIES

Some zinc is certainly present in porphyry copper fluids, as indicated by the analysis of fluid inclusion decrepitation products (Chapter 4), but little zinc is deposited in the ore zone. A study of zinc speciation may be useful in explaining this. Chloride species which could transport significant zinc in vapour include $ZnCl_2$, Zn_2Cl_4, $NaZnCl_3$, $Na_2Zn_2Cl_6$, the K-analogues of these species, and possibly $ZnFeCl_4$. Again, the potassium species will be assumed to behave as the sodium ones.

Na-bearing species. The complexes $NaZnCl_3$, and $Na_2Zn_2Cl_6$ were reported by Bloom *et al.* (1970) who gave these thermochemical data:

$$2NaCl + 2ZnCl_2 = Na_2Zn_2Cl_6 \qquad \ldots 10.31$$

$$\Delta H = -53.8 \text{ kcal/mole}$$

$$NaCl + ZnCl_2 = NaZnCl_3 \qquad \ldots 10.32$$

$$\Delta H = -18.3 \pm 3.4 \text{ kcal/mole.}$$

All species are gaseous, and the temperature range is 577 - 777 K. Since these enthalpies depend largely on bond dissociation energies and bond lengths (Hastie, 1975), they are not significantly temperature-dependent and can be extrapolated. Hastie's rules give

$$\Delta S_{10.31} = -90 \pm 15 \text{ cal/deg.mole}$$

$$S_{10.32} = -30 \pm 5 \text{ cal/deg.mole.}$$

At 1000 K, $\log k_{10.32}$ is -2.6

$$\log \frac{f_{NaZnCl_3}}{f_{ZnCl_2}} = \log k_{10.32} + \log f_{NaCl}$$

$$\leq -4.4 \quad (\text{if } \log f_{NaCl} \leq -1.8).$$

$$\text{Log } k_{10.31} = -7.9 \text{ at 1000 K, and}$$

$$\log \frac{f_{Na_2Zn_2Cl_6}}{f_{ZnCl_2}} = \log k_{10.31} + 2 \log f_{NaCl} + \log f_{ZnCl_2}$$

$$\leq -11.5 + \log f_{ZnCl_2}$$

If $f_{ZnCl_2} < 500$ ($P_{tot.} = 500$ atm), $\log \frac{f_{Na_2Zn_2Cl_6}}{f_{ZnCl_2}} \leq -8.8$.

$ZnCl_2$ clearly predominates over the NaCl-$ZnCl_2$ complexes at 1000 K, and a similar result applies at 850 K.

Fe-bearing species. The thermochemical data for the reaction

$$ZnCl_2 + FeCl_2 = ZnFeCl_4 \quad (Cl\text{-}Zn\langle^{Cl}_{Cl}\rangle Fe\text{-}Cl) \qquad \ldots 10.33$$

can be estimated by Hastie's rules.

$$\Delta S = -30 \pm 5 \text{ cal/deg.mole}$$

$$\Delta H \text{ (bond)} = -0.2 \ (\bar{D}_{Zn-Cl} + \bar{D}_{Fe-Cl}) = -34 \pm 2 \text{ kcal/mole}$$

($\bar{D}_{A-Cl}$ for ACl_2; data from Vedeneyev *et al.*, 1966).

ΔH (coulombic repulsion) = 0 (because the ionic radii of Fe^{2+} and Zn^{2+} are equal; Weast, 1975). Hence there is no stability enhancement, and the species should be unimportant relative to $ZnCl_2$ and $FeCl_3$. To test this:

$$\text{At 1000 K, } \Delta G_{10.33} = 4 \pm 7 \text{ kcal/mole}$$

$$\text{and } \log k_{10.33} \leq 0.7$$

$$\log \frac{f_{ZnFeCl_4}}{f_{ZnCl_2}} = \log k_{10.33} + \log f_{FeCl_2}$$

$$\leq -14.7 \pm 1.0 \text{ at HM.}$$

$ZnCl_2$. Thus only $ZnCl_2$ (and possibly its dimer) are important. The fugacity of $ZnCl_2$ can be estimated roughly from the reaction

$$ZnS \text{ (solid)} + 2HCl = ZnCl_2 + H_2S \qquad \ldots 10.34$$

at 850 K, approximately the formation temperature of 103014, in which there is sphalerite. No explicit thermodynamic data for $ZnCl_2$ gas are

available, but Barin & Knacke (1973) give ΔG_f^o for the liquid (-128.7 kcal/mole), and the equilibrium vapour pressure. It will be assumed that $f_{ZnCl_2} = P_{ZnCl_2} = 6.6 \times 10^{-2}$ atm.

$$ZnCl_2\ (liq) = ZnCl_2\ (gas) \quad \ldots 10.35$$

For pure liquid, $\log k_{10.35} = \log f_{ZnCl_2} = -1.2$, and $\Delta G_{10.35} = 4.7$ kcal/mole. Thus ΔG_f^o $ZnCl_2$ (gas) $\simeq$ -124 kcal/mole. So for reaction 10.34, using only data from Barin & Knacke,

$$\log k_{10.34} = -3.7$$

$$\text{and } \log f_{ZnCl_2} = \log k_{10.34} - \log f_{H_2S} + 2 \log f_{HCl}$$

$$= -3.7 \pm 1.8$$

The calculation would not give a meaningful result at 1000 K because ZnS does not appear to be stable at Panguna at that temperature. If the amount of $ZnCl_2$ in the salt-rich liquid is the same at 850 K and 1000 K, the amount of Zn in the vapour at 1000 K should be much larger than at 850 K. Vapour pressures of pure liquid ZnCl increase about sixteenfold over the same temperature interval (Barin & Knacke, 1973).

MOLYBDENUM SPECIES

Both the oxides and chlorides of Mo are volatile, and the +4, +5 and +6 valence states may be important. There are thus many reactions to consider. Thermochemical data are available for the following (all species gaseous):

$$MoO_2 + 4HCl = MoCl_4 + 2H_2O \quad \ldots 10.36$$

$$MoO_2 + \tfrac{1}{2}O_2 = MoO_3 \quad \ldots 10.37$$

$$MoO_3 + H_2O = MoO_2(OH)_2 \quad \ldots 10.38$$

$$MoO_3 + 2HCl = MoO_2Cl_2 + H_2O \quad \ldots 10.39$$

$$MoO_3 + 6HCl = MoCl_6 + 3H_2O \quad \ldots 10.40$$

$$MoCl_5 + HCl + \tfrac{1}{4}O_2 = MoCl_6 + \tfrac{1}{2}H_2O \quad \ldots 10.41$$

The rules used previously cannot be applied to complex halide species of molybdenum. Table 10-6 is a listing of the equilibrium constants and fugacity ratios for the equations above under Panguna conditions. The +6 oxidation state predominates, largely as OH-bearing species. Glemser & Wendlandt (1963) have suggested that even larger hydroxy-oxide species may be the most significant in the transport of Mo. The species $Mo_7O_{18}(OH)_6$ is consistent with the chemical - transport data at pressures up to 330 atm. At higher pressures, they suggested a species involving two H_2O molecules. There are no thermochemical data for these species, but their predominance would be consistent with the stability trend established for the simpler species. Certainly, all available data suggest the predominance of hydroxy-oxide species under Panguna conditions. Krauskopf (1964), concluded that oxides predominated over chlorides under most f_{HCl} conditions at 1 kbar total pressure.

There is no evidence that molybdenite is a stable solid phase at Panguna at magmatic temperatures. If molybdenite was stable at 850 K (e.g. in 103014, where several type III inclusions gave $T_h > 580^{\circ}C$), the equilibrium fugacity of MoO_2 would have been as follows.

$$MoO_2 + S_2 = MoS_2 \text{ (solid)} + O_2 \qquad \ldots 10.42$$

Mills (1974) gives estimates of ΔG°_f for MoS_2.

$$\log k_{10.42} = 13.3$$

$$\log f_{MoO_2} = -\log k_{10.42} + \log f_{O_2} - \log f_{S_2}$$

$$= -24.1 \pm 1.5$$

and from the data in Table 10-6, $\log f_{MoO_2(OH)_2} = -3.6 \pm 1.5$

Table 10-6

MOLYBDENUM SPECIES

At 1000 K, log f_{H_2O} = 2.6, log f_{HCl} = 0.1 ± 0.5, log f_{O_2} = -11.0 (HM)

Reaction	log $k_{10.i}$	
10.36	11.2	log $[f_{MoCl_4}/f_{MoO_2}]$ = 6.4 ± 2.0
10.37	7.9	log $[f_{MoO_3}/f_{MoO_2}]$ = 7.6
10.38	7.5	log $[f_{MoO_2(OH)_2}/f_{MoO_3}]$ = 10.1
10.39	10.6	log $[f_{MoO_2Cl_2}/f_{MoO_3}]$ = 8.4 ± 1.0
10.40	-8.35	log $[f_{MoCl_6}/f_{MoO_3}]$ = -15.6 ± 3.0
10.41	-5.2	log $[f_{MoCl_6}/f_{MoCl_5}]$ = -9.1 ± 0.5

At 850 K, log f_{H_2O} = 2.4, log f_{HCl} = -0.7 ± 0.6, log f_{O_2} = -15.3

Reaction	log $k_{10.i}$	
10.36	15.7	log $[f_{MoCl_4}/f_{MoO_2}]$ = 8.1 ± 2.4
10.37	8.8	log $[f_{MoO_3}/f_{MoO_2}]$ = 8.5
10.38	9.6	log $[f_{MoO_2(OH)_2}/f_{MoO_3}]$ = 12.0
10.39	13.7	log $[f_{MoO_2Cl_2}/f_{MoO_3}]$ = 9.9 ± 1.2
10.40	-6.0	log $[f_{MoCl_6}/f_{MoO_3}]$ = -17.4 ± 3.6
10.41	-5.0	log $[f_{MoCl_6}/f_{MoCl_5}]$ = -10.7 ± 0.6

DISCUSSION OF VAPOUR CHEMISTRY

The fugacities of the various important metal species can now be compared.

	850 K	1000 K
log f_{CuCl}	-28.3	-10 ± 5 ?
log f_{NaFeCl_3}	-15 ± 2	-11 ± 2
log f_{ZnCl_2}	-3.7 ± 1.8	? (> -3.7 ± 1.8)
log $f_{MoO_2(OH)_2}$	-3.6 ± 1.5	? (> -3.6 ± 1.5)

Under magmatic conditions (T 1000 K) the transport of Fe in the vapour is insignificant. The transport of Cu is also unimportant if log f_{CuCl} < -6.8, which seems likely on the basis of the deliberate broad limits (log f_{CuCl} = -10 ± 5) arising from the rough calculation on equilibrium 10.23. If all of the metals have relative volatilities that are similar under magmatic conditions to those at 850 K, then it may be possible to separate Zn and Mo from Cu and Fe in the process of evolving a boiling salt-rich liquid from silicate melt and crystals. This could account for the general lack of Zn in porphyry coppers, and for the separation of Mo from Cu in certain deposits.

The condensation of salt-rich liquid by the Henley & McNabb (1978) mechanism will fractionate whatever metals are carried in the vapour into the condensate to some extent. No Henry's Law constants are available. Whether or not this leads to the formation of porphyry-molybdenum deposits, Cu and Mo may behave differently enough to be separated under porphyry copper conditions. That Zn should follow Mo, on the indications given here, is a problem, because Zn-enrichment is not characteristic of porphyry molybdenums.

Lastly, the likely copper concentration of the salt-rich condensate can be examined. For 1 ppm of Cu in vapour consisting otherwise of water,

the mole fraction of CuCl is

$$\frac{1/63.5}{1/63.5 + 10^6/36} = 6 \times 10^{-7} \text{ for dimeric } H_2O.$$

At a total pressure of 800 atm, then, $P_{CuCl} = 4.8 \times 10^{-4}$ atm $\simeq f_{CuCl}$ for a vapour concentration of 1 ppm. At 1000 K, log f_{CuCl} has been estimated at -10 ± 5. Under conditions at which CuCl is dominant (log $f_{CuCl} < -6.8$) the concentration of Cu in the vapour is less than 1 ppb; the presence of, say, 5% NaCl in the vapour makes little difference to the calculation. If all of the copper is transferred to a liquid consisting of 50% NaCl and 50% H_2O, then 10% of the mass of the vapour is being condensed and the copper is enriched 10 times to less than 10 ppb. If the vapour contained only 2% NaCl, the enrichment factor would be 25 and the upper limit on copper concentration in the liquid 25 ppb. This falls short of the observed copper concentrations in type III inclusions by many orders of magnitude, and would be a further argument against any significant copper deposition from the condensates of the magmatic vapour. This, as stated earlier, seems likely from the broad overlap of the limits of f_{CuCl} for equilibrium with hematite and chalcopyrite, and for the dominance of CuCl in the vapour. It appears possible, however, to derive a salt-rich liquid rich in copper for log f_{CuCl} between -5 and -6. Clearly, better thermochemical data for the Cu,Fe sulphides are required if this problem is to be resolved beyond doubt.

The findings of this study can be compared with those of Krauskopf (1964). Under the conditions T = 1100 K, log $f_{H_2O} = 3$, log $f_{O_2} = -8$, log $f_{\Sigma S} = 1$, log $f_{HCl} = 0$, he found that

log $f_{Cu_3Cl_3}$	-1
log f_{FeCl_2}	-5
log f_{ZnCl_2}	-2
log f_{MoO_3}	-2

and at 900 K, $\log f_{H_2O} = 3$, $\log f_{O_2} = -14$, $\log f_{\Sigma S} = -1$, $\log f_{HCl} = -1$

$$\log f_{Cu_3Cl_3} \quad -7$$

$$\log f_{FeCl_2} \quad -8$$

$$\log f_{ZnCl_2} \quad -5$$

$$\log f_{MoO_3} \quad -5$$

The estimates made in this study for magmatic conditions apply to intermediate conditions. Both studies agree on the high volatility of Zn and Mo. The volatilities of Cu and Fe are considerably higher in Krauskopf's results than in those of this study. In particular, the importance of Cu_3Cl_3 according to Krauskopf contrasts with its insignificance according to this work. Both studies are limited by unreliable thermochemical data for the Cu,Fe sulphides.

THE ACIDITY OF THE SALT-RICH LIQUID

The salt-rich liquid presents its own problems of speciation, but a consideration of this serves little purpose at present. It is sufficient to remark that all potential vapour species, dominant or otherwise, must exist in the liquid, and probably do so in different relative proportions. The consequences of mineral precipitation in veins and of wallrock alteration will be dealt with here.

K-feldspar, or K-feldspar + sericite, commonly forms an inner alteration selvage to quartz-Cu,Fe sulphide veins. A quartz-sericite assemblage without K-feldspar was noted in only one case, 103021. Sericite-albite assemblages without K-feldspar occur along the boundary between salt-rich liquid and groundwater. To a good approximation, the molality of KCl remained constant in the salt-rich liquids so that any increase in molality of HCl would drive the liquid towards the sericite field (Montoya & Hemley, 1975). The alteration assemblages show that this did not happen

in general; the K-feldspar - sericite boundary was not crossed. Montoya & Hemley's diagrams can be used, with estimates of the molalities of NaCl and KCl at Panguna, to show that the range of pH in which albite and sericite coexist at 400°C is close to the buffered pH of the K-feldspar - sericite assemblage. There appears to have been a control on the amount of HCl in the salt-rich liquids. The reactions controlling HCl include:

(i) precipitation of quartz. Dissolved quartz is presumed to be in the form of an alkali silicate.

$$Na_2O.nSiO_2 + 2HCl = 2NaCl + nSiO_2 + H_2O \quad \ldots 10.43$$

(ii) precipitation of sulphides, e.g. chalcopyrite, pyrite - see below for equations (10.53, 10.54).

(iii) precipitation of anhydrite.

$$CaCl_2 + H_2SO_4 = CaSO_4 + 2HCl \quad \ldots 10.44$$

The sources of $CaCl_2$ and H_2SO_4 are discussed below.

(iv) wallrock alteration. Biotite is by far the most abundant alteration product associated with quartz-Cu,Fe sulphide veins at Panguna; reactions involving this mineral all either consume or produce HCl. Biotite usually replaces plagioclase and amphibole of either igneous or early hydrothermal origin. Ford (1976) gives analyses of amphiboles and all fall in a range between actinolite and hornblende. Here, reactions are written for both end members, $Ca_2(Mg,Fe)_5Si_8O_{22}(OH)_2$ and $Ca_2(Mg,Fe)_4Al_2Si_7O_{22}(OH)_2$, and for the anorthite and albite components of plagioclase.

(a) Plagioclase to biotite.

$$CaAl_2Si_2O_8 + 2KCl + 6(Mg,Fe)Cl_2 + 4SiO_2 + 8H_2O =$$
$$2K(Mg,Fe)_3AlSi_3O_{10}(OH)_2 + CaCl_2 + 12HCl \quad \ldots 10.45$$

$$NaAlSi_3O_8 + KCl + 3(Mg,Fe)Cl_2 + 4H_2O =$$
$$K(Mg,Fe)_3AlSi_3O_{10}(OH)_2 + NaCl + 6HCl \quad \ldots 10.46$$

(b) Hornblende to biotite.

$$Ca_2(Mg,Fe)_4Al_2Si_7O_{22}(OH)_2 + 2KCl + 2H_2O + 2(Mg,Fe)Cl_2 = 2K(Mg,Fe)_3AlSi_3O_{10}(OH)_2 + 2CaCl_2 + SiO_2 + 2HCl \quad \ldots 10.47$$

(c) Actinolite and plagioclase to biotite.

$$Ca_2(Mg,Fe)_5Si_8O_{22}(OH)_2 + CaAl_2Si_2O_8 + (Mg,Fe)Cl_2 + 2KCl + 2HCl = 2K(Mg,Fe)_3AlSi_3O_{10}(OH)_2 + 3CaCl_2 + 4SiO_2 \quad \ldots 10.48$$

$$Ca_2(Mg,Fe)_5Si_8O_{22}(OH)_2 + NaAlSi_3O_8 + KCl + 8HCl = K(Mg,Fe)_3AlSi_3O_{10}(OH)_2 + 2CaCl_2 + 2(Mg,Fe)Cl_2 + NaCl + 8SiO_2 + 4H_2O \quad \ldots 10.49$$

(d) Hornblende and plagioclase to biotite (combining a and b).

$$Ca_2(Mg,Fe)_4Al_2Si_7O_{22}(OH)_2 + 4KCl + CaAl_2Si_2O_8 + 3SiO_2 + 8(Mg,Fe)Cl_2 = 4K(Mg,Fe)_3AlSi_3O_{10}(OH)_2 + 3CaCl_2 + 14HCl \quad \ldots 10.50$$

$$Ca_2(Mg,Fe)_4Al_2Si_7O_{22}(OH)_2 + NaAlSi_3O_8 + 3KCl + 5(Mg,Fe)Cl_2 + 6H_2O = 3K(Mg,Fe)_3AlSi_3O_{10}(OH)_2 + 2CaCl_2 + NaCl + SiO_2 + 8HCl \quad \ldots 10.51$$

The reactions above are written to conserve aluminium, which shows only small variations between fresh and altered rocks at Panguna (Ford, 1978). The reactions by which sanidine replaces biotite and chlorite replaces biotite both consume HCl, but these are considered unimportant beside the other reactions above. Likewise, the reactions depositing vein material should be insignificant because of the sheer volume of biotitised rock in the orebody, with the possible exception of the deposition of quartz in parts of the orebody where quartz veins make up 5 to 10% of the total volume.

The biotite-amphibole-plagioclase reactions are summarised below as a table, giving the numbers of moles of HCl produced (+) or consumed (-) per mole of reactant on conversion to biotite.

	Albite	Anorthite	No plagioclase
Actinolite	-8	-2	—
Hornblende	+8	+14	+2
No amphibole	+6	+12	—

In the intrusions, the alteration of plagioclase predominates, so that there will be a net increase of HCl in the fluid (this may be partly compensated, but not completely, by the consumption of HCl as SiO_2 is supplied from the fluid to alter anorthite). In the Panguna Andesite amphibole of the amphibole-plagioclase-magnetite alteration assemblage is entirely altered, and the plagioclase partly. Since the volume of a mole of amphibole is nearly three times that of a mole of plagioclase, the simultaneous conversion of a mole of each in a rock consisting of approximately equal volumes of each is probably a reasonable approach to reality. If a mole of $Ab_{50}An_{50}$ reacts with a mole of $Hb_{50}Ac_{50}$ to give biotite, interpolation of the numbers in the table gives about 3 moles of HCl added to the fluid.

If this extra HCl is not taken up by some other means, sericite will replace K-feldspar. The sporadic chloritisation of biotite, the replacement of biotite by K-feldspar near veins and the deposition of quartz in veins may all be in part a response to local HCl build-up. However, minerals not favoured by increasing HCl content (sulphides and anyydrite) also form in the veins and wallrock. This suggests that some other means of removing HCl is operating. The most obvious one is boiling, for which there is evidence in the form of type II inclusions throughout the deposit. Boiling would thus appear to be an essential element of the porphyry copper mechanism in deposits in which sericite is not an important component of the potassic alteration assemblage. Sericite - K-feldspar assemblages are characteristic of veins cutting the

Biotite Granodiorite (and also occur to some extent in the other porphyries). This is consistent with the predominance of the alteration of plagioclase in the porphyries and the consequent release of large quantities of HCl.

SULPHIDE AND SULPHATE DEPOSITION

Although the main sulphur-bearing species in the vapour is SO_2, it will be shown in Chapter 11 that sulphur isotope data are consistent with a predominance of H_2S in the salt-rich liquid. Only 10 - 20% of the sulphur in the liquid is carried as SO_2. In the vapour, SO_2 will decompose as the temperature falls, probably according to the reaction

$$4SO_2 + 4H_2O = H_2S + 3H_2SO_4 \quad \ldots 10.52$$

(Holland, 1967, p.421). The same could be suggested for the salt-rich liquid, although the chemical evolution is different. The liquid appears to maintain a constant SO_2:H_2S ratio, between 1:9 and 1:4 (see fig. 11-3), while H_2S is withdrawn as Cu,Fe sulphides, so that SO_2 must be withdrawn simultaneously. As sulphate is formed, it will combine with Ca^{2+} from the alteration of plagioclase to give anhydrite. A sufficient explanation of the vein assemblages should account for these features:

(i) The salt-rich liquids are saturated in Cu,Fe sulphides and anhydrite over the whole temperature range, from magmatic temperatures to 400°C.

(ii) In the high-temperature veins (e.g. 102675, 102676 and 102998) anhydrite is more abundant than sulphides; sulphides become much more abundant, probably more so than anhydrite, at about 500°C and below (this is difficult to judge because of the solution of anhydrite, but there is nothing to suggest a large-scale removal of anhydrite from wallrock at lower temperatures).

Reaction 10.52 is incapable of accounting for the increase of sulphide relative to sulphate at lower temperatures, although it seems necessary to account for the generation of sulphate at all temperatures, and if it is the only important reaction at high temperatures, could account for the high sulphate to sulphide ratio in the high-temperature veins. Other reactions for the decomposition of SO_2 may become important below 500°C: e.g. for the formation of chalcopyrite

$$6CuCl + 6FeCl_2 + SO_2 + 11H_2S = 6CuFeS_2 + 2H_2O + 18HCl \quad \ldots 10.53$$

and for pyrite

$$9FeCl_2 + 2SO_2 + 4H_2S = 3FeS_2 + 6FeCl_3 + 4H_2O \quad \ldots 10.54$$

The reaction forming chalcopyrite removes SO_2 and H_2S in a molar ratio 1:11, and this will tend to deplete the liquid in H_2S (according to the ratios arising from the isotope study). Reaction 10.52 will enrich the liquid in H_2S. A combination of the two processes could account for the constant ratios at lower temperatures.

The reduction of Mo^{6+} species to form molybdenite could also contribute to the oxidation of Fe^{2+} or SO_2, although the quantities involved would be very small.

METAL ZONING

According to the textures described in Chapter 4, pyrite deposition generally preceded the deposition of chalcopyrite and bornite. The distribution of bornite and digenite relative to chalcopyrite, and of sphalerite relative to the Cu,Fe sulphides are further features that require explanation in a complete chemical model of ore deposition. The formation of a mole of biotite (according to the average reaction considered above in the context of acidity) would consume one mole of $(Mg,Fe)Cl_2$, while the alteration of plagioclase alone causes a larger

depletion of Fe and Mg in the liquid. Ford (1976) has suggested that the formation of biotite might be a necessary condition for the deposition of Cu,Fe sulphides instead of pyrite and magnetite, through the decrease it brings about in the concentration of Fe species. The liquid may thus evolve in composition, first depositing pyrite, then chalcopyrite, and finally becoming sufficiently enriched in copper over iron to deposit bornite with or without digenite. It is unlikely however, that the situation is as simple as that. The removal of volatiles by boiling may also affect the replacement of pyrite by chalcopyrite and chalcopyrite by bornite. The chemistry of ore deposition at the edges of the deposit may also have been complicated by additions from groundwater (see Chapter 9).

THE OXIDATION STATE OF MAGMATIC FLUIDS

The occurrence of hematite and the expulsion of much SO_2 (see Chapter 11) are consistent with a high oxidation state in the magma and the fluids it was exsolving at the time of copper deposition at Panguna. Magnetite is the usual iron oxide phase in crystallising magmas (e.g. non-mineralised Kaverong Quartz Diorite, where sphene and ilmenite also occur). Oxidation therefore seems to have taken place before copper mineralisation, and Ohmoto & Rye (in press) have suggested the diffusive loss of hydrogen as a possible mechanism. The degree of oxidation of an ordinary pluton (i.e. one without porphyry copper mineralisation) seldom, if ever, attains the degree observed at Panguna. Thus there is little to suggest that diffusion, which ought to be equally effective in all plutons, brings about the oxidation in porphyry coppers. Hematite has been reported in other deposits, e.g. Bingham (Roedder, 1971), Sar Cheshmeh (Etminan, 1977), Frieda (appendix, this study), and there is evidence of

more extreme oxidation at El Salvador (see Chapter 11). The expulsion of two fluids from the magma is evidenced in each of these deposits just as it is at Panguna.

In a magma which has begun exsolving water and other volatiles, the fugacity of hydrogen is governed by the gaseous reaction

$$H_2O = H_2 + \tfrac{1}{2}O_2 \qquad \ldots 10.55$$

$$\log f_{H_2} = \log k_{10.55} + \log f_{H_2O} - \tfrac{1}{2} \log f_{O_2}$$

At 1100 K, $\log k_{10.55} = -8.9$. If exsolution starts at $\log f_{O_2}$ = HM-3 (the estimate of Carmichael *et al.*, 1974, for calc-alkaline magmas with amphibole phenocrysts) and $\log f_{H_2O} = 2.8$, then $\log f_{H_2} = -0.2$. The fugacity coefficient of hydrogen under these conditions is 1.2 (Newton, 1935; critical parameters from Weast, 1975) so that the corresponding partial pressure of hydrogen is 0.5 atm, by the Lewis & Randall Rule. This is a substantial pressure in terms of the ability of a vapour phase to carry hydrogen away from the magma. Continued removal of vapour will therefore lead to the oxidation of the magma and fluids by the loss of hydrogen. At $\log f_{O_2}$ = HM the hydrogen fugacity is -1.7, and at HM+1, -2.2. The degree of oxidation will be limited by the decline of the partial pressure of hydrogen.

The expulsion of magmatic volatiles is therefore implicated in the oxidation process, not only at Panguna, but in many porphyry coppers. This mechanism was also suggested to explain progressive oxidation during the crystallisation of the Finnmarka complex, Norway, by Czamanske & Wones (1973). This means that the production of oxidised fluids ought to be preceded by the production of reduced fluids, all as part of a single, continuous process. There is evidence for this (except for the continuity of the process) at Panguna where phase A mineralisation, usually hematite-bearing, was superimposed on to a slightly more extensive and more

pervasive amphibole-plagioclase-magnetite alteration with associated sphene (cf. oxidation state of unaltered Kaverong Quartz Diorite). There is meagre evidence (specimen 103049) that a boiling salt-rich liquid was involved in the formation of the amphibole-bearing assemblage, and that the water in equilibrium with another specimen was of magmatic origin (Ford & Green, 1976). The phase A pyritic halo, described by Fountain (1973) as being most intensely developed at the outer boundary of the amphibole-bearing assemblage, may also have been deposited by the reduced fluids. The pyrrhotite replaced by pyrite in 103029 may also belong to this hydrothermal phase.

Chivas (1976) recognised oxidation resulting from the expulsion of volatiles at the Koloula porphyry copper prospect, Guadalcanal. He attributed part of the copper mineralisation to the first, relatively reduced, fluids which were boiling salt-rich liquids (although the fluid inclusions of these are said to contain hematite by Chivas & Wilkins, 1977).

There is nothing to suggest that the reduced fluids at Panguna deposited copper, although they may have deposited sulphur in the pyritic halo and iron as magnetite and pyrite. Together with the apparently general association of copper deposition and oxidised fluids in porphyry coppers, this suggests that the evolution of copper-rich fluids from the silicate melt is dependent on the state of oxidation of the fluids.

CHAPTER ELEVEN: SULPHUR ISOTOPE STUDY

INTRODUCTION

A small number of samples was examined at the isotope laboratory of the C.S.I.R.O. Minerals Research Laboratories, North Ryde, New South Wales, under the guidance of Messrs. J.W. Smith and M.S. Burns.

Sulphide samples were separated physically if possible, but anhydrite was dissolved away from chalcopyrite in HCl, and samples bearing pyrite, sphalerite and galena were subjected to a chemical separation. A weighed sample was reacted first with cold 1N HCl in a reflux apparatus with a magnetic stirrer. A stream of nitrogen was passed through the reactants to collect any H_2S, and was then passed through a trap containing $AgNO_3$ solution. Any Ag_2S formed was collected by filtration, dried and weighed. The reactants (minerals + acid) were also filtered, the residue being kept for the next stage and the filtrate for analysis by atomic absorption spectrophotometry. The residue was placed in cold 2N HCl and the whole process was repeated, and the residue from that stage was processed a third time with hot 2N HCl. The final residue, pyrite or chalcopyrite (they cannot be separated by this process) was dried in a nitrogen atmosphere. The three Ag_2S samples and the pyrite (in this case) were burned as described below. Since the process does not separate the minerals quantitatively, the filtrate analyses (Pb, Zn, Cu and Fe) are used to determine the contributions of each mineral to the measured $\delta^{34}S$ of each Ag_2S sample.

Powdered sulphide samples (10 mg of pyrite, 20 mg of others) were ground with excess Cu_2O and burned at 900°C in a vacuum. Any water vapour in the gaseous products was separated out with an acetone-dry ice

freezing mixture, and any CO_2 was separated from SO_2 with a pentane freezing mixture (Sakai & Yamamoto, 1966).

Anhydrite samples were first converted to $BaSO_4$ by solution in hot HCl and precipitation with $BaCl_2$. Weighed $BaSO_4$ samples were reduced to BaS with graphite at 1100°C under a stream of nitrogen (basically the method of Rafter, 1957). The BaS was leached out and filtered into $AgNO_3$ solution, and the resulting Ag_2S was recovered and burned as above.

$\delta^{34}S$ was measured for each SO_2 sample on a mass spectrometer relative to a laboratory standard. In the case of determinations on Ag_2S from anhydrite, a second standard (seawater sulphate taken as +20.2‰) was also checked. Since this was found to give +19.1‰ relative to the other standard, all $\delta^{34}S$ readings on sulphate sulphur were corrected according to a linear interpolation between the two standards.

As is customary, the isotopic variation is expressed as $\delta^{34}S$, defined as

$$\delta^{34}S = \left[\frac{^{34}S/^{32}S \text{ (sample)}}{^{34}S/^{32}S \text{ (standard)}} - 1 \right] \times 1000 \text{ ‰}$$

The standard is troilite from the Cañon Diablo meteorite. The fractionation of ^{34}S between minerals A and B is expressed as

$$\Delta_{A-B} = \delta^{34}S_A - \delta^{34}S_B$$

Recently, Rees (1978) criticised the method of determining $\delta^{34}S$ on SO_2 samples. He presented inter-laboratory data which showed poor agreement due to the "memory" effect - the retention of SO_2 in mass spectrometer inlet valves between measurements - and to unaccounted-for oxygen isotope interference. The interference is unavoidable when SO_2 is used. On the basis of determination on SF_6, free of both drawbacks,

Rees *et al.* (1978) have recalibrated seawater sulphate at $\delta^{34}S$ = 20.99‰. The temperatures quoted here may therefore be in slight error because seawater sulphate was taken as +20.2‰. Studies of the isotopic variation in a single mineral across a deposit will not be greatly affected, provided all measurements are made in the one laboratory. The determination of temperatures from isotopic fractionation (which, by virtue of the need of a calibration curve, will generally involve data from more than one laboratory) will be subject to unknown error. The uncertainty in sulphate-sulphide temperatures, already large according to the calibration data (Ohmoto & Rye, in press), will be increased because the disagreement between laboratories tends to be larger at higher $\delta^{34}S$ (Rees, 1978). In this study and in another of sulphur isotopes at Panguna (Ayres *et al.*, in press) and in a study of the calibration (used here) of the galena-sphalerite-pyrite thermometer (Smith *et al.*, 1978) all readings were made in the same laboratory.

THERMOMETRY

Sphalerite-pyrite veins. Sphalerite-pyrite pairs were obtained from six veins, a sphalerite-galena pair from one and sphalerite-galena-pyrite from one. In the last (103473) the expected fractionation order (galena < sphalerite < pyrite) was reversed and the results were rejected. A high result for one of the Ag_2S samples in 103471 was also rejected because the yield of the burn was low, and it led to a low Δ(sphalerite-pyrite) compared with the other sample, which was comparable with other specimens. The $\delta^{34}S$ and Δ values are set out in Table 11-1.

The mineragraphic study (Chapter 3) confirmed that sphalerite and galena were in equilibrium in 103480. This was the only specimen in which pyrite also appeared to be in equilibrium with sphalerite, but no

$\delta^{34}S$ could be measured for the pyrite because of the presence of tennantite in the final residue. The galena-sphalerite pair gave a temperature of 300°C. Three of the pyrite-sphalerite pairs in apparent textural disequilibrium gave similar temperatures (270 - 310°C). The other two pairs gave much lower temperatures.

The only comparable fluid inclusion data are from 103042 (see Chapter 6) which did not have enough galena or sphalerite for isotopic study. The pressure-corrected trapping temperatures were 330 ± 5°C. Taken altogether, the various temperature estimates indicate an average temperature near 300°C for sphalerite-pyrite mineralisation. Osatenko & Jones (1976) report a similar temperature, 266°C, for a sphalerite-pyrite pair from Valley Copper, British Columbia.

Anhydrite-Chalcopyrite. Two samples were obtained from diamond drill core BVP 88 for this study. Ayres *et al.* (in press) made measurements on two other samples. All of the data have been converted to temperatures using calibration equations cited in Ohmoto & Rye (in press), viz.

$$T = \frac{2.85 \times 10^{-3}}{(\Delta \pm 1)^{\frac{1}{2}}} \qquad \text{(for } T > 673 \text{ K)}$$

Note that the temperatures published by Ayres *et al.* differ substantially from those accepted here (Table 11-2). The temperature range compares favourably with the fluid inclusion temperature range for quartz-Cu,Fe sulphide mineralisation. In the cases of 102675 and 102676, the temperatures match the fluid inclusion data for quartz from 102676 (T_h = 600 to >700°C).

Table 11-1

$\delta^{34}S$, Δ AND TEMPERATURE MEASUREMENTS ON PYRITE-SPHALERITE VEINS

Specimen	$\delta^{34}S$, ‰			Δ, ‰	T°C*
	galena	sphalerite	pyrite		
103048		+0.2	+2.4	2.2	<150
103481		+1.2	+2.4	1.2	270
103475		+1.6	+3.1	1.5	200
103476		+0.6	+1.7	1.1	310
103471		+1.6	+2.7	1.1	310
103473	-1.5	-1.0		2.5	300

* using data from Smith *et al.* (1978).

Table 11-2

$\delta^{34}S$, Δ AND TEMPERATURES FOR ANHYDRITE-CHALCOPYRITE PAIRS

Specimen	$\delta^{34}S$, ‰		Δ, ‰	T°C§
	anhydrite	chalcopyrite		
102675	+7.6	+0.4	7.2	797±70
102676	+11.5	+0.5	11.0	588±40
34640†	+16.0	-0.1	16.1	438±22
34641†	+11.0	+0.2	10.8	597±40

† from Ayres *et al.* (in press), who gave temperatures of 350°C and 520°C.

§ data cited in Ohmoto & Rye (in press).

VARIATION OF $\delta^{34}S$ IN TIME AND SPACE

Pyrite. Pyrite samples examined in this study had $\delta^{34}S$ values ranging between +0.5 and +3.1‰ (+2.4, excluding veins with appreciable sphalerite). Ayres *et al.* (in press) found a similar range of 0.0 to +2.3‰. All available measurements for pyrite have been plotted on a map of the deposit (fig. 11-2). Fig. 11-1 shows specimen locations for the sulphur isotope study. There is no systematic distribution of $\delta^{34}S$ if the data are considered in this way. The data of Ayres *et al.* do not lend themselves to classification in terms of vein-types; most of the pyrite samples had been classified by association with alteration types. Even where a vein type was specified, it is not possible to relate Ayres' classification (after Fountain, 1972) to that used here. Thus only the measurements made in this study can be classified according to vein type.

Apart from the high ^{34}S content of the pyrite from sphalerite-pyrite veins, no real trend is visible, probably because there are not enough samples for most of the vein types.

Chalcopyrite. The range of $\delta^{34}S$ given by Ayres *et al.* is -1.6 to +1.5‰ within the orebody, and one is -2.5‰ outside the orebody. Given the number of samples involved, the trends suggested by Ayres *et al.* (viz. a difference in mean $\delta^{34}S$ between samples from near the Leucocratic Quartz Diorite and samples from near the Biuro Granodiorite, and an enrichment in ^{34}S towards the northwest) do not seem to be significant.

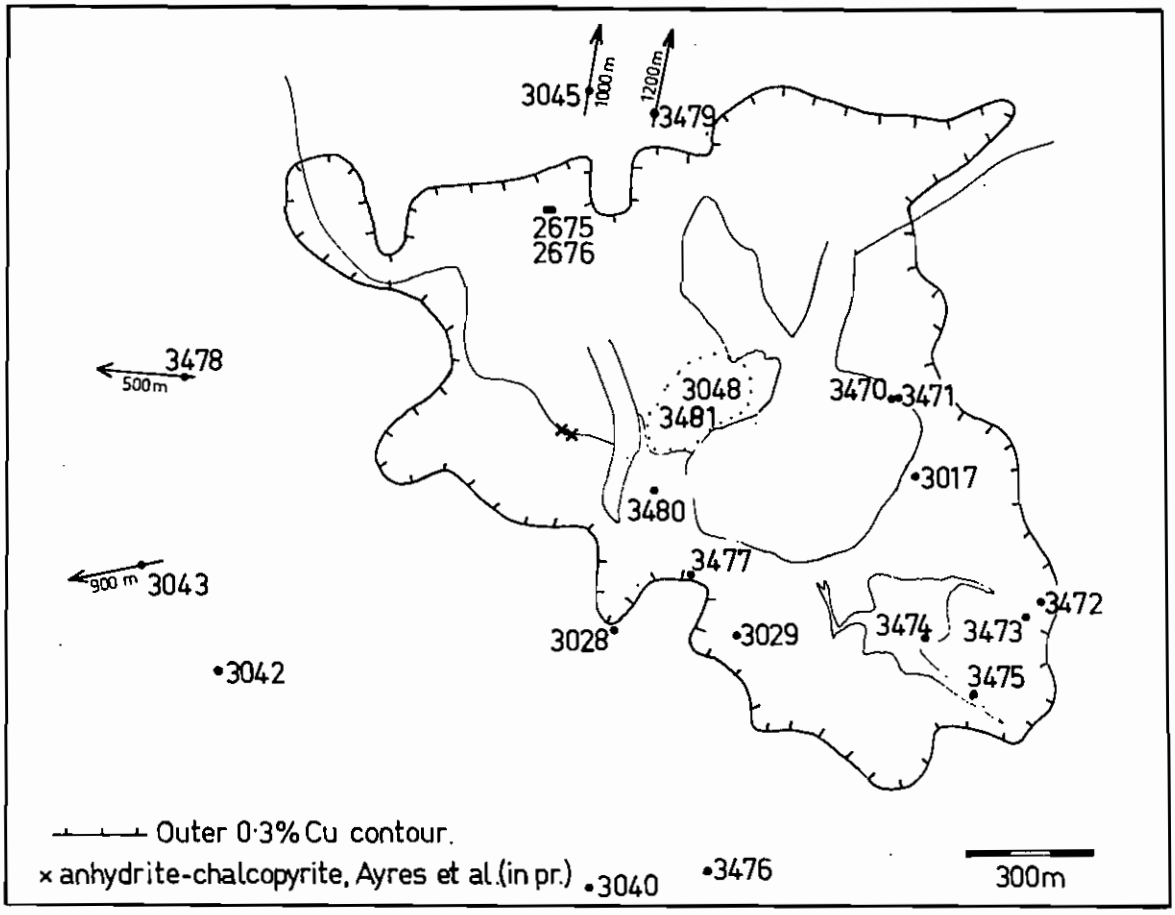

Fig. 11-1 Locality map of specimens used in the sulphur isotope study. Geological contacts and outer 0.3% Cu contour as in fig. 2-3.

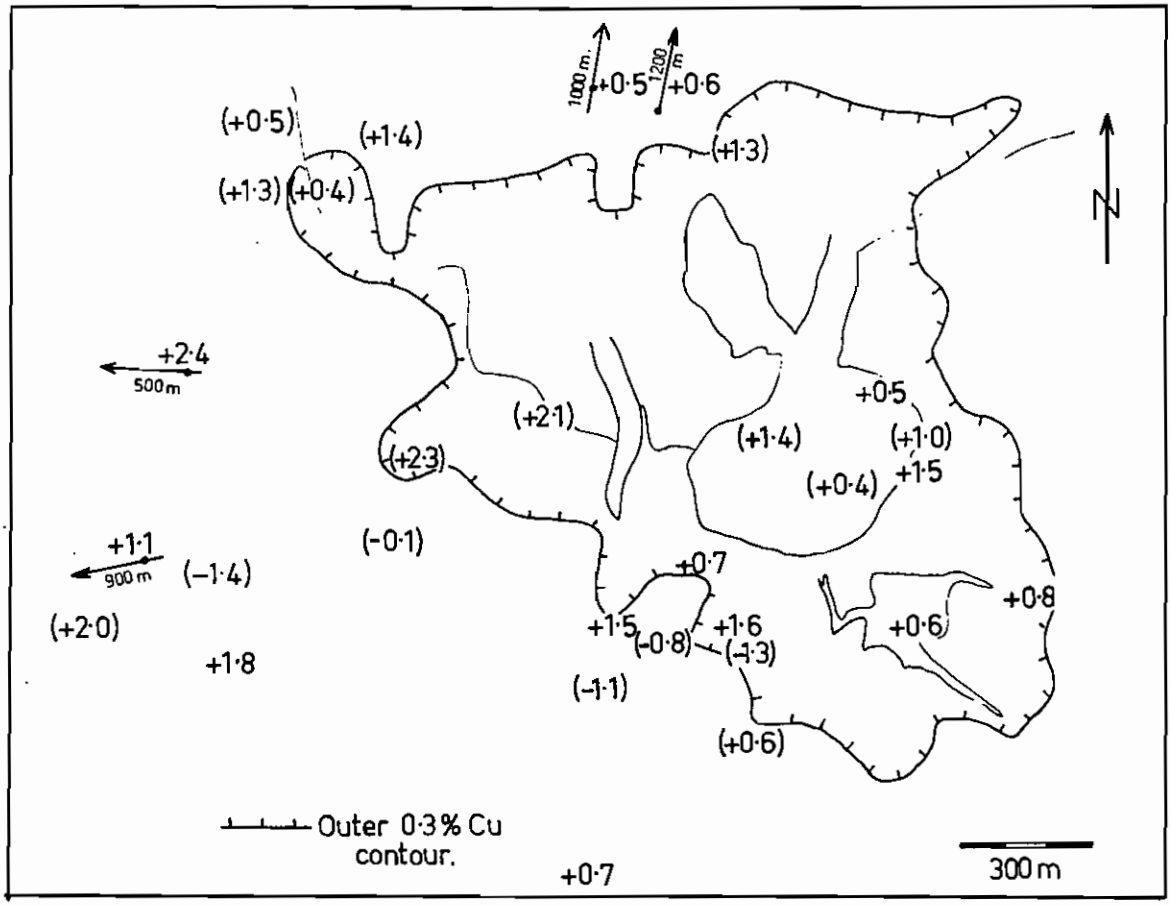

Fig. 11-2 Distribution of $\delta^{34}S$ of pyrite at Panguna. Data in parentheses from Ayres *et al.* (in press). Geological contacts and outer 0.3% Cu contour as in fig. 2-3.

Table 11-3

SULPHIDE $\delta^{34}S$ VALUES, CLASSIFIED BY VEIN TYPE (see Table 3-1)

Vein type	This study		Ayres *et al.*		
	Specimen	$\delta^{34}S_{py}$, ‰	Specimen	$\delta^{34}S_{py}$, ‰	$\delta^{34}S_{ccp}$, ‰
(ii)	103029	+1.6	40961?	0.0	-0.3
			40962?		
			34640		-0.1
			34641		+0.2
			34644		+0.1
			34645		+0.9
			34647		-0.5
			34648?	+2.0	
			40963		-1.6
			27967		-0.2
(iv)	103028	+1.5			
QP assoc.	103017	+1.5			
	103040	+0.7			
external	103479	+0.6			
	103045	+0.5			
	103043	+1.1			
(v)	103470	+0.5			
(vi)	103474	+0.6			
(viii)	103472	+0.8			
(ix/x) sp.	103042	+1.8			
no sp.	103477	+0.7	30643	+0.8 (Listed under ccp by Ayres *et al.*)	
	see also Table 11-1.				
Other	103478	+2.4	Pyrites associated with biotite alteration: -1.4, +0.4, +0.5, +0.6, +1.3, +1.3, +2.0, +2.1, +2.3		

FURTHER EXAMINATION OF ANHYDRITE-CHALCOPYRITE FRACTIONATION

Field & Gustafson (1976) prepared a plot of $\delta^{34}S$ of coexisting sulphides and sulphates as a function of Δ, i.e. effectively as a function of temperature. They explained that the data will plot as two straight lines if three conditions are met:-

1. The sulphur reservoir was effectively infinite;
2. The $\delta^{34}S$ of the sulphur reservoir remained constant;
3. There was a constant ratio of oxidised to reduced sulphur species throughout mineralisation.

Field & Gustafson found this to be so for anhydrite and sulphides at El Salvador. There were two trends, one pair of lines (for anhydrite and Cu,Fe sulphides) converging to $\delta^{34}S = +1.6‰$ and the other (for anhydrite and pyrite) to +6.8‰ at $\Delta = 0.0‰$. For any intercept on the $\Delta = 0$ axis it is possible to calculate a family of lines giving $\delta^{34}S$ variation in anhydrite and a sulphide as a function of Δ and the ratio of oxidised to reduced sulphur species. This was done for pyrite and anhydrite by those authors (who assumed that oxidised sulphur would be present as sulphate in the liquid, and reduced sulphur as H_2S) for $\delta^{34}S = 0‰$ at $\Delta = 0‰$. The $\delta^{34}S$ value to which the lines defined by actual measurements converge gives the isotopic composition of the sulphur reservoir.

A similar diagram has been prepared for the four pairs of data from Panguna. A pair of straight lines is defined, and these give a $\delta^{34}S$ value near 1‰, within the range shown, at the point of convergence (fig. 11-3).

The assumptions of Field & Gustafson warrant further attention. Given the straight line plots, the three numbered assumptions above seem justified. In view of the nature of the hydrothermal system, however,

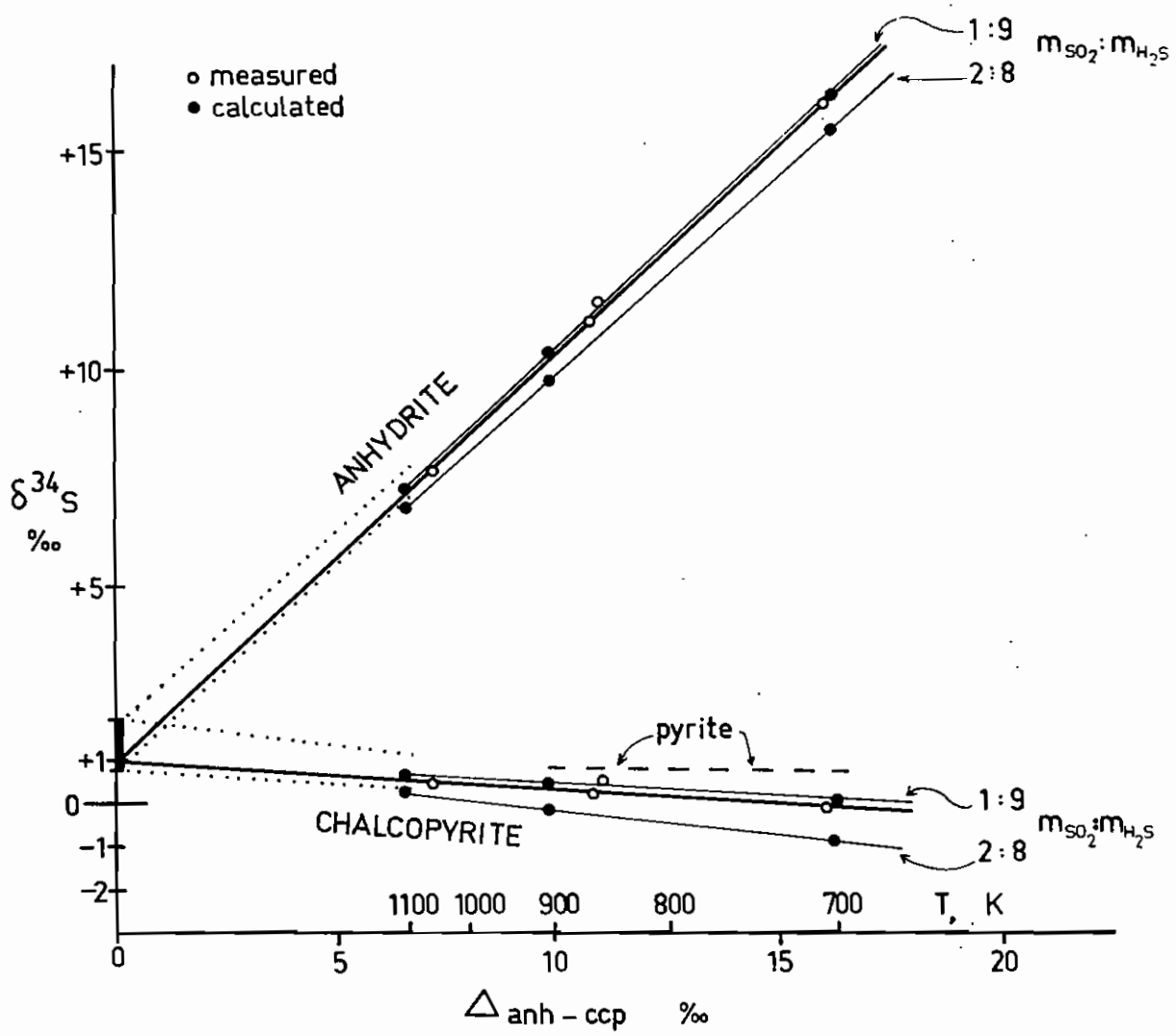

Fig. 11-3 $\delta^{34}S$ in anhydrite-chalcopyrite pairs as a function of Δ(anhydrite-chalcopyrite). Open circles and thick black lines are for measurements on Panguna samples. The dotted lines are limits on the position of the thick black lines. The black circles and thin black lines are calculated (see text) for the indicated molar ratios of oxidised to reduced sulphur species in the salt-rich liquid. The dashed line gives the $\delta^{34}S$ variation of a small amount of pyrite in isotopic equilibrium with the other minerals.

the meaning of the "sulphur reservoir" concept should be re-examined. The $\delta^{34}S$ value at the convergence of the two straight lines is not an estimate of the isotopic composition of magmatic sulphur. It is only an estimate of the bulk isotopic composition of the initial salt-rich liquid (which precipitates the sulphides and sulphates at lower temperatures). The implied constancy of $\delta^{34}S$ in the sulphur reservoir (assumption 2) is thus a constancy in the salt-rich liquid, implying a constraint on $\delta^{34}S$ of the magma in which the salt-rich liquids originated. The infinite supply of sulphur (assumption 1), however, refers to the salt-rich liquid only. Thus assumptions 1 and 2 are independent, and both are necessary. At temperatures below 750 K, the situation will be more complicated because of the possibility of adding sulphur from groundwater, and of depositing pyrite either before or with chalcopyrite. A small amount of pyrite in equilibrium with chalcopyrite would have the $\delta^{34}S$ values shown in fig. 11-3, with little variation as a function of temperature. Both pyrite and groundwater would affect only a small interval - the lowest temperature part - of the range of Δ being considered, so that ignoring them would not greatly affect the arguments used here. Likewise, deviation from the infinite reservoir hypothesis is most likely in the salt-rich liquid at low temperatures where most of the sulphides were deposited. All of these effects might have to be considered in a study based mainly on lower temperature sulphate-sulphide pairs.

$\delta^{34}S$ IN THE SULPHIDES, SULPHATES & FLUIDS AS A FUNCTION OF f_{O_2}

Sulphur in the liquid and vapour at temperatures over 673 K is present as SO_2 and H_2S (Barnes & Czamanske, 1967) and not as SO_4^{2-}. The sulphate in anhydrite probably originates from the decomposition of SO_2,

which becomes an unimportant species near 673 K under porphyry copper f_{O_2} conditions. The calculation of a family of curves giving $\delta^{34}S$ as a function of $\Delta_{anh-ccp}$ under the conditions at Panguna is based on the following equation:

at temperature T, given values for $\Delta_{SO_2-H_2S}$; Δ_{anh-H_2S}; Δ_{ccp-H_2S} ($\simeq 0$) [all fractionation data are from Ohmoto & Rye (in press) ; see Table 11-4]; $m_{H_2S}:m_{SO_2} = a:1-a$

$$\delta^{34}S_{liq} = a\,\delta^{34}S_{H_2S} + (1-a)(\delta^{34}S_{H_2S} + \Delta_{SO_2-H_2S})$$

$$= 1 \text{ (value taken from fig. 11-3).}$$

Whence, $\delta^{34}S_{ccp} = \delta^{34}S_{H_2S}$

and $\delta^{34}S_{anh} = \delta^{34}S_{H_2S} + \Delta_{anh-H_2S}$

Some of the curves are plotted in fig. 11-3. The curves bracket $m_{H_2S}:m_{SO_2}$ between 9:1 and 8:2. The ratio 9:1 will be adopted for the purposes of the following calculations.

Thus, at 1100 K,

$$1 = 0.9(\delta^{34}S_{H_2S}) + 0.1(\delta^{34}S_{H_2S} + 3.4)$$

and $\delta^{34}S_{H_2S} = +0.7‰$

$\delta^{34}S_{SO_2} = +4.1‰$.

Since the vapour contains effectively only SO_2 (see Chapter 10), $\delta^{34}S_{vap} = +4.1‰$.

In this relatively simple situation, the $\delta^{34}S$ of the fluids, sulphides and sulphates depends on the oxygen fugacity. The higher the oxygen fugacity, the higher will be $m_{SO_2}:m_{H_2S}$ in the liquid, the steeper the sulphide lines and therefore the larger the difference in $\delta^{34}S$ between the liquid and the sulphides, and the smaller the difference between the liquid and the anhydrite.

Table 11-4

FRACTIONATION AMONG SULPHUR SPECIES

T	ΔSO_2-H_2S	$\Delta HS^--H_2S^*$	$\Delta_{ccp}-H_2S^*$	$\Delta CaSO_4-H_2S^*$
700	9.1	-0.7	-0.10	16.3
800	6.8	-0.7	-0.08	12.5
900	5.3	-0.7	-0.06	9.9
1000	4.2±0.5	-0.7±0.2	-0.05±0.08	8.0±1.0
1100	3.4	-0.7	-0.04	6.6

* extrapolated

Data from Ohmoto & Rye (in press). All values in ‰.

Under any conditions at which sulphate and sulphide coexist, the $\delta^{34}S$ of chalcopyrite will decrease with decreasing temperature. This ought to be reflected as a zonation of $\delta^{34}S_{ccp}$ with outward decrease. The smallness of the decrease implied by fig. 11-3 for Panguna must make zonation difficult to detect if there is also scatter in the data. Ayres *et al.* give a $\delta^{34}S$ range of 3‰ for Panguna chalcopyrite, compared with the predicted decrease of <1‰ in fig. 11-3. However, the prediction corresponds with the isotopic zonation reported by Field (1966) at Bingham, where there is an outward decrease in $\delta^{34}S$. The apparent contrast between salt-rich liquid ($m_{SO_2}:m_{H_2S} \simeq 1:9$) and the vapour ($f_{SO_2}:f_{H_2S} = 10^{3.9}$ at 1000 H, HM) deserves comment. The large difference may be an artefact of thermodynamic assumptions (standard states and activity coefficients), possibly implying that one of the gas species interacts strongly with another chemical species in the liquid. Alternatively, the assumption that SO_2 is the only oxidised sulphur species in the liquid may be at fault.

COMPARISON WITH OTHER DEPOSITS

Coexisting pairs of anhydrite and sulphide have been examined in relatively few porphyry copper deposits. For El Salvador (Field & Gustafson, 1976) and Frieda (Appendix 3), there were sufficient data to plot curves like those in fig. 11-3. Limited fluid inclusion studies of both deposits (Gustafson & Hunt, 1975 and appendix, this study) show that the hydrothermal systems consisted of boiling salt-rich liquid, comparable with the Panguna system. The isotopic data for Frieda and El Salvador both give converging pairs of straight lines, two pairs at El Salvador and possibly two at Frieda. From the discussions above, the slopes of the lines and the intercept on the $\delta^{34}S$ axis are the most important parameters for comparison.

The $\delta^{34}S$ lines for anhydrite and chalcopyrite or bornite converge at about +1.6‰ in the case of El Salvador. The ratio of oxidised to reduced sulphur species, using SO_2 as the oxidised species instead of SO_4^{2-}, is recalculated as follows:

$$\delta^{34}S_{liq} = 1.6 = \delta^{34}S_{H_2S} \cdot m_{H_2S} + \delta^{34}S_{SO_2} \cdot m_{SO_2}$$

(where $m_{H_2S} + m_{SO_2} = 1$). From Field & Gustafson's diagram, at $\Delta = 10.0‰$ (T = 900 K), $\delta^{34}S_{ccp} = -3.0‰$. From Table 11-4, $\Delta_{SO_2-H_2S} = 5.3‰$ and $\Delta_{ccp-H_2S} \simeq 0‰$ at 900 K, so that

$$m_{H_2S} = 0.13 \quad \text{and} \quad m_{SO_2}/m_{H_2S} = 7:1 \ .$$

Thus conditions were more oxidising than at Panguna. As an alternative measure of this, the difference in $\delta^{34}S$ between the liquid and the Cu,Fe sulphides at El Salvador is 4.6 to 7.6‰, greater than at Panguna.

Anhydrite-pyrite mineralisation at El Salvador gives a very different pair of lines. These converge to +6.8‰, and have slopes indicating high oxygen fugacity. Field & Gustafson concluded that a correction to the pyrite data may be required. A subtraction of 3‰ from $\delta^{34}S_{py}$ would correct temperature estimates (see below) and align the pair of lines so as to indicate a single source-composition of sulphur.

The difficulty with pyrite does not seem to arise in the case of Frieda (Appendix 3). In summary, the two pairs of lines (one pair of which, as drawn, coincides exactly with the Panguna curves) may reflect mineralisation from two different centres. If so, the slope of the steeper sulphide line is greater than at Panguna, indicating a higher oxidation state. The pairs of lines both converge near +1‰.

Sulphide data from other selected deposits are listed in Table 11-5. The sulphide from El Salvador is isotopically very light compared with the other deposits. Other deposits with low $\delta^{34}S$ are known,

Table 11-5

SULPHUR ISOTOPE DATA FOR PORPHYRY-TYPE MINERALISATION FROM SELECTED DEPOSITS

Deposit	$\delta^{34}S$ range, ccp ‰	$\delta^{34}S$ range, py ‰	Reference
Panguna	-1.6 to +1.5	0.5 to +2.4	Ayres *et al* (in press); this study.
Frieda	-3.5, +0.1	-1.6 to +2.1	this study
Bingham (central)	-2.9 to -0.1	-0.4 to +1.1	Field (1966)
Butte (deep zone)	-3.0 to 0.0	-1.0 to +2.7	Lange & Cheney (1971)
Valley Copper	-3.3 to +1.5	-3.1	Osatenko & Jones (1976)
El Salvador (except peripheral)	-5.3 to -3.1	-5.1 to -0.3	Field & Gustafson (1976)

e.g. Yerington, Nevada (Field, 1966, data for undifferentiated sulphides). Panguna sulphides are a little heavier than the others. The range for pyrite is displaced about 2‰ in the positive direction in each case. If this difference reflects the temperature of formation, then the temperature would be less than 250°C, considerably lower than other estimates. At El Salvador, coexisting pyrite-chalcopyrite pairs have been examined, and they give apparently erroneous temperatures. At Panguna, it is at best uncertain whether chalcopyrite and pyrite were ever in equilibrium; the same may apply to the other deposits.

All information points to Cu,Fe sulphide-anhydrite pairs as the most useful and reliable source of data on porphyry copper mineralisation. In a well-controlled and sufficiently detailed study, pyrite may yield additional insight. The variety of pyrite occurrences at Panguna suggests that very careful sampling would be necessary.

THE ISOTOPIC COMPOSITION OF MAGMATIC SULPHUR

The near-zero $\delta^{34}S$ values of porphyry copper sulphides have in the past been taken to indicate that magmatic sulphur in these systems also had $\delta^{34}S$ near 0‰. The fixing of much sulphur as anhydrite (likely even in deposits where it has not been observed because it has been dissolved away), and the removal of large amounts as SO_2 in vapour imply that this approach is greatly oversimplified. Field & Gustafson's suggestion that the point of convergence of curves such as those in fig. 11-3 represents the isotopic composition of magmatic sulphur is also inadequate in any system in which two fluid phases separated from the crystallising magma.

Two extreme cases are to be considered. In the first, the magmatic volatiles separate in isotopic equilibrium with the silicate liquid,

i.e. without depleting the magmatic sulphur reservoir significantly. H_2S in the salt-rich liquid will therefore be in equilibrium with HS^- in the magma (Ohmoto & Rye, in press). At Panguna, $\delta^{34}S_{H_2S} = +0.7‰$ so that $\delta^{34}S_{HS^-} = 0.0‰$.

In the second case, the volatiles remove all sulphur from the magma. The $\delta^{34}S$ of all the volatiles taken together is the same as the magmatic $\delta^{34}S$. The problem becomes one of knowing the relative proportions of vapour and salt-rich liquid, and the oxidation states of the fluids. The evolution of an early, boiling salt-rich liquid at relatively low oxygen fugacity has been discussed in Chapter 10.

Using the estimates of magmatic volatile content cited in Chapter 10 (viz. for 1 kg magma, 15 g H_2O and 1 g NaCl), and assuming the evolution of salt-rich liquid of 65% NaCl and vapour of 2% NaCl, the molar ratio of vapour and liquid is found (from a calculation similar to those performed in Chapter 10) to be 0.034:0.61 for dimers in the vapour, $\simeq$ 1:18.

In the vapour evolved during copper mineralisation (1100 K, HM and 800 atm) $P_{SO_2} > 6$ atm (Chapter 10), i.e. $X_{SO_2} > 0.01$ and 18 moles of vapour contain more than 0.18 moles S as SO_2.

If one mole of salt-rich liquid contains enough sulphur to form chalcopyrite corresponding to 1900 ppm Cu (Chapter 5), i.e. 1900 ppm S, and 65% NaCl, the mole fraction of S as chalcopyrite is

$$\frac{0.19/32}{65/58.5 + 35/18 + 0.19/32} \simeq 1.9 \times 10^{-3}$$

If the molar ratio of $SO_2:H_2S$ in the liquid is 1:9, and if sulphate forms by reaction 10.52, this corresponds with a total sulphur mole fraction of

$$1.9 \times 10^{-3} \left[1 + [\tfrac{1}{4}/(9 + \tfrac{3}{4})]\right] \simeq 1.9 \times 10^{-3}$$

Doubling the above figure to account (roughly) for sulphur lost by boiling in the ore-zone, the mole fraction of sulphur in the liquid becomes about 4×10^{-3}.

$$\text{Thus, } \frac{\text{moles S in liquid}}{\text{moles S in vapour}} < \frac{4 \times 10^{-3}}{0.18} = \frac{1}{45}$$

SO_2 is also the dominant sulphur species in the vapour down to $\log f_{O_2} = HM - 3$ ($k_{10.15}$ from Table 10-6; $\log f_{H_2O} = 2.8$). If more sulphur is carried in the vapour than in the liquid under all f_{O_2} conditions, then $\delta^{34}S_{magma} \simeq \delta^{34}S_{SO_2}$ summed over the whole process of expulsion of volatiles. Late, relatively oxidised fluids must have removed all sulphur remaining in the magma which would therefore have had $\delta^{34}S = +4.1‰$ at that stage. Early, relatively reduced fluids may have removed sulphur in isotopic equilibrium with magmatic sulphur, before significant depletion of the reservoir. Since this sulphur was removed as SO_2, the initial $\delta^{34}S$ of the magmatic sulphur would have been greater than +4.1‰ . How much greater depends on the amount of sulphur carried in the reduced fluids, and there is no information about this.

Again using the calculation of the number of moles of liquid and vapour expelled by a kilogram of magma, it is possible to estimate the amount of sulphur lost from the magma as volatiles. Considering only the sulphur in the vapour, for which the limits $X_{SO_2} = 0.01$ to 0.1 were set in Chapter 10, the number of moles of S lost as vapour would be 6.1×10^{-3} to 6.1×10^{-2}, and the weight 0.2 to 2.0 g. The estimates of X_{SO_2} apply only to the relatively oxidised vapours expelled during copper mineralisation. If, say, half of the volatiles were expelled in that condition, then 0.1 to 1.0 g S would leave the magma during copper mineralisation. The more reduced half of the fluids might be expected to carry less SO_2 because of the lower oxygen fugacity, but no estimate is possible. In any case, the amount of S carried in the fluids would be

no less than 0.1 to 1.0 g, a quantity to be compared with the amount of S remaining in unaltered Kaverong Quartz Diorite (0.3 g/kg, analyses from Ford, 1976). Thus isotopic equilibria could well be subject to a depletion effect, even for the minimum quantities estimated here, and the results would approach those of the second case discussed above.

The problem of the isotopic composition of magmatic sulphur is thus a difficult one, dependent for its solution on a complete understanding of the processes by which volatiles are evolved and expelled from the magma. The speculations here are founded on guesses as to the relative quantities of oxidised and reduced fluids, and the amount of sulphur in the reduced fluids.

Comment. Less than 2% of the sulphur expelled from the magma during copper mineralisation is carried in salt-rich liquid (see calculation above). The figure used in the calculation was a minimum estimate of the amount carried away as vapour. Earlier fluids may also have removed significant sulphur, and the mineralising salt-rich liquid itself may not deposit all of the sulphur it contains. Thus the formation of a porphyry copper fixes little, probably much less than 1%, of the sulphur expelled from the magma, and much sulphur may be available for mineralisation higher in the hydrothermal system.

CONCLUSIONS

The sequence of mineralisation at Panguna porphyry copper deposit comprises many types and episodes of veining, including the quartz-Cu,Fe sulphide veins associated with the copper mineralisation. Fluid inclusions in quartz of these veins contain three types of fluid: dense salt-rich liquid, low-density water-rich vapour, and brines of low to moderate salinity unsaturated in NaCl at room temperature. The fluids may be grouped into two systems, one of salt-rich liquid in equilibrium with vapour, the other of low to moderate salinity brine. The two systems were distinct in the ore-zone.

The composition of the salt-rich liquid, in terms of the system $NaCl-KCl-H_2O$, ranged between 76% and 46% salts by weight in inclusions which had nucleated sylvite. The NaCl content varied from 60% to 30% while the KCl content remained constant at 16 ± 2%. Salt-rich liquids with $T_s NaCl < 320^{\circ}C$ had not nucleated sylvite, except for one inclusion which had 22% KCl and 27% NaCl. The K/Na ratio of the salt-rich liquids ranged from 0.46 to 0.17 (atomic proportions), increasing as the salinity decreased and, in general, as the temperature decreased. Na, K, Fe and Cl are the predominant ions in leachates of crushed quartz; Ca, SO_4 and minor Mg are also present. Chlorides of Na, K and Ca (minor Mn, Zn), a Cu,Fe sulphide and possibly apatite have been identified among the daughter salts of opened inclusions of salt-rich liquid. Volume measurements on chalcopyrite crystals in fluid inclusions indicate an original copper concentration near 1900 ppm in the salt-rich liquid from a vein formed at temperatures below $550^{\circ}C$. The density of the salt-rich liquids lay in the range 1.2 - 1.5 g/cm^3. The temperatures of these liquids varied between $350^{\circ}C$ and $700^{\circ}C$ or higher.

Salt-rich liquid deposited quartz-Cu,Fe sulphides, anhydrite and iron oxides and was associated with the development of potassic alteration assemblages. They may also have deposited earlier amphibole-magnetite-quartz veins. Some, at least, were of magmatic origin, because primary salt-rich inclusions occur in quartz phenocrysts. The temperature and salinity distributions of the salt-rich liquids, combined with field data, indicate three phases (A, B and C) of quartz-Cu,Fe sulphide mineralisation from different centres. Phase A, the earliest, took place while the Kaverong Quartz Diorite was at near-magmatic temperatures (>700°C) to the north of the orebody and was bounded to the south and southwest by a zone at 350° - 430°C. This zone corresponds closely with the 0.3% Cu ore-grade contour and is parallel to a pyritic halo beyond the orebody. T_SNaCl values were 450° - 490°C except along this zone, where they fell below 420°C. Prior to phase A copper mineralisation, a hydrothermal system of similar extent brought about pervasive alteration of the Panguna Andesite to an amphibole-plagioclase-magnetite assemblage. Before this, the Panguna Andesite may have undergone thermal metamorphism to biotite hornfels at the contact of the Kaverong Quartz Diorite.

Two later phases, B and C, occurred after a long period of cooling and may have been partly concurrent. Phase B, which seems to have comprised two stages, was associated with the emplacement of the Leucocratic Quartz Diorite. Temperatures exceeded 600°C at the centre and T_SNaCl values varied between 390°C and 490°C. The cell of mineralisation was bounded by a halo of pyrite veins and possibly by another of fluids at or near the critical point. Phase C postdated the Biuro Granodiorite. Temperatures exceeded 580°C and T_SNaCl values attained 570°C at the centre. A group of veins with T_SNaCl < 400°C east of the

Biotite Granodiorite may be part of the phase C boundary, which has not otherwise been located.

Brines of low to moderate salinity, in terms of the system $NaCl-H_2O$, covered the whole composition range of solutions unsaturated at 25°C. Brines of 0 - 5 wt. % eq. NaCl predominated. Formation temperatures (corrected for pressure) ranged between 160°C and 400°C. The brines deposited quartz-pyrite veins and were associated with some of the phyllic alteration. They also appear to have been associated with the deposition of sphalerite-pyrite and pyrite-clay veins near 300°C. Isotopic evidence (Ford & Green, 1977) combined with fluid inclusion evidence, indicates that these were meteoric waters. No regular temperature or salinity distributions were found for the brines of low to moderate salinity. They were present outside the zones of ore-deposition during phases A, B and probably C, and inundated the orebody between phases A and B, and again after the waning of phases B and C. They were present throughout the cooling of the ore zone from 400°C to below 200°C, and may have been involved in the formation of the post-mineralisation pebble dykes that intersect the hot centres of phases B and C. The opening of large fractures is thought to have carried groundwater into rock hot enough to cause violent boiling.

The fluids near the critical point at 400°C (the QP association of Chapter 6) are thought to represent the boundary of the region of two coexisting fluids from which copper was deposited in each phase of fluid circulation. The critical pressure of the fluids (270 - 280 bars) is a minimum estimate of the pressure at the edge of the system, to be compared with a maximum estimate of 290 bars based on the behaviour of gas-rich inclusions, and an estimate of 200 - 300 bars based on the vapour pressures of saturated salt-rich liquids. Under a hydrostatic pressure regime, this implies a depth of formation of about 3 km.

With the critical pressure of the QP association as a boundary pressure, the phase behaviour of salt-rich liquid in fluid inclusions is found to compare closely with the behaviour predicted in the literature for boiling NaCl-H_2O liquids, provided supersaturation is permitted in the real system in place of saturation, and despite the presence of significant KCl in the real liquids. The evolution of the liquids was as follows: unsaturated, boiling salt-rich liquid was expelled from the magma, and cooled by boiling to saturation and supersaturation at temperatures probably near 500°C. Further cooling was in part due to mixing with cooler, more dilute liquid so that the salt-rich liquids became unsaturated again by about 430°C. During phase C, some liquids were concentrated by boiling to 75% salinity without mixing. Dilution and cooling of the boiling liquids continued from 430°C to 400°C, at which temperature the compositions of the liquid and gas had converged to a single, critical composition.

The compositional variation of the salt-rich liquids, a straight-line trend on the NaCl-KCl-H_2O triangular diagram, is consistent with the mixing of two salt-rich liquids, one of about 65% salts and low K/Na, derived from the magma, and the other containing at most 45% salts and with a higher K/Na, probably derived from groundwater by boiling. Both would have contained the same concentration, about 16% (wt.) of KCl. The K/Na ratios of magmatic salt-rich liquids are consistent with equilibrium between the liquids and the rims of plagioclase phenocrysts in the various stocks. No buffering mechanism can be suggested for salt-rich liquid derived from groundwater.

Salt-rich liquid probably ascended from crystallising magma to the ore-zone by the pumping action of the difference between lithostatic pressure in the magma and hydrostatic pressure in the ore-zone. At a level

probably determined by the presence of groundwater, salt-rich liquid moved horizontally into the country rocks, then descended, because of its density, through the ore-zone.

The critical-point boundary proposed for the region of two fluid phases can continue at most 600 m above present levels of exposure. The nature of the boundary over the two-phase region cannot be inferred. Below the exposed ore-zone, the salinity at the critical-point boundary, if it and groundwater persist to depth, would increase with depth.

At 1000 K, 500 bars and log f_{O_2} at the hematite-magnetite boundary, vapour leaving the magma would have had the following chemical parameters:

$\log f_{O_2}$	$= -8.8$	$\log f_{NaCl}$	< -1.8
$\log f_{S_2}$	$= -7.1 \pm 2.3$	$\log f_{CuCl}$	$= -10 \pm 5$
$\log f_{SO_2}$	$= 0.6 \pm 1.0$	$\log f_{NaFeCl_3}$	$= -11 \pm 2$
$\log f_{H_2S}$	$= -3.3 \pm 1.0$	$\log f_{ZnCl_2}$	$> -3.7 \pm 1.8$ *
$\log f_{H_2O}$	$= 2.6$	$\log f_{MoO_2(OH)_2}$	$> -3.6 \pm 1.5$ *
$\log f_{HCl}$	$= 0.1 \pm 0.5$	(* values at 850 K)	

when in equilibrium with an assemblage of quartz, anhydrite, rutile, molybdenite, sphalerite and Cu,Fe sulphide, and with $X_{SO_2} < 0.1$. Values at other conditions are tabulated in the text. Enhanced volatility in mixed halide systems brings about a significant increase in the volatility of iron only, but does not lead to significant vapour transport of iron. The metal-bearing species above are the predominant species for each metal except for Na ($NaOH.H_2O$ predominating) and Mo [$Mo_7O_{18}(OH)_6$ predominating]. Zinc and molybdenum may separate (in vapour) from iron and copper (in liquid) by virtue of their greater volatility. The formation from magmatic vapour of a salt-rich condensate with the copper concentration observed in fluid inclusions of salt-rich liquid is unlikely unless

$f_{CuCl} > 10^{-6 \cdot 8}$. The chemical appraisal of the vapour plume mechanism of Henley & McNabb cannot be improved without better thermochemical data.

Since biotite is the most abundant alteration product associated with copper mineralisation, the acidity of the salt-rich liquid must be dominantly controlled by the formation of biotite from amphibole and plagioclase. The acidity of the salt-rich liquid should show a net increase, driving the liquid towards equilibrium with sericite rather than the observed K-feldspar, or K-feldspar + sericite. The formation of anhydrite and sulphides also produces HCl, so that boiling may be necessary in addition to the precipitation of quartz in order to take up excess HCl and avoid the formation of large quantities of sericite. The alteration reactions also control the activity of $FeCl_2$ in the liquid, and may therefore control the distribution of bornite and chalcopyrite.

The decomposition of SO_2 may account for the presence of the sulphate fixed as anhydrite but cannot account for the increase in sulphide deposition below 500°C. Reactions such as the reduction of SO_2 by Fe^{2+} may be significant at lower temperatures.

The high oxidation state of the magmatic fluids during copper mineralisation reflects the loss of H_2 in earlier fluids, those responsible for amphibole-magnetite-plagioclase alteration in the Panguna Andesite prior to phase A. There is no evidence of the deposition of copper by the reduced fluids, which appear to have been salt-rich liquid and vapour. The transport of copper may thus be dependent on the oxygen fugacity.

Sulphur isotope data yielded temperatures near 300°C for sphalerite-pyrite veins, and 400 - >800°C for anhydrite-chalcopyrite pairs. No space or time variation of $\delta^{34}S$ in pyrite or chalcopyrite could be detected in the data available. Pyrite has a $\delta^{34}S$ range of +0.5 to +3.1‰, chalcopyrite (Ayres *et al.*, in press) -1.6 to +1.5‰ and anhydrite +7.6 to +16.0‰. The salt-rich liquid which deposited anhydrite and sulphides had

$\delta^{34}S$ = 1‰. The $\delta^{34}S$ values of the liquid and the solid phases should vary as a function of oxygen fugacity and are not simply related to the $\delta^{34}S$ value of magmatic sulphur.

The evolution of salt-rich liquid from crystallising magma, the condensation of salt-rich liquid from cooling magmatic vapour, the boiling of groundwater and groundwater convection driven by heat from the intrusive centre - all suggestions by other authors regarding the mechanism of porphyry copper formation - may all have contributed to the formation or evolution of the Panguna deposit. The association of salt-rich liquid with copper is definite. The continuity of K/Na ratios between salt-rich liquids in veins and in the magma, along with the improbability of significant copper transport in the vapour under porphyry copper conditions implies that liquid expelled direct from the magma, and not condensate, was responsible for the mineralisation. Some metals and sulphur may have been derived from groundwater.

Further work at Panguna could examine the amphibole-bearing veins and alteration in greater detail, if the quality and quantity of specimens permit. More detailed work on the composition and properties of inclusions (solid and fluid) in quartz phenocrysts may also yield interesting data on processes occurring in the magmas. Any extension of the sulphur isotope study should, at the outset, be limited to anhydrite-chalcopyrite pairs (which are not common) or to chalcopyrite samples with temperature control. Depth was not considered as a spatial variable for the set of samples used in this study, so that ultimately, a new set of samples from the deepened pit may make an interesting comparative study.